# Identifying the roles of *dead ringer* in the *Drosophila* eye

A thesis submitted for the degree of Doctor of Philosophy

Jane Sibbons, B.Sc. (Hons.)

School of Molecular and Biomedical Sciences, Genetics discipline
Centre for the Molecular Genetics of Development
The University of Adelaide

September, 2004

# Table of Contents

# Table of Figures



# Table of Tables

# Abstract

The *Drosophila* Dead ringer (Dri) protein is a founding member of the ARID family of transcription factors, which play important roles in many important biological processes. *dri* is essential for *Drosophila* development, with mutations in *dri* resulting in embryonic lethality. Although some of the roles of Dri have been identified in the embryo, little is known about its roles in later stages of development. This study has focused on the role of Dri in the *Drosophila* eye. *dri* expression in larval eye imaginal discs was shown to be restricted to a subset of photoreceptor (R) cells, R1-R6 and R8, with expression beginning several rows behind the morphogenetic furrow. Expression in R1-R6 was found to persist in adults, but expression in R8 was downregulated during pupal development.

To determine if *dri* plays a role in *Drosophila* eye development or function, somatic *dri* mutant clones spanning the entire eye were produced. Significantly, *dri* was found to be essential for fly vision. Further analysis aimed at understanding the cellular and molecular basis for the blindness revealed that *dri* mutant R cells are specified correctly during the third larval instar stage, consistent with expression some time after the onset of differentiation, but that a subset of R1-R6 axons pass through the correct layer of the optic lobe, the lamina, and terminate in the second optic ganglia, the medulla. The mistargeted R1-R6 axons were found to persist in the adult optic lobe, but the mild mistargeting phenotype appeared unlikely to cause blindness. In the adult eye, *dri* was expressed in R1-R6 cells, an expression pattern identical to the light-sensing Rhodopsin 1 (Rh1) gene, *ninaE*. This pattern of *dri* expression and the blindness phenotype suggested that Dri may regulate the expression of *ninaE*. Indeed, a dramatic reduction in the level of Rh1 protein was observed in *dri* mutant eyes, but the *ninaE* transcript level was found to be unaffected, indicating that *dri* was not regulating *ninaE* transcription or mRNA stability. However, *dri* was found to be necessary for the regulation of one or more factors required for the processing or turnover of Rh1 as the loss of Dri resulted in age-dependent and light-independent retinal degeneration. The rate and severity of retinal degeneration increased if *dri* mutant eye mosaic flies were exposed to light, suggesting that *dri* may also regulate one or more components of the visual transduction pathway.

# Declaration

This work contains no material which has been accepted for the award of any other degree or diploma in any university or tertiary institution and, to the best of my knowledge and belief, contains no material previously published or written by another person, except where due reference has been made in the text.

I consent to this copy of my thesis, when deposited in the University library, being available for loan and photocopying.

Jane Sibbons

# Acknowledgments

Firstly I must thank my supervisor Rob Saint, for allowing me independence, having faith in me, being available to give me advice when needed and for providing such a fun place to work. Thank you also to Barry Dickson for allowing me to visit your lab during the course of my PhD and Kirsten Senti who taught me so much in such a short amount of time.

Thank you to the members of the Genetics discipline, the Centre for the Molecular Genetics of Development, particularly Helli, members both past and present of the Saint lab, with special thanks to Donna Crack, Hazel Dalton and Tetyana Shandala for reading this thesis.

Thanks to all the flies that gave their heads for this research.

Thank you to my family and friends, who supported me though this PhD, I really appreciated it.

Finally thank you to Chris, without your love and support, this journey would have been so much harder and thank you to Connor for giving me another focus, love you both.

# Chapter 1: Introduction

## 1.1 Transcription factors and animal development

Development of an animal begins with a single cell, and progression through a program of proliferation and differentiation of numerous cell types generates the adult animal. Differentiation requires cell type specific expression of appropriate factors at the correct time of development. Regulation of transcription is a key process for the differential expression of genes in different cell types, so it is not surprising that transcription factors play a major role in development. In the *Drosophila* embryo, transcription factors such as the products of the patterning genes *bicoid* and *dorsal*, act during axis formation to regulate the transcription of other transcription factor genes. For example, Dorsal activates the mesoderm genes, *twist* and *snail* (reviewed by Chasan and Anderson, 1993). The establishment of segments utilizes different transcription factors, such as Kruppel, Hairy, Even skipped and Engrailed (reviewed by Chasan and Anderson, 1993). Transcription factors utilized early in embryogenesis are often reused later in organogenesis. For instance, *twist* expression is required for mesoderm formation, but is also required for the expression of *tinman*, a gene important in heart development (reviewed by Chasan and Anderson, 1993). In the larval eye, transcription factors such as Atonal, Rough, Glass, Bar and Prospero are important for differentiation of the components of the eye (reviewed by Dickson and Hafen, 1993), while Glass, and Prospero are involved later in regulating factors required for the vision of the adult fly (Mismer and Rubin, 1989; Moses and Rubin, 1991; Cook et al., 2003).

### *1.1.1 The ARID family of transcription factors*

The ARID (AT Rich Interacting Domain) family, as the name suggests, binds to AT rich sequences in DNA and regulates gene expression (Herrscher et al., 1995; Gregory et al., 1996; Valentine et al., 1998; Hader et al., 2000; Watanabe et al., 2002). This thesis will investigate one of the founding members of this family, Dead ringer/Retained, which will be referred to as Dead ringer (Dri) for the remainder of this thesis. The aims of the work described in this thesis were to investigate the biological roles of Dri during *Drosophila* eye development and function. In the following sections I will firstly describe the general characteristics of ARID genes and proteins. Secondly, what is known about Dri will be discussed in detail, including the embryonic roles, and finally I will discuss the components of the visual system and the visual transduction pathway in *Drosophila*.

## 1.2 The ARID family of proteins

Members of the ARID family have been identified in many organisms including the yeast (*Saccharomyces cerevisiae*), the nematode (*Caenorhabditis elegans*), the zebrafish (*Danio rerio*), the fly (*Drosophila melanogaster*), the mouse (*Mus musculus*) and humans (*Homo sapiens*). Family members include *S. cerevisiae* SWI1 (Peterson and Herskowitz, 1992), *D. melanogaster* Dead ringer/Retained, (Gregory et al., 1996) and Osa/Eyelid (Treisman et al., 1997b; Vazquez et al., 1999), *C. elegans* CFI-1 (Shaham and Bargmann, 2002), *D. rerio* Dri1 and Dri2 (Kortschak, 1999), mouse Bright (Herrscher et al., 1995), mouse and human Jumonji (Takeuchi et al., 1995), Smcy and Smcx (Agulnik et al., 1994b; Agulnik et al., 1994a), human Retinoblastoma Binding Proteins 1 (RBP1) and RBP2 (Fattaey et al., 1993), Bright Dead ringer Protein (BDP) (Numata et al., 1999), Modulator Recognition Factor 1 (MRF-1) and MRF-2 (Huang et al., 1996) and DRIL1 (Kortschak et al., 1998). This family can be divided into three distinct subgroups; 1) the JUMONJI family that share a jumonji domain and the core ARID, 2) the other proteins that contain a core ARID domain but have no other domain similarities and 3) proteins that contain extended regions of homology both N-terminal and C-terminal to the core ARID, known as the extended ARID (eARID) (Kortschak et al., 2000). Dri is a member of the eARID subfamily.

### *1.2.1 The Jumonji group of proteins*

Proteins that belong to the JUMONJI family include both human and mouse JUMONJI, SMCY, SMCX, RBP1 and PLU-1 and human RBP2 (Fattaey et al., 1993; Agulnik et al., 1994b; Agulnik et al., 1994a; Takeuchi et al., 1995; Berge-Lefranc et al., 1996; Lu et al., 1999; Barrett et al., 2002). This group of proteins is named after the jumonji (jumj) domain. The jumj domain has two regions of homology, the jumjN, the N-terminal-most region of homology adjacent to the ARID domain and the jumjC region positioned at the C-terminus of the protein. Although the jumjN and jumjC appear to be at opposite ends of the protein, secondary structure may result in these regions co-operating to become one domain (Balciunas and Ronne, 2000). The JUMONJI family of proteins has a wide variety of functions, including differentiation of the mammalian heart and other tissues, X-inactivation and cell cycle regulation (Fattaey et al., 1993; Agulnik et al., 1994a; Wu et al., 1994; Takeuchi et al., 1995; Nevins, 1998; Lu et al., 1999; Staehling-Hampton et al., 1999; Quadbeck-Seeger et al., 2000; Toyoda et al., 2000; Chan and Hong, 2001; Kitajima et al., 2001). Interestingly, JUMONJI preferentially binds to AT rich sequences but can bind to other sequences (Kim et al., 2003) while RBP2 binds to DNA in a non-site specific manner (Chan and Hong, 2001).

### *1.2.2 Other core ARID family members*

The SWI/SNF complex in yeast is a well-characterized chromatin-remodelling complex with one of the members, SWI1 containing an ARID domain (Peterson and Herskowitz, 1992). It is noteworthy that the ARID domain in SWI1 is dispensable for the function of this gene (C. Peterson, personal communication). Homologues of the SWI/SNF complex are found in many organisms including *Drosophila*, mice and humans and have a wide range of functions, including regulating the cell cycle and differentiation (Treisman et al., 1997b; Vazquez et al., 1999; Collins and Treisman, 2000; Dallas et al., 2000; Kozmik et al., 2001; Brumby et al., 2002; Hurlstone et al., 2002; Inoue et al., 2002). Osa, the *Drosophila* orthologue of SWI1, is required for segmentation and maintenance of the correct pattern of expression of some homeotic genes and negatively regulates the Wingless pathway (Treisman et al., 1997b). Osa also interacts with Brahma and Moira, two other non-ARID SWI members, to regulate the cell cycle and negatively regulate neural development of bristle cells (Collins et al., 1999; Staehling-Hampton et al., 1999; Vazquez et al., 1999 Collins and Treisman, 2000; Brumby et al., 2002; Heitzler et al., 2003). Homologues of Osa have been found in both mice and humans and, like Osa, these proteins are expressed in a wide range of tissues and can interact with the human homologue of Brahma (Dallas et al., 2000; Nie et al., 2000; Kozmik et al., 2001; Hurlstone et al., 2002; Inoue et al., 2002).

MRF-1 and MRF-2 were identified by their ability to bind to sequences similar to those found in the promoter region of the human cytomegalovirus (HCMV) major immediate-early gene enhancer (Huang et al., 1996). Recently, MRF-2 has been implicated in smooth muscle differentiation (Watanabe et al., 2002). The murine homologue, Desrt (developmentally and sexually retarded with transient immune abnormalities) has also been identified (Lahoud et al., 2001; Ristevski et al., 2001). This protein has been found to be developmentally important, with homozygous mutant mice showing reduced viability (Lahoud et al., 2001; Ristevski et al., 2001).

### *1.2.3 The extended ARID group of proteins*

The extended ARID sub-family consists of proteins including *Drosophila melanogaster* Dri (Gregory et al., 1996), murine Bright (Herrscher et al., 1995), *C. elegans* CFI-1 (Shaham and Bargmann, 2002), *D. rerio* Dri1 and Dri2 (Kortschak R.D. 1999) human Bright Dead ringer Protein (BDP/DRIL2) (Numata et al., 1999) and DRIL1 (Kortschak et al., 1998). Dri, Bright, BDP and CFI-1 have all been shown to bind DNA in a site-specific manner (purineATTAA for Dri and purineATa/tAA for Bright). To date, they have been found only in the metazoan lineage (Herrscher et al., 1995; Gregory et al., 1996; Numata et

al., 1999; Kortschak et al., 2000; Shaham and Bargmann, 2002). Like the other subgroups of ARID proteins, the members of the extended ARID group have a wide variety of functions including developmental, cell cycle and tissue specific gene regulation (Herrscher et al., 1995; Gregory et al., 1996; Webb et al., 1998; Numata et al., 1999; Shandala et al., 1999; Iwaki et al., 2001; Peeper et al., 2002; Shaham and Bargmann, 2002; Shandala et al., 2002; Shandala et al., 2003; Haberman et al., 2003; Ma et al., 2003). Interestingly, the extended ARID subgroup shares another region of homology C-terminal to the eARID. This second region is referred to as the REKLES domain, named after the near conserved residues at the beginning of this domain (Herrscher et al., 1995; Kortschak et al., 2000). The REKLES domain in Bright has been shown to be important for self-association (Herrscher et al., 1995).

*1.2.3.1 Bright*

Bright binds to the nuclear matrix attachment region (MAR) flanking the intronic enhancer element (Eμ) and proximal to the promoter of the immunoglobulin heavy chain (IgH) gene. Bright activates transcription of the IgH gene in mature B cells (Herrscher et al., 1995). The MAR is known to alter chromatin structure and Bright has the ability to bend DNA on binding to the promotor region (Kas et al., 1993; Pemov et al., 1998; Stein et al., 1998; Kaplan et al., 2001). Yeast two-hybrid experiments have identified components of the promyelocytic leukemia (PML) nuclear bodies, Speckled Protein 100 (Sp100) and the lymphoid specific LYSp100B, that interact with Bright (Zong et al., 2000). The PML nuclear bodies are important for gene expression and it has been proposed that Bright allows components of the PML nuclear bodies access to the MAR to regulate gene expression (Webb, 2001).

*1.2.3.2 Bright Dead ringer Protein*

BDP, like Bright, can bind to the MAR *in vitro*. BDP has also been shown to interact with the Retinoblastoma protein via the ARID domain, and therefore is implicated in inhibiting cell proliferation (Numata et al., 1999).

*1.2.3.3 DRIL1/E2FBP1*

DRIL1, which is most similar to Bright binds to the E2F1 transcription factor and is also known as E2F Binding Protein 1 (E2FBP1). DRIL1 has been shown to overcome RAS-induced senescence by downregulating the Rb/E2F1 pathway (Peeper et al., 2002). Recently it has been demonstrated that DRIL1 is regulated by the binding of p53 to the second intron of DRIL1, resulting in the upregulation of DRIL1 when cells were exposed to UV damage (Peeper et al., 2002; Ma et al., 2003). Additionally it was found that the introduction of

DRIL1 cDNA to tumour cells results in less BrdU labelled cells, indicating that DRIL1 inhibits cell growth. This inhibition of cell growth was found to be dependent on p53 (Ma et al., 2003). Like Bright, DRIL1 has also been shown to bind to Speckled Protein 100 (Sp100) *in vitro* and *in vivo* and to UbcH9, the small ubiquitin-like modifier (SUMO-1), *in vitro*. Both Sp100 and UbcH9 are components of the PML-Nuclear Bodies (PML-NBs) (Gong et al., 1997; Seeler and Dejean, 1999; Maul et al., 2000; Negorev et al., 2001). It has been shown previously that p53 also interacts with PML-NBs (Ferbeyre et al., 2000). Unlike in the mouse where Bright and Sp100 co-localised within PML-NBs (Zong et al., 2000), in TIG-3 cells PML-NBs and DRIL1 did not co-localise. The forced co-localisation, by overexpressing DRIL1, results in the disintegration of the PML-NBs (Fukuyo et al., 2004). The overexpression of DRIL1 also results in the de-sumoylation of proteins such as Sp100 and p53, although DRIL1 has no homology to a SUMO-1 hydrolase or SUMO-1 ligase and therefore this effect is unlikely to be direct (Fukuyo et al., 2004). Deletion analysis revealed that the ARID domain was important for the disintegration of the PML-NBs (Fukuyo et al., 2004). The converse studies where DRIL1 was knocked down by siRNA designed to the mRNA of DRIL1, showed that a reduction in DRIL1 led to growth suppression of primary fibroblast cells due to an increase in expression of Sp100 and p53. In addition, the number and density of PML-NBs increased (Fukuyo et al., 2004). The molecular mechanisms of the action of DRIL1 in the PML-NBs and E2F1 pathways are yet to be elucidated.

#### *1.2.3.4 CFI-1*

The *C. elegans* protein CFI-1 is implicated in the differentiation of subtypes of neural cells in the hermaphrodite nervous system. CFI-1 is also expressed in a muscle-restricted pattern (Shaham and Bargmann, 2002).

## 1.3 ARID domain structure

The three dimensional structure of the ARID domain in Dri has been determined by NMR analysis (Iwahara and Clubb, 1999; Iwahara et al., 2002). The Dri ARID region consists of eight α helices and a short β-hairpin (Iwahara and Clubb, 1999; Iwahara et al., 2002) (Figure 1.1 A and B). Dri differs from the core ARID protein, MRF-2, by having two additional alpha helices (H1 and H8) and a β-hairpin at the position of the loop in MRF-2 (Zhu et al., 2001; Iwahara et al., 2002) (Figure 1.1). Interestingly part of the core ARID (H5-H7 in Dri) forms a helix-turn-helix (HTH) structure that contacts the major groove of DNA.

## Figure 1.1 The structure of the ARID domain in Dri

**(A)** Sequence alignment of the extended, N-terminal extended and core ARID proteins. The positions of the conserved helices are shown in red, the additional R1 and R8 helices represented in blue and the position of the helix-turn-helix (HTH region) is indicated in black. The conserved residues that contact the minor groove are indicated in green while the residues that contact the major groove of DNA are indicated in yellow. The B1 and B2 regions indicated in this diagram are also the positions of the more flexible loop structures found in MRF-2. The red stars indicate the sequences of Dri and MRF-2. Image reproduced from Iwahara *et al*, 2002.

**(B)** Ribbon structure of the Dri-ARID domain bound to DNA. The helix-turn-helix binds to the major groove of DNA while the H8 and B1 and B2 binds to the minor groove. Image reproduced from Iwahara *et al*, 2002.

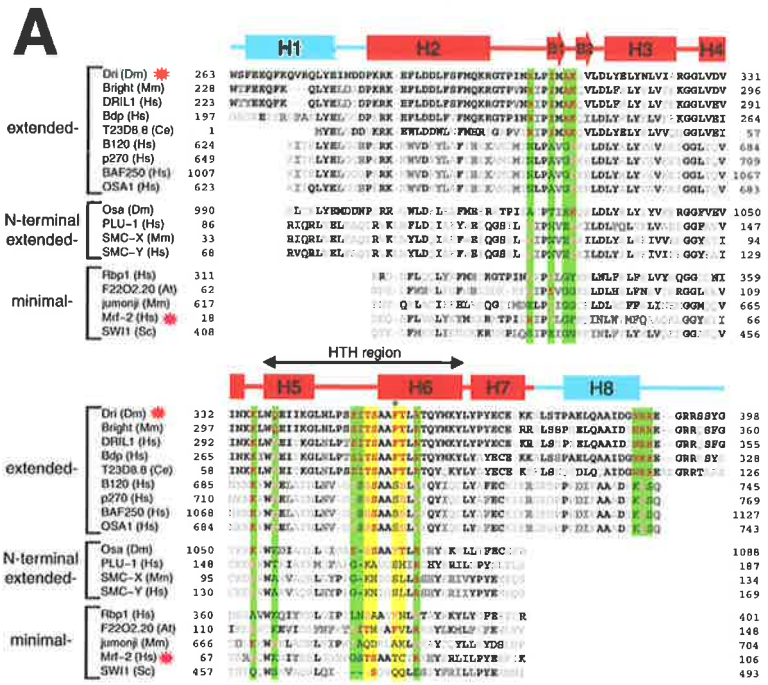
A
H1
H2
B1
B2
H3
H4
extended-
N-terminal extended-
minimal-
HTH region
H5
H6
H7
H8
B
Cyt17
Gua14
H4
H8
H3
H5
H7
H6
B1
B2
H2
H1
Phe265
Thy3
Ade28

The residues that are thought to provide AT specificity (TSXXF/T within the HTH) are conserved in MRF-2 and the extended ARID members, but not in other proteins containing a core ARID domain (Zhu et al., 2001; Iwahara et al., 2002) (Figure 1.1 A). The β-hairpin and loop structures in Dri and MRF-2, as well as the additional helix H8 in Dri, makes contact with the minor groove of DNA (Zhu et al., 2001; Iwahara et al., 2002) (Figure 1.1 B). In the presence of distamycin (which disrupts minor groove binding), the binding-affinity of Bright was reduced, indicating that interactions with the minor groove of DNA are important for stabilizing the interaction with DNA (Herrscher et al., 1995).

## 1.4 Embryonic expression of *dri* and the known target genes of Dri regulation

The embryonic expression pattern of *dri* has been extensively characterized (Gregory et al., 1996; Shandala et al., 2003). There is both a maternal and zygotic contribution in the developing *Drosophila* embryo. The maternally contributed *dri* transcript and protein are uniformly distributed, while zygotic *dri* expression is initially ubiquitous until gastrulation when expression is temporally and spatially restricted (Gregory et al., 1996). Following gastrulation, expression is refined to rings of cells around the foregut and midgut junction, the pharyngeal muscles, amnioserosa, the ring glands, clypeolabrum, salivary ducts, a distinct row of cells in the hindgut and several cells in each lobe of the brain (Gregory et al., 1996). It has recently been shown that *dri* is expressed in a subset of longitudinal glial cells in the developing central nervous system (CNS) and is important for the migration of those cells (Shandala et al., 2003). In the absence of *dri* a mild axonal fasciculation defect is observed, presumably as a result of the glial defects, as *dri* expression is not observed in neural cells that generate these axons (Shandala et al., 2003).

Dri has been shown to regulate the expression of embryonic genes such as *buttonhead*, *argos* (Shandala et al., 1999), *prospero* (*pros*), *locomotion defects* (*loco*) (Shandala et al., 2003), *zerknullt* (*zen*) (Valentine et al., 1998) and *huckebein* (*hkb*) (Hader et al., 2000). Of these, only *zen* and *hkb* transcription have been shown to be directly regulated by Dri. Dri has been demonstrated to form a multi-protein complex that represses these genes (Valentine et al., 1998; Hader et al., 2000). Dri and Cut (a homeobox domain protein) bind to similar sites within the ventral repression region (VRR) of *zen* and are both required for repression of *zen* expression on the ventral side of the developing embryo (Valentine et al., 1998). Interestingly, the loss of *dri* results in ventral activation of *zen*, indicating that Dri may play a role in inhibiting the intrinsic activation of Dorsal (a morphogen) (Valentine et al., 1998). Within the promoter region of *zen*, Dri and Dorsal binding sites are adjacent and *in*

*vitro* analysis revealed that both Dorsal and Dri interact with, and cooperatively recruit the repressor protein Groucho (Valentine et al., 1998). Analysis of the promotor region of *hkb* revealed that, similar to *zen*, both Dorsal and Dri binding sites are present and Groucho is recruited to repress expression on the ventral side of the embryo (Hader et al., 2000). However unlike *zen*, the binding sites are not adjacent to each other and the increased distance between the Dri and Dorsal binding sites suggests that Dorsal cannot be interacting with Groucho, as Dri has been shown to be necessary for Groucho recruitment (Hader et al., 2000). The authors suggest that at the *hkb* promotor region the activity of Groucho is to quench the Dorsal activation activity (Hader et al., 2000). This study also found that the Groucho-mediated repression can be overcome by receptor tyrosine kinase signalling via Torso, but it is unclear at this stage whether phosphorylation is interfering with Groucho activity or the ability of Dri to recruit Groucho (Hader et al., 2000). Surprisingly, and in contrast to the studies of regulatory DNA segments described above, *dri* mutant embryos do not exhibit dorsal defects that would be indicative of the loss of either *zen* or *hkb*. This indicates that *dri* is playing a redundant role in dorsal determination.

Dri appears to also be able to activate transcription. In *dri* mutant embryos the expression of *argos* (an inhibitor of the EGF receptor) is abolished in the terminal regions of the embryo, but expression continues in the cephalic furrow (Shandala et al., 1999). It is unclear at this stage whether this activation of *argos* by Dri is direct or indirect. Additionally, in *dri* mutant embryos *pros* and *loco* expression is lost in a subset of longitudinal glial cells, although direct regulation by Dri is yet to be demonstrated (Shandala et al., 2003).

In contrast to these embryonic studies, the role of *dri* later in development has not been extensively investigated. Initial characterisation of the expression pattern of *dri* during larval stages indicated that *dri* is expressed in the developing eye disc in a subset of photoreceptor cells (T. Shandala, personal communication). This thesis examines in detail the expression pattern and role of *dri* during eye development and in the adult eye. The cellular, molecular and genetic basis of eye development and function are discussed in the following sections.

## 1.5 Differentiation of the components of the adult eye

The *Drosophila* eye has been well characterised and consists of approximately eight hundred ommatidia, each of which comprise eight photoreceptor cells (R cells), four cone cells, eleven pigment cells (two primary, six secondary and three tertiary cells) and three bristle cells. The eight photoreceptor cells and cone cells differentiate during the third larval

instar stage, while the pigment and bristle cells differentiate during pupal stages. The secondary and tertiary pigment and bristle cells, known as interommatidial cells, form a hexagonal lattice structure that surrounds the R cells and the cone cells (reviewed by Wolff and Ready, 1993; and Freeman, 1997).

Differentiation of the adult eye begins during the third larval instar and is completed during the pupal stages. The site of initial differentiation coincides with the morphogenetic furrow, a morphological landmark, associated with organizer activity that progresses from posterior to anterior. Cells in the morphogenetic furrow arrest in G1 phase, the nuclei of these cells drop basally and the shape of the cells changes to create the morphogenetic furrow (Ready et al., 1976; Tomlinson, 1985) (Figure 1.2 A). Differentiation of the photoreceptor cells occurs posterior to this furrow (Tomlinson et al., 1987; Wolff and Ready, 1991). Movement of the morphogenetic furrow is dependent on Hedgehog, a secreted protein, which is expressed several rows behind the morphogenetic furrow. Hedgehog induces the progression of the morphogenetic furrow from posterior to anterior across the eye imaginal disc (Heberlein et al., 1993; Ma and Moses, 1995; Treisman and Heberlein, 1998).

Within the morphogenetic furrow, proneural clusters are established by the expression of *atonal* (Jarman et al., 1994; Jarman et al., 1995; Dokucu et al., 1996; Baker and Yu, 1997). The proneural cluster is further reduced to a single *atonal*-expressing cell, the presumptive R8, when the expression of *rough* and *E(Spl)* in the neighbouring cells downregulates *atonal* in those cells (Dokucu et al., 1996; Baker and Yu, 1997). In the presumptive R8 cell, *senseless* represses *rough* expression. In a *senseless* mutant, Rough is expressed in the presumptive R8 cell resulting in it adopting an R2 or R5 cell fate (Frankfort et al., 2001). It was initially believed that the R8 cell was required for the sequential recruitment of the other R cells, however in a *senseless* mutant R8 cells are not established but other R cells are still recruited (Frankfort et al., 2001).

Recruitment of the other photoreceptor cells occurs in a defined order (reviewed by Wolff and Ready, 1993). R2 and R5 are recruited first, followed by R3 and R4 and then R1 and R6, with R7 being the final photoreceptor cell recruited. Recruitment of the R1-R7 photoreceptor cells, but not R8, is dependent on the *Drosophila* EGF Receptor (DER) (Xu and Rubin, 1993; Freeman, 1996). The Notch pathway also plays a significant role in eye development (Brennan and Moses, 2000) but it is not discussed further here. As the R8, R2, R5, R3 and R4 cells differentiate, their nuclei move to the apical surface of the eye disc.

## Figure 1.2 The differentiation and components of the *Drosophila* eye

(**A**) A schematic diagram of a third larval instar eye disc. The nuclei of a subset of cells move to the basal surface of the eye disc forming the morphogenetic furrow, which moves from posterior to anterior across the eye disc. Directly after the morphogenetic furrow, R8 is differentiated and the R8 nucleus moves to the apical surface of the eye disc before being displaced by apical localisation of the nuclei of the R2 and R5 cells (one of which is shown here). In the more posterior ommatidia the R2 and R5 nuclei are displaced by the apical movement of the R3 and R4 nuclei (one of which is shown here). R3 and R4 nuclei are displaced by the apical movement of the R1 and R6 nuclei (one of which is shown here), which then become displaced by the apical movement of the R7 nucleus and, finally, by the cone cells.

Images reproduced from Wolff and Ready (1993).

(**B**) A schematic representation of an adult ommatidium. A longitudinal view of an ommatidium shows the position of all of the components of the eye. Rh: rhabdomere. PP, SP and TP: primary, secondary and tertiary pigment cells. CC: cone cells. L: lens, B: bristle cell, A: photoreceptor cell axon M: basal membrane. On the right hand side are cross sections at three positions along the apical-basal axis of the ommatidium. AC, PC, EQC and PCL referred to the position of the cone cells (AC: the anterior cone cell, PC: the posterior cone cell, EQC: the equatorial cone cell and PLC: the polar cone cell). The second cross section is a more apical section. The R7 rhabdomere (in green) is positioned between the R1 and R6 rhabdomeres (in pink). In the more basal section the smaller R8 rhabdomere (in pink) is observed between R1 and R2 (in pink) rhabdomeres.

Images reproduced from Dickson and Hafen (1993).

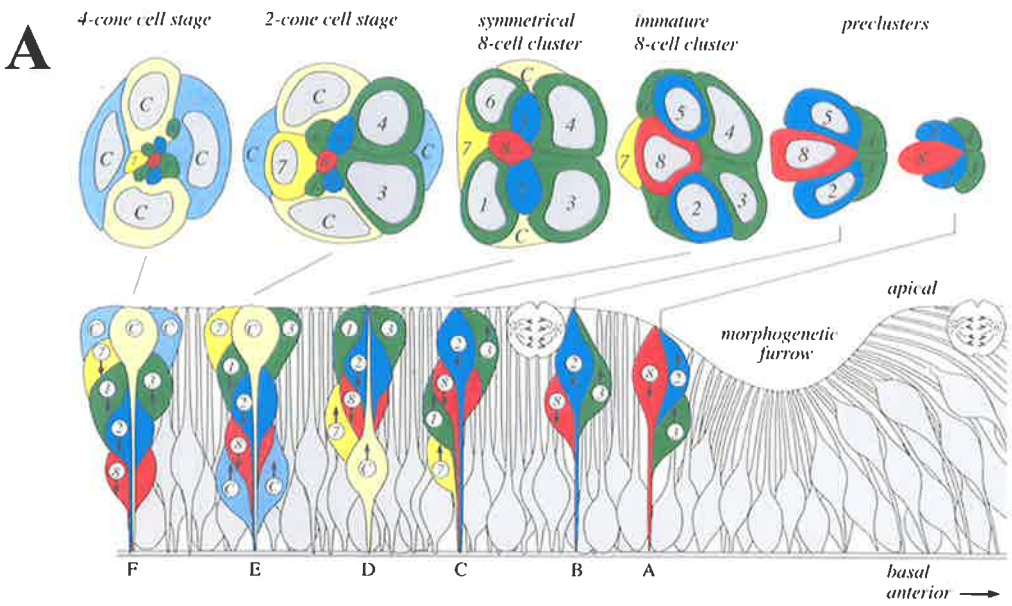
A
4-cone cell stage
2-cone cell stage
symmetrical 8-cell cluster
immature 8-cell cluster
preclusters
apical
morphogenetic furrow
F
E
D
C
B
A
basal anterior

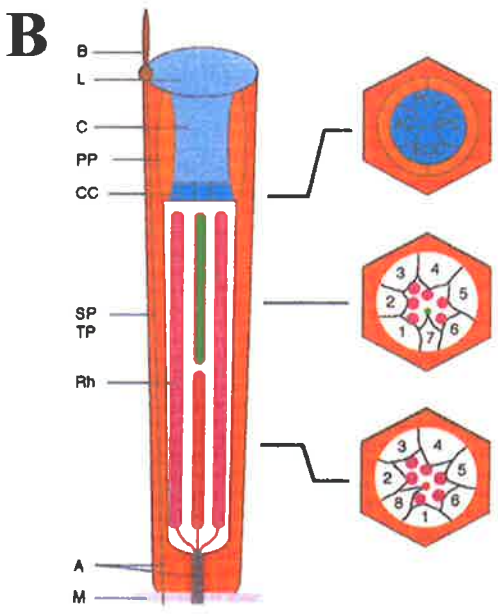
B
B
L
C
PP
CC
SP
TP
Rh
A
M

The nuclei move basally with the arrival at the apical surface of the nuclei of newly differentiating R1 and R6 cells. The nucleus of the R7 cell, the last of the R cells to differentiate, arrives apically as the R8, R2, R5, R3 and R4 nuclei move basally. Finally, the cone cells move apically while the nuclei of the R1, R6 and R7 cells move basally (Figure 1.2 A). Once the cone cells are at their final position they secrete the lens. The end result of this photoreceptor cell activity is a specific position for each photoreceptor cell within the ommatidium. Rhabdomeres of the R1, R2, R3, R4, R5 and R6 cells, the outer photoreceptor cells, extend the length of the ommatidium, while the R7 rhabdomere lies directly above the R8 cell (reviewed by Wolff and Ready, 1993) (Figure 1.2 B).

During pupal development the primary, secondary and tertiary pigment cells of the retina differentiate. These cells secrete pigment providing visual insulation for the R cells and giving the adult eye its colour. They also form a lattice around the R cells and cone cells (reviewed by Wolff and Ready, 1993). The total number of cells within the eye imaginal disc is greater than that required to form the ommatidia. Removal of the excess cells occurs at 42 hours after puparium formation, where all undifferentiated cells undergo apoptosis resulting in a hexagonal ommatidial lattice (reviewed by Dickson and Hafen, 1993). DER transmits a survival signal that regulates the expression of the pro-apoptotic gene *hid* (Kurada and White, 1998). The activity of DER in differentiated cells results in a decreased level of Hid, while undifferentiated cells have increased levels of Hid and undergo apoptosis (Kurada and White, 1998).

## 1.6 Axon connections between the developing eye and brain

During the late larval and early pupal stages of *Drosophila* development, axons from the newly differentiated photoreceptor cells are directed through the optic stalk to the optic lobe in the developing brain (reviewed by Meinertzhagen and Hanson, 1993). The axons from a single ommatidium cluster together to form an axon bundle, which assembles with other bundles at the posterior of the eye disc and moves through the optic stalk to the optic lobe (Figure 1.3 A and B). The assembly of the axon bundles at the posterior of the eye disc is dependent on retinal basal glia (RBG) cells (Rangarajan et al., 1999). The RBG cells originate in the optic stalk and migrate into the basal surface of the eye disc as the photoreceptor cells differentiate (Choi and Benzer, 1994). If the RBG cells are induced to migrate past the newly differentiated R cells, then the axons from these R cells will migrate anteriorly towards the morphogenetic furrow instead of posteriorly towards the optic stalk (Rangarajan et al., 1999; Hummel et al., 2002).

## Figure 1.3 The termination of the R cell axons in the optic lobe

**(A)** A diagrammatic representation of the axons of one third larval instar ommatidium showing that the R1-R6 axons terminate in the lamina while the R8 axon terminates in the medulla.

**(B)** mAb 24B10 antibody staining of a wild type eye-brain complex showing the photoreceptor axons innervating the brain. os: optic stalk; la: lamina and me: medulla. (Image reproduced from Poeck et al, 2001).

**(C)** A diagrammatic representation of the position of the monopolar neurons and the glial cells in the larval optic lobe. sg: satellite glial cells; LF: lamina furrow; L1-L5: monopolar neurons; eg: epithelial glial cells; mg: marginal glial cells; meg: medulla glial cells. R1-R6 axons terminate between the eg and the mg. The lamina glial cells migrate from the glial precursor cell area (GPC) to the lamina plexus during the third larval instar stage. (Image reproduced from Poeck et al, 2001).

**(D)** Horizontal section (prepared by the author) through a wild type adult head stained with mAb 22C10, which stains all axons. The eye is to the left hand side. la: lamina, me: medulla, lo: lobula. The arrowhead points to the M3 layer of the medulla where the R8 axons terminate. The arrow points to the M6 layer where the R7 axons terminate.

**(E)** A schematic diagram of neural superposition of R1-R6 axons. Axons from one ommatidium synapse with axons from neighbouring ommatidia (see section 1.6.2.3). (Image reproduced from Clandinin et al, 2001).

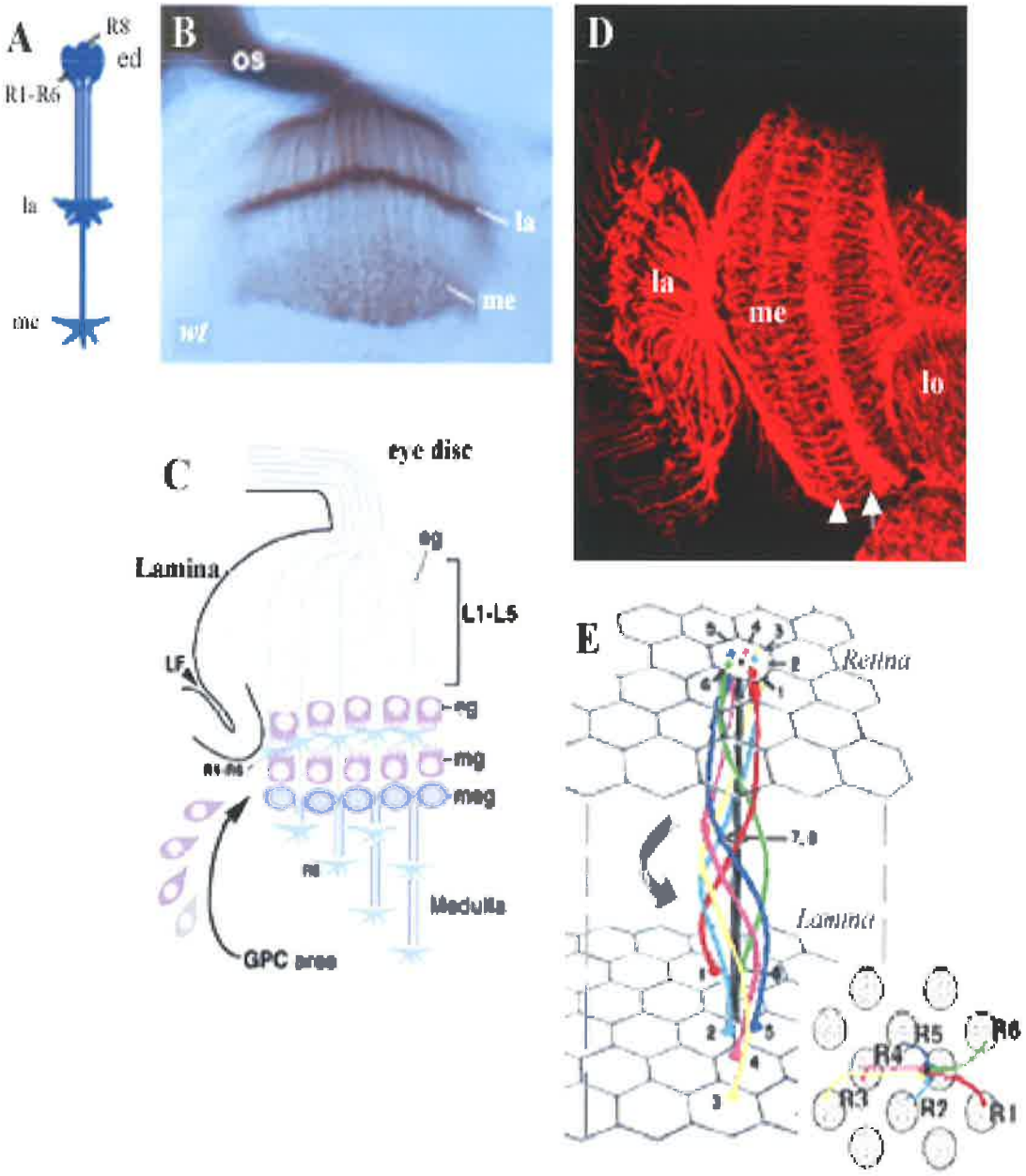
A
R8
ed
R1-R6
la
me
B
OS
la
me
wz
D
la
me
lo
C
eye disc
Lamina
eg
L1-L5
LF
eg
mg
meg
R8
Medulla
GPC area
E
Retina
7, 8
Lamina
R5
R6
R4
R3
R2
R1

Each of the R cell axons migrates and terminates in a precise location within the optic lobe. R8 axons are the first to extend, moving through the optic stalk to the optic lobe and terminating in the second ganglion, the medulla. These are followed by R1-R6 axons. Each bundle of R1-R6 axons rotates 180 degrees from its initial position within the ommatidium before terminating in the lamina between two layers of glial cells (epithelial and the marginal glial cells) to form the lamina plexus (Figure 1.3 A and B) (reviewed by Meinertzhagen and Hanson, 1993). The lamina (the structure closest to the eye disc) consists of cartridges containing glial cells and monopolar neurons (L1 to L5), which surround the photoreceptor cell axons (Figure 1.3 C). The differentiation of the monopolar neurons is dependent on innervation by axons from the eye (Salecker et al., 1998). The mature monopolar neurons respond to light impulses by sending a signal into the medulla where it is be processed (reviewed by Meinertzhagen and Hanson, 1993). The R7 axons follow R1 to R6 axons during pupal stages but instead of terminating with the R1-R6 axons in the lamina they continue and terminate in the second ganglion of the optic lobe, the medulla (reviewed by Meinertzhagen and Hanson, 1993). During later pupal stages the R7 and R8 axons separate into two different layers of the medulla. R8 axons terminate in the M3 layer (closest to the lamina) while R7 axons terminate in the M6 layer (Fischbach and Dittrich, 1989) (Figure 1.3 D).

### *1.6.1 R1-R6 axons terminate in the lamina*

R1-R6 axons are involved in three distinct behaviours when they innervate the optic lobe. The axons recognise a signal in the lamina that causes the expansion of the growth cones and thus termination of these axons. Secondly, the innervation of R1-R6 axons causes the differentiation of the neural cells in the lamina, and finally, during pupal stages the R1-R6 axons undergo a process known as neural superposition, where the axons from one ommatidium synapse with axons from neighbouring ommatidia.

#### *1.6.1.1 R1-R6 axon termination*

Glial cells play a vital role in the targeting of R1-R6 axons. There are three types of lamina glial cells, the epithelial, marginal and medulla glial cells, which surround the R1-R6 axons and neurons in the lamina cartridge (Figure 1.3 C). These glial cells migrate from the glial precursor cell (GPC) area to the lamina plexus (Perez and Steller, 1996; Huang et al., 1998) where they are proposed to produce a signal that terminates the growth cones of R1-R6 axons (Poeck et al., 2001). Poeck and colleagues (2001) showed that in *nonstop* (*not*) mutant animals, the R1-R6 axons pass through to the medulla. Nonstop encodes an ubiquitin specific protease. In a *not* mosaic animal the epithelial, marginal and medulla glial cells were inhibited from migrating from the GPC area to the lamina plexus.

Differentiation of the glial cells was not affected as the number of glial cells increased in the GPC while the number of glial cells at the lamina plexus had decreased in the *not* mutant animal. Furthermore, late expressing markers were not affected. NOT was expressed in the lamina glial cells and the optic lobe. Therefore, these results suggested that a signal for termination of the R1-R6 axons in the lamina originates from the lamina glial cells (Poeck et al., 2001), although the identity of this signal is unknown. The destruction of proteins by ubiquitination within the lamina glial cells must be required for the migration of these cells (Poeck et al., 2001). Interestingly, another protein found to be required for glial cell migration was JAB1/CSN5 (Suh et al., 2002). Members of this family have been implicated in protein degradation and signalling pathways (Lyapina et al., 2001; Schwechheimer and Deng, 2001; Zhou et al., 2003). Like *not*, JAB1/CSN5 is required for migration of the epithelial and marginal glial cells from the GPC to the lamina plexus and in the absence of these glial cells, the R1-R6 axons fail to terminate in the lamina (Suh et al., 2002). Interestingly, medulla glial cells are not affected. However, JAB1/CSN5 is expressed in the lamina plexus, the medulla neuropil and the cytoplasm of the R cells, but not in the glial cells. Mosaic analysis showed that loss of *jab1/csn5* in the eye also results in the lamina glial cells not migrating. Together these observations suggest that a signal produced from the R cell axons promotes the migration of lamina glial cells to the lamina plexus (Suh et al., 2002). Despite the identification of some of the proteins required for R1-R6 axon targeting, the protein required to recognize the signal from the glial cells remains unknown.

Brakeless was the first nuclear factor to be reported to play a role in axon guidance rather than in the differentiation of the eye (Rao et al., 2000; Senti et al., 2000). The Brakeless protein is expressed in all cells anterior to the morphogenetic furrow and in a subset of ommatidial cells posterior to the furrow, however it is unclear at this stage if Brakeless is expressed in all R cells or a subset of them (Rao et al., 2000; Senti et al., 2000). In *bks* mosaic eyes, most of the R1 to R6 axons do not terminate in the lamina but pass through to the medulla. A recent paper by Kaminker and colleagues (2002) showed that Bks negatively regulates *runt* (*run*) expression in R2 and R5 cells. Run is a transcription factor expressed exclusively in R7 and R8 cells (Kania et al., 1990; Canon and Banerjee, 2000). In a *bks* mosaic animal Run is inappropriately expressed in R2 and R5 cells. Interestingly, the over-expression of Run in R8, R2 and R5 cells, results in the other R axons that normally terminate in the lamina, passing through to the medulla (Kaminker et al., 2002). This result suggests that R2 and R5 axons are required for the correct pathfinding of the R cell axons that extend later and terminate in the lamina (Kaminker et al., 2002). The downstream proteins regulated by Run are unknown at this time.

Some of the proteins required for the adhesion of R1-R6 axons in the lamina have been identified. The Receptor Tyrosine Phosphatases, LAR and PTP69D are required for the R1-R6 axons to terminate in the lamina (Garrity et al., 1999; Newsome et al., 2000a). PTP69D is a multi-domain protein that consists of two protein tyrosine phosphatase (PTP) domains, an extracellular component containing Ig domains, fibronectin type III repeats (FNIII), and a membrane-proximal CAM-like region. The introduction of deletions or point mutations in each PTP domain rescues the R1-R6 axon phenotype, but mutations in both domains do not, suggesting that the PTP domains can compensate for each other (Garrity et al., 1999). Deletion studies of the extracellular components of PTP69D revealed that the FNIII domains are required for R1-R6 axon targeting (Garrity et al., 1999). As mentioned above, LAR is also required for R1-R6 axons to stop in the lamina, as some R2 and R5 axons in a *LAR* mosaic eye-brain complex pass through to the medulla (Clandinin et al., 2001).

One protein that responds to tyrosine signalling is the adaptor protein Dreadlocks (Dock) (Garrity et al., 1996). Dock contains three src homology 3 (SH3) domains and one SH2 domain and is found in R cell growth cones and the medulla neuropil. Loss of Dock results in R1-R6 axons terminating in the medulla (Garrity et al., 1996). Studies in which point mutations were introduced into the SH3 domains showed that the SH3-2 domain is required for correct R-cell projection, but that the other domains are not (Rao and Zipursky, 1998). Pak (p-21-activated kinase) is a serine/threonine kinase (Ste20) family member that interacts with this SH3-2 domain of Dock in a yeast two hybrid assay, as well as *in vivo* (Hing et al., 1999). The loss of Pak results in the disruption of the projections from the eye disc to the optic lobe but not the differentiation of the R cells or target area of the lamina (Hing et al., 1999). The overexpression of Pak in a *dock* mutant rescues the *dock* phenotype, suggesting that Pak is downstream of Dock. The Pak protein contains an N-terminal regulatory region that inhibits the C-terminal kinase domain (Frost et al., 1996; Zhao et al., 1998). The regulatory region contains a PXXP domain that interacts with Dock (Hing et al., 1999), a CRIB (Cdc42/Rac Interaction Binding) domain, and a proline rich region that binds PIX, a guanine nucleotide exchange factor (Manser et al, 1998). All three of these domains are required for Pak activity within the R-cells (Hing et al., 1999).

Another Ste20 kinase, but of a different subfamily than Pak, is Misshapen (Msn). Msn also interacts with the SH3-1 and SH3-2 domains of Dock (Su et al., 2000). Misshapen differs in structure from Pak with an N-terminal kinase domain that contains the PXXP domain but no PIX domain (Su et al., 1998). Like Pak, Dock interacts with the PXXP domain of Msn in a yeast two-hybrid assay and genetic analysis showed that *msn* was downstream of

*dock* (Ruan et al., 1999; Su et al., 2000). Msn is required for R1-R6 axons to terminate in the lamina, and is found in the R cell axons and the medulla neuropil (Ruan et al., 1999). Interestingly, the over-expression of Msn results in the early termination of the R cell axons, suggesting that Msn responds, via Dock, to the stop signal in the lamina that terminates the R1-R6 axons (Ruan et al., 1999). Reducing one copy of *bifocal* (*bif*), a cytoskeletal regulator, suppresses the gain-of-function Msn phenotype (Ruan et al., 2002). Bif co-localises with F-actin (Bahri et al., 1997) and in a *bif* mutant F-actin is disorganized (Ruan et al., 2002). Bif is expressed in the R cell axons and loss of the protein results in R1-R6 axons passing through to the medulla. Bif interacts with the kinase domain of Msn and becomes phosphorylated *in vitro* (Ruan et al., 2002). Transfection assays of Cos cells showed that Msn causes the redistribution of Bif and F-actin and reduces the number and length of filopodia structures that were observed, compared to when Bif alone was transfected (Ruan et al., 2002). The authors propose that unidentified proteins upstream of Dock recognize a signal from the glial cells in the lamina, resulting in Dock and Msn interacting and Bif being phosphorylated. The F-actin would therefore be redistributed and less filopodia occur, leading to the termination of the growth cones of R1-R6 axons (Ruan et al., 2002). However, in a Dock mutant not all axons pass through to the medulla suggesting that more than one pathway is involved in the termination of R1-R6 axons.

*1.6.1.2 Neuron differentiation within the lamina*

As the photoreceptor axons penetrate the lamina they promote the G1-arrested lamina precursor cells (LPC) to undergo their final synthesis phase and differentiate into neuronal (L1-L5) cells (Huang et al., 1998). This establishes the lamina cartridge, where the ommatidial axons and the cartridge units interact (Figure 1.3 B) (Huang et al., 1998). The secreted signalling molecule, Hedgehog (Hh), causes the LPCs to undergo the final cell cycle (Huang et al., 1998). While Hh regulates cell cycle progression, it is the EGFR pathway that causes the differentiation of the neurons (Huang et al., 1998). The ligand, Spitz, is transported down the R cell axons to the lamina, where it is secreted and induces the EGF receptor pathway, which in turn activates *argos* expression, resulting in the differentiation of five monopolar neurons (Huang et al., 1998). Although the lamina neurons are required for vision in adult flies, they are not required for the termination of the R1-R6 growth cones. Poeck and colleagues (2001) showed that in a *hh* allele that specifically affects the visual system, the lamina neurons are not formed but the R1-R6 axons terminate in the lamina (Poeck et al., 2001).

*1.6.1.3 Neural superposition*

During pupal stages the axons in the brain undergo further organisation into the structures that are required in the adult visual system. The lamina undergoes a phenomenon known as neural superposition where the ommatidial bundles defasciculate and migrate to their neighbouring synaptic partners (reviewed by Meinertzhagen and Hanson, 1993). There are two features of neural superposition, the R axons project in a particular pattern relative to the other axons from the same ommatidium (Figure 1.3 E) and the projection is oriented towards the dorsoventral axis of the eye with R3 axons always moving towards the equator (Figure 1.3 E) (reviewed by Meinertzhagen and Hanson, 1993; Clandinin and Zipursky, 2000). Clandinin and Zipursky (2000) have established, by analysing mutants that alter the cell fate of the R cells, that R3 and R4 axons are required for the correct targeting of the remaining axons within the lamina and R1 and R6 axons are required for the correct targeting of R2 and R5 but not R3 and R4 axons (Clandinin and Zipursky, 2000). Analysing mutants that have an altered orientation of the R cells within the ommatidium has shown that the R3 axons rotate 180 degrees to the position of the R3 ommatidium. In mutant animals where the mis-orientation of the ommatidium is severe, such as in *frizzled* mutants, where the R cells are mis-orientated by 180 degrees, the R3 axon was also mis-orientated by 180 degrees (Clandinin and Zipursky, 2000). In *nemo* mutants in which the R cells are mis-orientated by 45 degrees, the axons in the lamina defasciculate and project normally (Clandinin and Zipursky, 2000). The loss of cell surface proteins such as N-Cadherin (Lee et al., 2001), Flamingo (a protocadherin) (Lee et al., 2003b) and LAR (Clandinin et al., 2001) all disrupt this phenomenon and therefore are important for neural superposition of the R axons.

*1.6.2 R7 and R8 axons terminate in the medulla*

Unlike the R1-R6 axons, R7 and R8 axons terminate in a different layer of the adult optic lobe. R8 axons terminate in the M3 layer of the medulla, the layer closest to the lamina, while R7 axons terminate in the M6 layer (Figure 1.3 D). Extensive studies have been undertaken to identify proteins that are required in these axons for them to terminate in a different layer. Interestingly many of the proteins required for the correct targeting of the R1-R6 axons are also required for R7 and R8 axon targeting.

*Drosophila* LAR, a receptor tyrosine phosphatase, is required for the correct targeting of R7 axons to the medulla. In *LAR* mosaic eye-brain complexes the R7 axons initially target to the correct layer of the medulla during pupal stages, but shortly after retract to the R8 layer. This phenotype was found to persist into adulthood (Clandinin et al., 2001; Maurel-Zaffran et al., 2001). Another receptor tyrosine phosphatase, PTP69D, which is required for

the correct targeting of R1-R6 axons, is also required for R7 axon targeting (Newsome et al, 2000a). The similarity in phenotype between LAR and PTP69D led Maurel-Zaffran and colleagues (2001) to investigate whether these two proteins were involved in activating the same signalling pathway and found the over-expression of LAR in all R cells could compensate for the loss of PTP69D but the opposite was not true (Maurel-Zaffran et al., 2001). Domain swapping experiments revealed that the extracellular component of the LAR protein was required for the correct targeting of R7 axons in a *LAR* mosaic animal, although more R7 axons were correctly targeted if the PTP69D intracellular domain was present than if no intracellular domains were present (Maurel-Zaffran et al., 2001). Furthermore, the intracellular domains of PTP69D fused to the extracellular component of LAR restored the correct targeting of R7 in *PTP69D* mosaic retinas. Interestingly, the rescue of LAR specifically in R8 cells partially rescues the R7 phenotype indicating that there is interaction between R8 and R7 axons. Maurel-Zaffran et al (2001) then investigated the potential signalling pathways involved with LAR and PTP69D, it had been previously established in motor axon guidance (Wills et al., 1999) that Enabled and Abl interact with the intracellular domain of both LAR and PTP69D. Dosage sensitive studies that scored the number of R7 axons targeted correctly in *LAR* mosaic eyes revealed that the loss of one copy of *enabled* but not *abl*, results in a more severe phenotype than the *LAR* mosaic alone. Furthermore, the over-expression of Ena rescues the *LAR* mosaic phenotype (Maurel-Zaffran et al., 2001), suggesting that Ena can interact with LAR. Likewise, the loss of *trio* (a guanine nucleotide exchange factor) also enhanced the *LAR* phenotype and overexpression of Trio rescued it, suggesting that Trio is also involved in the signal transduction pathway of LAR (Maurel-Zaffran et al., 2001). N-Cadherin and LAR have a similar phenotype in the visual system and may act together in targeting R7 axons (Lee et al., 2001). These two proteins are known to interact in other systems (Kypta et al., 1996; Brady-Kalnay et al., 1998) but this hypothesis has not been investigated as yet in the *Drosophila* visual system.

*trio* also genetically interacts with *dock* and *pak* (Newsome et al., 2000b). The *trio* mosaic phenotype is interesting in that a subset of axons bypass the medulla completely and misroute between the medulla and the underlying lobula (Newsome et al., 2000b). The Trio protein consists of an N-terminal domain, Spectrin repeats, two Guanine nucleotide exchange factor (GEF) domains, two SH3 domains and Ig and kinase domains. It is found uniformly distributed in the R-cell axon (Newsome et al., 2000b). Mutation studies within the Trio protein revealed that the GEF1 and the N-terminal domain show the same phenotype as a *trio* mosaic suggesting that these two domains are required for Trio function. Over-expression of the GEF1 domain results in a gain-of-function phenotype, where almost no axons entered the

optic lobe. Interestingly adding a myristylation signal to the GEF1 domain, which results in its attachment it to the membrane, enhanced this phenotype (Newsome et al., 2000b). Therefore, the intracellular regulation of Trio is vital for the integrity of the axons (Newsome et al., 2000b). The GEF activity of Trio could activate three Rho-GTPases, Rac1, Rac2 and Mtl. The authors showed that Pak could bind to the activated (GTP-bound) form of Rac, suggesting a model in which Trio activates Rac, which then binds to Pak and alters the cytoskeleton of the axons (Newsome et al., 2000b). This model is supported by genetic interactions between *pak*, *dock* and *trio*. The downstream targets of Pak are unknown at this time.

Recently it has been found that the insulin-like receptor (DInR) interacts with Dock in a yeast-two hybrid assay and *in vivo* (Song et al., 2003). In fact, the autophosphorylation of a tyrosine residue in DInR was required for Dock interaction in yeast (Song et al, 2003). DInR is found in the R cell axons and the target regions of the brain. Dock is an SH2-SH3 domain protein whose role in the correct targeting of the axons is well established (Garrity et al., 1996). In *dinr* mosaic retina, the R1-R6 axons fail to terminate in the lamina and the R8 axons showed a blunt-end morphology. This suggests that DInR is required for correct targeting of the axons by recruiting a downstream pathway via Dock following DInR autophosphorylation (Song et al., 2003).

As described above, many of the proteins that are required for R7 and R8 targeting are also required for R1-R6 targeting. The reasons why the R cell axons terminate in different layers of the optic lobe are yet to be elucidated.

### *1.6.3 Genetic Screens undertaken to identify proteins required for the correct targeting of R axons*

To identify genes whose protein products are important in the guidance and attachment of the visual axons, two independent genetic screens have recently been carried out (Newsome et al., 2000a; Clandinin et al., 2001; Lee et al., 2001). Both screens utilised EMS to induce mutations and mitotic clones to generate mutant eye cells, followed by either immunohistochemical analysis or behavioural tests to identify genes required for normal eye-brain wiring (Newsome et al., 2000a; Clandinin et al., 2001; Lee et al., 2001).

#### *1.6.3.1 The immunohistochemical screen*

The screen by Newsome and colleagues (2000) aimed to identify genes involved specifically in axon guidance and attachment of those axons to the correct layer during

development. Many of the genes required for axon guidance in the visual system may play earlier roles during embryogenesis. Thus mutations in such genes may be lethal. To overcome this problem Newsome and colleagues designed a novel system that involved creating somatic clones specifically in the developing eye that spanned the entire eye. Specifically, an enhancer region of a gene expressed at the outset of eye development, *eyeless*, was utilised to drive the yeast recombination gene, FLP, during embryogenesis in cells that will become the eye (Hauck et al., 1999). The FLP protein creates double stranded DNA breaks at specific sites known as FRT sites (Brand and Perrimon, 1993). One FRT chromosome carried EMS-induced mutations and the other FRT chromosome had a recessive cell lethal. In the presence of FLP, recombination can occur between the non-sister chromatids of the two FRT chromosomes which, when followed by mitosis, can produce one cell homozygous for the recessive lethal allele, which dies, and one cell homozygous for the mutagenised chromosome. Repeated rounds of mitotic recombination and mitosis result in the majority of the cells of the eye being homozygous for the mutagenised chromosome (Newsome et al., 2000a). Newsome and colleagues (2000) induced mutations in animals by EMS and used mass immunohistochemical staining with the antibody mAB 24b10, which stains all R cell axons, to detect axon guidance and attachment phenotypes. This antibody identifies most axons that enter the brain during the third larval instar stage (Figure 1.3 A and B). The mutant alleles responsible for the phenotypes were mapped and the gene characterized. Amongst the genes identified were those encoding *Drosophila* LAR, Trio, PTP69D, Flamingo and Brakeless (Newsome et al., 2000a; Newsome et al., 2000b; Senti et al., 2000; Maurel-Zaffran et al., 2001; Senti et al., 2003).

*1.6.3.2 The behavioural screen*

Blindness will result if axons do not target or attach to the correct layer during the third larval instar and pupal stages, or if the proteins required for visualisation of different wavelengths in the adult are not produced. To identify genes that are responsible for blindness, flies carrying mutant eyes generated by an approach similar to that described in the previous section underwent a series of behavioural tests (Gerresheim, 1988; Clandinin and Zipursky, 2000; Lee et al., 2001). An optomotor response test was undertaken to identify blind flies that no longer responded to white light. This optomotor response test involved placing adult mutant flies in a tube with a bar of light that moved. Wild type flies move in the opposite direction to the movement of the bar of light. However, flies with mutations in genes required for correct targeting and adhesion of the R1-R6 axons or visual transduction move randomly in the tube (Buchner et al., 1987; Clandinin and Zipursky, 2000). These mutant animals are then bred and the mutations mapped to identify the genes involved in these

pathways. Other behavioural tests were undertaken that allowed the identification of genes required for visualization of ultra violet (UV) light and green light. UV light is visualised by the R7 cell whose axons are targeted to the M6 layer of the medulla. Flies were placed in a T-maze with UV light illumination on one arm and green light on the other. Flies with mutations within the R7 axon or visual transduction pathway moved towards the green light, whereas wild type flies move towards the UV light (Gerresheim, 1988; Clandinin and Zipursky, 2000; Lee et al., 2001). This approach has identified genes encoding proteins such as PTP69D, LAR, N-cadherin, Flamingo, Nonstop, JAB1/CSN5 and Brakeless as being important for the correct targeting and attachment of the R cell axons (Garrity et al., 1999; Rao et al., 2000; Clandinin et al., 2001; Poeck et al., 2001; Lee et al., 2001; Suh et al., 2002; Lee et al., 2003a).

## 1.7 Visual transduction

The development of photoreceptor cells occurs in two stages. R cells differentiate during the third larval instar and during pupal development, while the expression of rhodopsins begins at late pupal stages and continues into adulthood. In the *Drosophila* eye, light is detected by G-protein coupled receptors of the Rhodopsin family. The opsin part of the receptor is a seven trans-membrane domain protein. Rhodopsins are found in the microvilli of the rhabdomere and play an essential role in both phototransduction and the survival of the retina (see section 1.7.2 and 1.7.4) (Scavarda et al., 1983; Leonard et al., 1992; Kumar and Ready, 1995a; Kumar and Ready, 1995b; O'Tousa et al., 1995). There are seven rhodopsins in *Drosophila*: six have been characterised and the seventh, Rh7, has been identified as a possible rhodopsin by sequence similarity to other rhodopsins (Papatsenko et al., 2001). The characterised rhodopsins, R1, R2, R3, R4, R5 and R6, are expressed in a non-overlapping pattern. The Rhodopsin1 (Rh1) protein product of the *neither inactivation nor afterpotential E,* (*ninaE*) gene is expressed in the outer photoreceptor cells, R1 to R6, and is involved in sensing blue light (Scavarda et al., 1983; Zuker et al., 1985a; Feiler et al., 1988; OTousa et al., 1989). Rh2 is expressed in the ocellus and detects violet light (Cowman et al., 1986; Feiler et al., 1988; Pollock and Benzer, 1988a). Rh3 and Rh4 are expressed in the inner photoreceptor cell, R7, which is responsible for the visualisation of UV light (Fryxell and Meyerowitz, 1987; Montell et al., 1987; Zuker et al., 1987; Feiler et al., 1992). Interestingly, Rh3 is expressed in approximately 30 percent of R7s with Rh4 being expressed in the remaining cells (Chou et al., 1996). Rh5 and Rh6 are expressed in R8, the other type of inner photoreceptor cell, and are involved in detecting blue and green light respectively, with the majority of the R8s expressing Rh6 (approximately 70 percent) (Huber et al., 1997; Salcedo et al., 1999). The expression of the inner R cell rhodopsins is coordinated within each

ommatidium (discussed in section 1.7.1.2). Approximately 30 percent of ommatidia, referred to as pale ommatidia, express Rh3 in the R7 cell and Rh5 in the R8 cell. The majority of the remaining ommatidia, termed yellow ommatidia, express Rh4 in the R7 cell and Rh6 in the R8 cell (Chou et al., 1996; Papatsenko et al., 1997; Chou et al., 1999). A small proportion of ommatidia at the dorsal rim area express Rh3 in both R7 and R8 cells (Fortini and Rubin, 1990).

### *1.7.1 Regulation of the rhodopsin genes*

Studies of the regulation of the rhodopsin gene family have revealed that all rhodopsins have two conserved *cis*-regulatory regions that are necessary for expression of the rhodopsins. The first element is the TATA box and the second region is known as the Rhodopsin Conserved Sequence 1 (RCS1) (Mismer and Rubin, 1989; Fortini and Rubin, 1990). Swapping the RCS1 sequences of different rhodopsin genes revealed that although RCS1 is important for *rhodopsin* expression within the eye, it is not responsible for photoreceptor cell type-specific expression (Mismer et al., 1988; Papatsenko et al., 2001). Comparisons of the RCS1 sequences within the known arthropod rhodopsins revealed a similarity to the P3 paired-class homeodomain binding sites that can bind Pax6 proteins (Sheng et al., 1997). In *Drosophila* the orthologues of the Pax6 proteins are *eyeless (ey)*, *twin of eyeless (toy)* and a related gene known as *eyes gone* (*eyg*). The *rh3*, *rh5* and *rh6* RCS1 sequences are significantly different from *rh1* and *rh4*, but similar to each other and genetic and molecular analyses have shown that the Pax6 homeodomain binds to the *ninaE* promotor region (Sheng et al., 1997; Papatsenko et al., 2001). However, experiments have established that Ey is not responsible for Rh1 expression (Punzo et al., 2001). At present it is unknown which of the remaining Pax6 genes are involved in *rhodopsin* expression. The RCS1 in *rh3*, *rh5* and *rh6* may therefore bind another transcription factor, perhaps one of the $K_{50}$ homeodomain proteins, which bind to similar sequences (Papatsenko et al., 2001).

It is interesting to note that there is very little similarity between the *rhodopsin* promotor regions outside the RCS1 even between Rh3 and Rh4, which are both expressed in R7 cells (Papatsenko et al., 2001). This has led to the hypothesis that the proximal region of the promotor is important for the restriction of rhodopsin expression to photoreceptor cells (Sheng et al., 1997) while the distal part of the promotor, which contains the Rh-specific sequence (also known as the Rhodopsin upstream sequences, RUS) that are unique to each of the rhodopsins (Fortini and Rubin, 1990; Papatsenko et al., 1997), are responsible for the photoreceptor cell type-specific expression (Fortini and Rubin, 1990; Papatsenko et al., 1997).

*1.7.1.1 Regulation of rhodopsin in R1 to R6*

The promotor region of *ninaE* has been extensively studied. Using serial dissection of the promoter region upstream of reporter genes, it has been established that approximately the first three hundred base pairs were required to produce the restricted expression of Rh1 (Mismer et al., 1988). Further dissection of this three hundred base pair region revealed the presence of three enhancer elements responsible for this expression. The enhancer elements are at positions -215, -162 and -120 base pairs upstream of the start of translation (Mismer et al., 1988). Glass was identified as the transcription factor that binds to the enhancer element at position -215 within the *ninaE* promotor region (Figure 1.4) (Moses and Rubin, 1991). Mutations in the Glass-binding site result in the loss of expression of the reporter gene, indicating that Glass is essential for the expression of Rh1 (Moses and Rubin, 1991). To date the factor that binds to the other enhancer region at position -142 has not been identified. The first 250 base pairs of the *ninaE* promotor region do not restore the wild type level of expression and it was subsequently discovered that there was another enhancer between positions -502 and -250 (Mismer and Rubin, 1989). However the transcription factor that binds to this region is yet to be discovered.

Deletion of the $K_{50}$ homeodomain binding sites within the *rh6* promotor region results in the partial extension of expression of Rh6 into R1-R6 cells (Tahayato et al., 2003). It has been established that Orthodenticle (Otd) binds to the *rh6* promotor region containing the $K_{50}$ sites and therefore this protein is required to inhibit *rh6* expression within R1-R6 cells (Tahayato et al., 2003) (Figure 1.4).

*1.7.1.2 Regulation of rhodopsin expression in R7 and R8*

The expression pattern of the rhodopsins within the inner photoreceptor cells is complicated by the coordinated expression of the rhodopsins within an ommatidium.

The loss of R8 cells but not R7 in the ommatidium does not alter the expression of either Rh3 or Rh4 in R7 cells, which suggests that the expression of these rhodopsins is not dependent on R8 cells (Chou et al., 1999). However, the loss of R7 cells results in the loss of Rh5 expression in R8 cells and the derepression of Rh6 suggesting that R7 cells are required for the expression of Rh5 and Rh6 is the default state for R8 cells (Chou et al., 1999).

Discovery of a rhodopsin upstream sequence (RUS) in the R8-specific genes, *rh5* and *rh6*, led to the identification of the R7 protein, Prospero, as a repressor of these rhodopsins in

R7 cells (Cook et al., 2003) (Figure 1.4). Sequence analysis has revealed that there are $K_{50}$ binding sites within the *rh3* and *rh5* promotor regions but not *rh4* and that Otd binds to these sites and enhances expression of *rh3* and *rh5* in pale ommatidia (Tahayato et al., 2003). However the factors that separate the ommatidia into yellow and pale are yet to be determined.

Mollereau *et al* (2001) has shown that *spalt major (salm)*, one of the transcripts of the *spalt* complex, is required to inhibit Rh1 expression within R7 and R8 cells. Salm is expressed in R3 and R4 cells during the third larval instar stage and becomes restricted to R7 and R8 during pupal development with expression continuing into adulthood. Loss of *salm* during the third larval instar stage has no effect on eye development. However if *salm* expression is absent during pupal stages, the R7 and R8 photoreceptor cells lose their fate and begin to express the normal R1-R6 cell-expressing rhodopsin Rh1, indicating that Salm is vital for the determination of the inner R cells (Mollereau et al., 2001) (Figure 1.4).

## Figure 1.4 Regulation of the different Rhodopsins

Ommatidia can be grouped into either pale or yellow ommatidia depending on the expression of the *rhodopsins*. A yellow ommatidium expresses *rh3* in R7 cell and *rh5* in the R8 cell while a pale ommatidium express *rh4* in the R7 cell and *rh6* in the R8 cell. *rh1* is expressed in the outer photoreceptor cells (R1-R6).

In the outer R1-R6 cells, Glass (Gl) activates expression of *rh1* while Orthodenticle (Otd) in conjunction with an unknown factor (Y) inhibits the expression of *rh6*.

In the yellow ommatidia, Prospero (Pros) inhibits expression of *rh6* in R7 cells and Spalt major (Salm) and Otd inhibit *rh1* expression in both R7 and R8 cells.

In the pale ommatidia, Salm and Otd inhibit *rh1* expression in both R7 and R8 cells. However, in this case Otd is an enhancer of *rh3* and *rh5* expression in R7 and R8 cells. *rh5* expression is inhibited in R7 cells by Pros and *rh3* expression is inhibited in R8 cells by an as yet unknown mechanism.

Image modified from Tahayato et al., 2003.

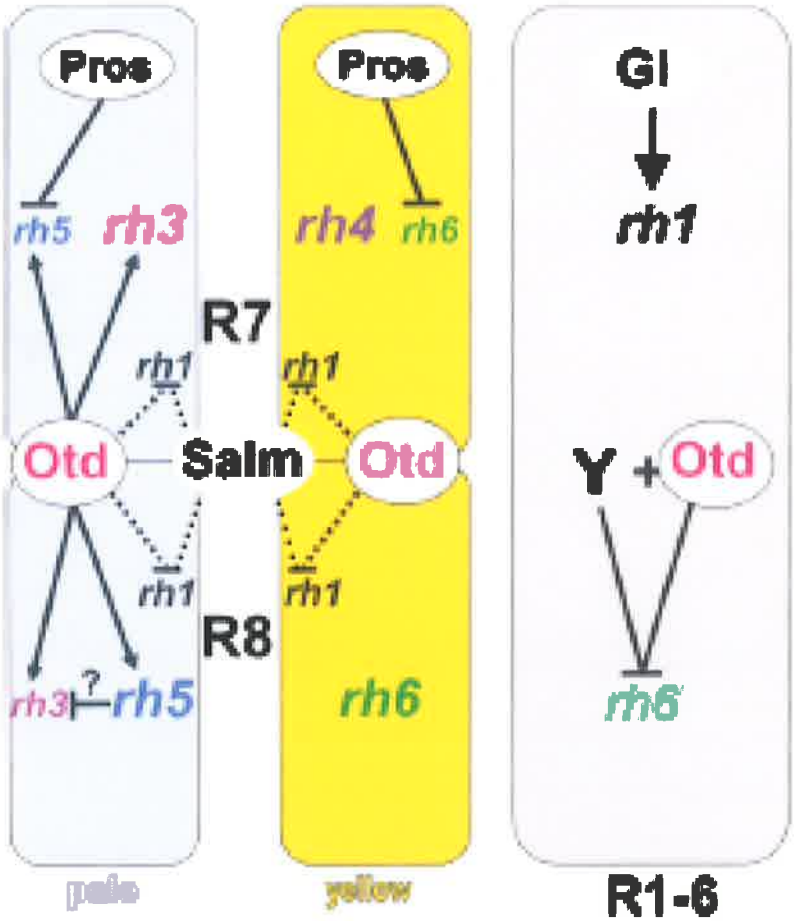
Pros
Pros
Gl
rh5
rh3
rh4
rh6
rh1
R7
rh1
rh1
Otd
Salm
Otd
Y
+
Otd
rh1
rh1
R8
rh3
?
rh5
rh6
rh6
pale
yellow
R1-6

*1.7.2 Light activation of the visual transduction pathway*

Different rhodopsins detect different wavelengths of light but activate the same light pathway. In the *Drosophila* eye, light (at 480nm) activation of rhodopsin (Rh) results in an isomerization to the activated form, Metarhodopsin (M), which then becomes phosphorylated by Rhodopsin Kinases (Hardie and Raghu, 2001). The formation of M leads to the activation of a G protein, $G_{\alpha p}$-GTP by releasing the $G_{\beta\gamma}$ component of $G_{\alpha\beta\gamma q}$-GDP, in the fastest known G coupling process (Ranganathan et al., 1991). Once $G_{\alpha q}$ becomes active, it in turn activates No Action Potential A (NorpA) which encodes phosopholipase C-beta (PLC). This generates second messengers by hydrolysing phosphatidyl inositol 4,5-bisphosphate ($PIP_2$) to produce soluble inositol-1,4,5-triphosphate ($InsP_3$) and membrane bound diacyl glycerol (DAG) (Hardie and Raghu, 2001). The activation of PLC and the release of the second messengers ultimately results in the opening of two calcium-permeable light-sensitive channels, Transient Receptor Potential (TRP) and TRP-like (TRPL) (Hardie and Raghu, 2001) (Figure 1.5). The gating of the TRP and TRPL channels requires polyunsaturated fatty acids (Chyb et al., 1999) but the exact mechanism is unknown. The influx of calcium causes depolarisation of the rhabdomere with a signal being sent down the R cell axons to the monopolar neurons, which in turn sends the message to the medulla where it can be processed (Hardie, 1991; Ranganathan et al., 1991; reviewed by Meinertzhagen and Hanson, 1993).

*1.7.3 Termination of the light pathway*

Once depolarisation has occurred all aspects of the signalling pathway must be turned off, rhodopsin must be inactivated, the secondary messages must be recycled and the TRP and TRPL channels must be closed.

The binding of Arrestin2 (Arr2) to the phosphorylated Metarhodopsin inactivates it by uncoupling M and $G_{\alpha q}$ (Hardie and Raghu, 2001). This interaction is transient and if it becomes stabilised then photoreceptor degeneration occurs. Arrestin is released from the phosphorylated Metarhodopsin by a $Ca^{++}$/Calmodulin dependent protein kinase C (which is also known as Inactivation No Afterpotential C or InaC) (Kahn and Matsumoto, 1997). The influx of calcium results in the activation of Calmodulin, which in turn activates the phosphatase Retinal Degeneration C (RdgC) (Lee and Montell, 2001). The role of RdgC is to dephosphorylate Metarhodopsin (Lee and Montell, 2001) reverting it back to Rhodopsin. Metarhodopsin can also revert back to Rhodopsin by exposure to another wavelength of light (580nm), resulting in Rh being able to respond to the next photon of light (Figure 1.5).

## Figure 1.5 The visual pathway in *Drosophila*

1) Light activates the Rhodopsin protein leading the isomerization of the receptor forming Metarhodopsin. 2) The associated G protein $G_{\alpha\beta\gamma q}$-GDP is activated ($G_{\alpha q}$) which in turn activates PLC to hydrolyse $PIP_2$ into the secondary messengers, $IP_3$ and DAG. 3) Calcium enters the cells via the TRP and TRPL channels leading to excitation of the photoreceptor cell.

The response is terminated by 4) the recycling of the second messengers: DAG is converted to PA by RdgA in the SMC, PA is converted to CDP-DAG via Cds, which becomes PI via PI synthase and is transported back to the microvilli by RdgB. In the microvilli PI is phosphorylated and becomes $PIP_2$. 5) After the activation of Rh to M, M becomes phosphorylated by rhodopsin kinases (RK). Arrestin 2 binds to the phosphorylated M and interferes with the interaction between M and $G_{\alpha q}$. M-P is dephosphorylated by RdgC and can be converted back to R by exposure to the 580nm of light. 3) The signalplex consists of the adaptor protein INAD, PKC, PLC, CaM, TRP and NinaC. INAD interacts with NinaC, a myosin III protein that interacts with actin and is required for the fast termination of the light response. INAD is also vital for the localization of PKC, PLC and TRP.

Image modified from Hardie, 2003

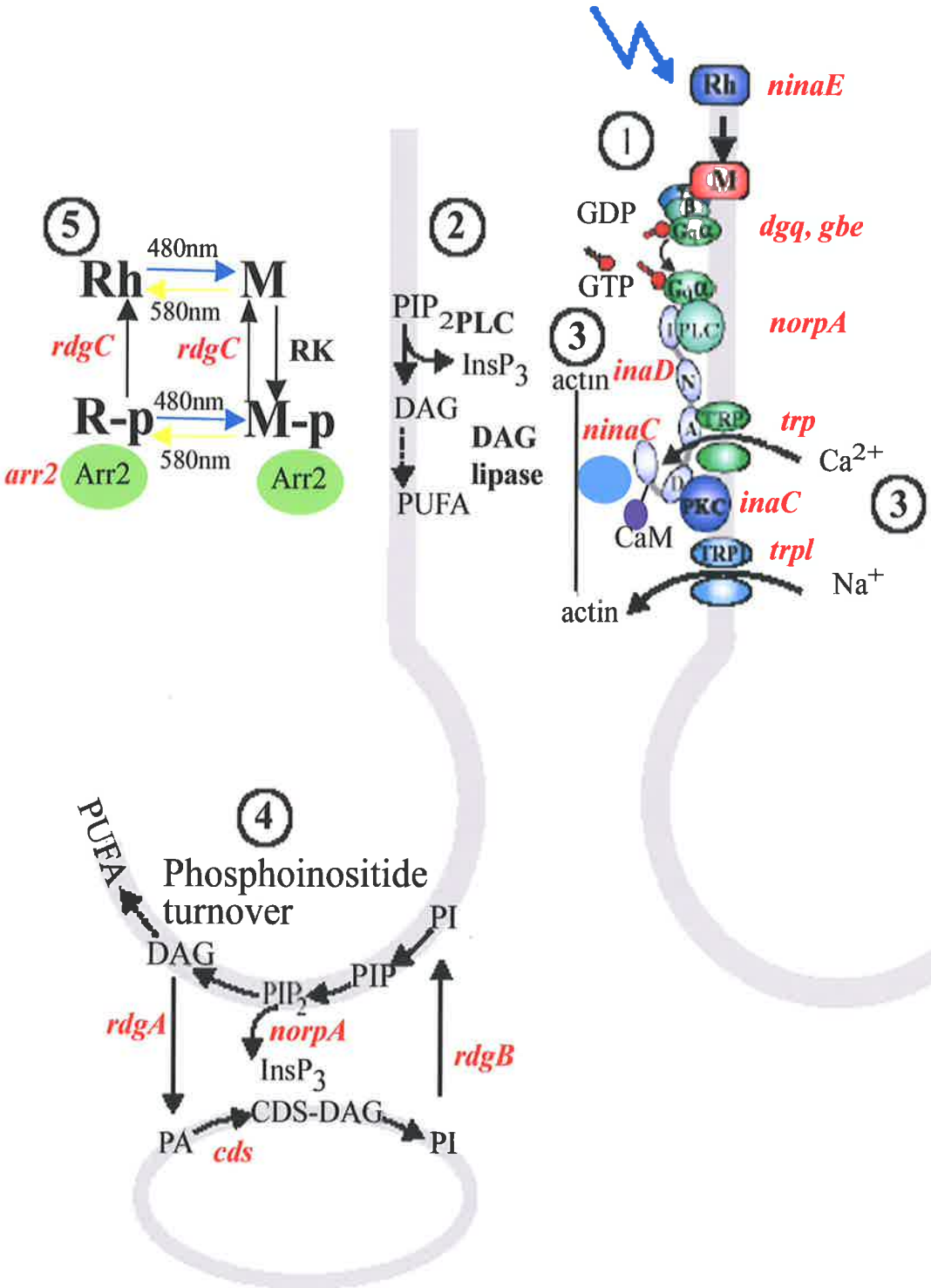
Rh
ninaE
1
M
GDP
dgq, gbe
GTP
norpA
3
actin
inaD
ninaC
trp
Ca2+
3
PKC
inaC
CaM
TRP
trpl
Na+
actin
2
PIP2
PLC
InsP3
DAG
DAG lipase
PUFA
5
480nm
Rh
M
580nm
rdgC
rdgC
RK
480nm
R-p
M-p
580nm
arr2
Arr2
Arr2
4
PUFA
Phosphoinositide turnover
PI
DAG
PIP
PIP2
rdgA
norpA
InsP3
rdgB
CDS-DAG
PA
cds
PI

The recycling of the second messengers is vital for termination of the light response. *retinal degeneration A* (*rdgA*), which encodes a DAG kinase, controls the DAG levels in the microvilli by converting the DAG to phosphatidic acid (PA) (reviewed by Hardie, 2003). PA is then converted into CDP-DAG by CDP-DAG-Synthase (Cds). This process occurs in the submicrovilli cisternae (SMC), which is a specialized smooth endoplasmic reticulum at the base of the microvilli. Inositol is incorporated in to the CDP-DAG, by PI synthase, to produce PI (reviewed by Hardie, 2003). The PI is transported from the SMC back to the microvilli by a PI transport protein Retinal Degeneration B, (RdgB). Once in the microvilli the PI undergoes a series of phosphorylation events to become $PIP_2$. When light activates the pathway $PIP_2$ becomes $InsP_3$ and DAG (reviewed by Hardie, 2003). Recently, it has been shown that the PI pathway and in particular RdgB and Cds are required for the correct localisation of Arr2 and NorpA to the rhabdomeres (Lee et al., 2003b) (Figure 1.5).

NorpA (PLC) is not only involved in the production of second messengers but also interacts with the signalling complex (known as the signalplex) that is formed around the TRP channels (Huber et al., 1996a; Shieh et al., 1997). Inactivation no afterpotential D (INAD) contains five PDZ domains (Shieh and Niemeyer, 1995) and is essential in this signalplex. The PDZ domains are protein interaction motifs enabling this protein to act as an anchor for other proteins. Proteins that interact with INAD include eye specific protein kinase C (INAC also known as PKC) (Huber et al., 1996b; Xu et al., 1998a), phospholipase C (PLC, NorpA) (Huber et al., 1996b; Chevesich et al., 1997), TRP (Sheih and Zhu, 1996) and TRPL (Xu et al, 1998), Neither Inactivation Nor Afterpotential C (NINAC) myosin III (Wes et al., 1999), and Rhodopsin itself (Chevesich et al., 1997; Xu et al., 1998b) (Figure 1.5). Calmodulin also interacts with the INAD protein but via a domain distinct from the PDZ domains (Chevesich et al., 1997; Xu et al., 1998b). The loss of INAD results in the mislocalisation of TRP over time (Chevesich et al., 1997) and is also essential for the localisation of PKC and PLC (Chevesich et al., 1997; Tsunoda et al., 1997). It was initially thought that INAD may be only required for the correct localisation of PLC, PKC and TRP and not actual signalling. However, analysis of the interaction between NINAC and INAD showed that the signalplex is also required to promote fast inactivation of the light response (Wes et al., 1999). NINAC interacts with actin, providing a link between the signalplex and the actin-based cytoskeleton (Hicks et al., 1996; Wes et al., 1999). The myosin domains within NINAC have been shown to be important for the deactivation of the light-signalling pathway (Wes et al., 1999) (Figure 1.5).

### *1.7.4 Degeneration of the rhabdomeres*

If genes that are required for vision in the *Drosophila* eye are mutated then degeneration of the photoreceptor cells will occur. There are two types of degeneration that are observed, light independent and light-dependent degeneration.

Light-independent degeneration occurs when mutations affect proteins such as Rhodopsin and the guanine triphosphatase (GTPase), Rac1 (Bentrop, 1998; Leonard et al., 1992; Chang and Ready, 2000), which are required to maintain the structure of the microvilli. In a *ninaE* mutant, the cortical actin cytoskeleton fails to be organized at the base of the rhabdomere resulting in its collapse into the photoreceptor cytoplasm (Kumar and Ready, 1995a; Chang and Ready, 2000). Rac1 is required for cytoskeletal organization and transgenic expression of *rac1* in a *ninaE* mutant rescues the degeneration observed in that mutant (Chang and Ready, 2000). Loss of genes required for the maturation of rhodopsin also leads to degeneration in a light-independent manner. Such genes include *neither inactivation nor afterpotential A*, which encodes a chaperone that folds the immature Rh1 to the mature form (Colley et al., 1995) and *rab6*, which encodes a GTPase that is required to transport Rh1 through the endoplasmic reticulum and golgi complex (Shetty et al., 1998).

Two forms of degeneration occur in a light-dependent fashion, apoptosis and necrosis. The apoptotic response is triggered when stabilised Metarhodopsin-Arrestin complexes form (Alloway and Dolph, 1999). A mutation in *norpA* results in light-dependent degeneration, even though the signalling pathway is not activated. It has recently been shown that mutations in the *norpA* and *rdgB* genes result in the formation of stabilised Rhodopsin-Arrestin complexes (Alloway et al., 2000). The removal of *arr2* rescues the light-dependent degeneration observed in these mutants as well the degeneration observed in *rdgC* mutants (Alloway et al., 2000; Kiselev et al., 2000). Close examination of the retinal degeneration observed in *norpA* mutants showed that the outer rhabdomeres underwent phagocytosis, which is a hallmark of apoptotic cell death (Alloway et al., 2000). Interestingly inhibiting caspase activity by over-expression of *p35* in the eye rescues the degeneration of the *rdgC* and *norpA* mutants (Davidson and Steller, 1998; Alloway et al., 2000). Also, inhibiting endocytosis via a dominant negative form of the dynamin homologue, *shibire*, which is essential for endocytosis, also inhibits the degeneration observed in *rdgC* and *norpA* mutants (Alloway et al., 2000; Kiselev et al., 2000). Arr2 interacts with clathrin-coated pits to internalise the Rhodopsin-Arrestin2 complexes during endocytosis. The long-term accumulation of these complexes results in apoptosis (Kiselev et al., 2000). *crumbs*, which is required for cell adhesion, is also necessary for survival of the photoreceptor cells. In *crumbs*

mutant animals, the rhabdomeres undergo light-dependent degeneration that can be inhibited by expressing *p35*, indicating that the degeneration is apoptotic and not necrotic (Johnson et al., 2002).

A number of mutations within genes that are required in the phototransduction pathway lead to necrotic degeneration. Mutations in the TRP ion channel and hypomorphic mutations in RdgA and Arr2 lead to degeneration in this manner. A missense mutation in the TRP ion channel that renders it constitutively active, results in degeneration of the photoreceptor cells within days of eclosion. However, loss of the TRP ion channel results in mild degeneration (Yoon et al., 2000), suggesting that the uncontrolled influx of calcium was responsible for the degeneration. Additionally, *rdgA* mutant animals, in which the second messengers are no longer recycled, undergo rapid light-dependent degeneration. However, introducing mutations in the *trp* and *trpl* ion channels into an *rdgA* mutant background inhibits this degeneration, indicating that the influx of calcium is responsible for the degeneration observed in *rdgA* mutants (Raghu et al., 2000). The loss of Arr2 leads to degeneration of the photoreceptor cells because of the continual activation of the signalling pathway. Interestingly, the degeneration in *arr2* mutants is not rescued by the expression of *p35*, indicating that degeneration in this case is not due to apoptosis but necrosis (Davidson and Steller, 1998; Alloway et al., 2000). These results taken together suggest that necrosis of the photoreceptor cells occurs when there is excessive activation of the signalling pathway that leads to increased intracellular calcium levels.

In yeast the sphingolipid pathway has been implicated in membrane trafficking by endocytosis (Zanolari et al., 2000). Therefore, Acharya and colleagues (2003) investigated this pathway in the *Drosophila* eye and found that both the necrosis and apoptotic pathways work through the shingolipid biosynthesis pathway (Acharya et al., 2003). The authors examined an *arr2* null mutant, which had been shown to induce necrosis of the photoreceptor cells (Dolph et al., 1993; Alloway et al., 2000). When over-expressing the *ceramidase* gene, one of the components of this pathway, in the eye of an *arr2* mutant, necrosis of the photoreceptor cells was rescued (Acharya et al., 2003). The same results were obtained when examining a *norpA* mutant, which has been shown to undergo apoptotic cell death rather than necrosis (Alloway et al., 2000). The sphingolipid biosynthesis pathway acts via clathrin-dependent endocytosis, as the over-expression of *ceramidase* also rescues the degeneration observed in the *shibire* mutant that disrupts clathrin-dependent endocytosis (Acharya et al., 2003). Therefore the sphingolipid pathway is required for the integrity of photoreceptor cells in the adult eye.

## 1.8 Aims and approaches of this thesis

Although studies into the embryonic expression pattern and role of Dri have been undertaken, the role of Dri later in development is not understood. Initial studies into the expression pattern of *dri* in the developing eye indicated that it was expressed in seven of the eight photoreceptor cells (T. Shandala, personal communications). Chapter 3 confirms and extends the analysis of the expression pattern of *dri* during the third larval instar, pupal and adult stages of development.

Dri is essential for the survival of the embryo and therefore the effect of loss of this protein later in development is difficult to examine. To overcome this problem, somatic clones that spanned the entire eye were generated. Chapter 4 describes the phenotypes associated with the loss of *dri* during the third larval instar stage of development

The expression pattern of *dri* in the adult eye suggests that it may have a function in that tissue. Chapter 5 discusses the role of *dri* in adult fly vision.

# Chapter 2: Methods and Materials

## 2.1 Abbreviations

APS - ammonium persulphate

DAB - 3, 3' diaminobenzidine

DTT - dithiothreitol

EDTA - ethylenediaminetetraacetic acid

HEPES - N-2-Hydroxyethylpiperazine-N-2-ethanesulphonic acid

HRP - Horse radish peroxidase

rpm - revolutions per minute

TEMED - N,N,N',N-tetramethylenediamine

## 2.2 Materials

### *2.2.1 Molecular weight markers*

**Protein**

Prestained molecular weight markers (NEB) sizes (in kDa): 175, 83, 62, 47.5, 32.5, 25, 16.5, and 6.5

BenchMark Prestained Protein ladder (Invitrogen) sizes (in kDa): 181.8, 115.5, 82.2, 64.2, 48.8, 27.1, 25.9, 19.4, 14.8 and 6.0.

### *2.2.2 Media, Buffers and Solutions*

***Drosophila* Media**

Fortified *Drosophila* medium contained 1% (w/V) agar, 18.75% compressed yeast, 10% treacle, 10% cornmeal (polenta), 2.5% tegosept mix (10% para-hydroxybenzoate in ethanol) and 1.5% acid mix (47% propionic acid/4.7% orthophosphoric acid)

**Buffers and solutions**

| | |
|---|---|
| Agarose gel loading buffer: | 50%(w/v) glycerol, 50mM EDTA, 0.1% (w/v) bromophenol blue |
| Cytoskeletal buffer: | 10mM Hepes (pH 7.4), 200mM sucrose, 3mM $MgCl_2$, 50mM NaCl, 0.5% Triton-X100, 0.02% $NaN_3$ |
| ECL - Solution A: | 5mL of 100mM Tris HCL (pH 8.5), 22µL of 90mM coumaric acid, 50µL of 250mM Luminol |
| Solution B: | 5mL of 100mM Tris HCL (pH 8.5), 3µL Hydrogen peroxide |

| | |
|---|---|
| 10X HEPES buffer: | 250mM HEPES, 150mM NaOAC, 2mM EDTA pH7.5 |
| FOFAL load buffer: | 200µL 37% formaldehyde, 1.6ml Formamide, 200ul of 10x HEPES buffer, bromophenol blue |
| 0.1 M Na buffer pH 7.2 | 68.4 mls of $Na_2HPO_4$ and 31.6 mls of $NaH_2PO_4$ |
| PBS: | 7.5mM $Na_2HPO_4$, 2.5mm $NaH_2PO_4$, 145mM NaCl |
| PBT: | 1x PBS, 0.3% Triton X-100 |
| Protein gel load buffer: | 125mM Tris pH6.8, 2% SDS, 6M Urea, Bromophenol blue |
| Protein gel running buffer (5X): | 1.5% (w/v) Tris-base, (w/v) glycine, 0.5% SDS |
| 20X SSC: | 3M NaCl, 0.3M sodium citrate |
| TAE: | 40mM Tris-acetate, 20mM sodium acetate, 1mM EDTA, pH8.2 |
| Western transfer buffer: | 50mM Tris-base, 0.3% Glycine, 0.04% (w/v) SDS, 20% methanol |

*2.2.3 Fly stocks*

| **General stocks (From Bloomington stock centre unless otherwise stated)** | *dri* stocks (kindly provided by T. Shandala) |
|---|---|
| *$w^{1118}$*<br>*UASnlacZ (II)*<br>*UASclacZ (II)*<br>*yw;FRT42DGMRhid;eyGal4UASflpase*<br>*CyO*<br>*FRT42D*<br>*X64 enhancer trap line*<br>(Kindly provided by G. Rubin)<br>*w; Sco ; Rh1Gal4 UASWGA*<br>*CyO*<br>(Kindly provided by H. Okano) | *w;FRT42Ddri$^1$*<br>*CyOTb*<br>*w;FRT42Ddri$^2$*<br>*CyOTb*<br>*w;UASdri3.5 (II)*<br>*w; +; UASdri4.7 (III)* |
| **Axon guidance stocks (kindly provided by B. Dickson)** | **Stocks produced during this PhD** |
| *yw eyFlpase2;FRT42D*<br>*yw eyFlpase2;FRT42Ddri$^3$*<br>*CyOy+*<br>*yw eyFlpase2;FRT42Dcl2R11.5* | *yw eyFlpase2;FRT42Ddri$^1$*<br>*CyOy+*<br>*yw eyFlpase2;FRT42Ddri$^2$*<br>*CyOy+* |

| | |
|---|---|
| *CyOy+* | *yw eyFlpase2glassLacZ;FRT42Ddri²* |
| | *CyOy+* |
| *yw eyFlpase2glassLacZ;FRT42Ddri³* | *yw eyFlpase2;FRT42D;ro-lacZ* |
| *CyOy+* | *CyOy+ +* |
| *yw eyFlpase2glassLacZ;FRT42Dcl2R11.5* | *yw eyFlpase2glassLacZ;FRT42Ddri¹* |
| *CyOy+* | *CyOy+* |
| *yw eyFlpase2;FRT42Ddri³;ro-lacZ* | *yw eyFlpase2 Rh1-lacZ;FRT42Ddri¹* |
| *CyOy+ +* | *CyOy+* |
| *yw eyFlpase2 Rh1-lacZ;FRT42Dcl2R11.5* | *yw eyFlpase2ato-myc;FRT42Ddri²* |
| *CyOy+* | *CyOy+* |
| *yw eyFlpase2 Rh1-lacZ;FRT42D* | |
| *CyOy+* | |
| *yw eyFlpase2 ato-lacZ;FRT42Ddri³* | |
| *CyOy+* | |
| *yw eyFlpase2 ato-lacZ;FRT42D* | |
| *CyOy+* | |
| *yw eyFlpase2;FRT42Ddri³;Rh6Gal4* | |
| *CyOy+ +* | |
| *yw eyFlpase2;FRT42DRh4-lacZdri³* | |
| *CyOy+* | |
| *yw eyFlpase2;FRT42Dcl2R1.5;UAS-lacZ* | |
| *CyOy+ +* | |
| *yw eyFlpase2glassLacZ;FRT42Dbks¹* | |
| *CyOy+* | |
| *yw eyFlpase2glassLacZ;FRT42Dbks²* | |
| *CyOy+* | |

### *2.2.4 Antibodies*

| **Primary antibodies** | **Dilution used** | **Provided by** |
|---|---|---|
| Mouse anti-Elav (9F8A9) | 1/10 on tissues | Developmental Studies Hybridoma Bank (DSHB) |
| Mouse anti-Prospero (MR1A) | 1/5 on tissues | DHSB |
| Mouse anti-c-myc (9E10) | 1/250 on tissues | DHSB |

| | | |
|---|---|---|
| purified by the IMVS | | |
| Mouse anti-mAb24B10 | 1/5-1/30 on tissues | DHSB |
| Mouse anti-mAb22C10 | 1/30 on tissues | DHSB |
| Mouse anti-Dachshund (mAbdac2-3) | 1/2 on tissues | DHSB |
| Mouse anti-Rhodopsin (4C5) | 1/50 on tissues<br>1/250 - 1/500 on Western blots | DHSB |
| Mouse anti-Boss | 1/1000 on tissues | H. Krämer |
| Mouse anti- α-tubulin | 1/10000 Western blots | Sigma |
| Guinea pig anti-Runt | 1/200 on tissues | J. Reinitz |
| Rat anti-Dri | 1/200 on tissues | R.D Kortschak |
| Rat anti-Elav (rat-Elav-7E8A10) | 1/10 on tissues | DHSB |
| Rabbit anti- β-galactosidase | 1/500 on tissues<br>1/5000 on Western blot | Rockland |

| **Secondary antibodies/ Tertiary complexes** | **Dilution used** | **Provided by** |
|---|---|---|
| Anti-Mouse-Rhodamine Red-X | 1/200 on tissues | Jackson Laboratories |
| Anti-Mouse Cy3 | 1/200 on tissues | Jackson Laboratories |
| Anti-Mouse Alexa488 | 1/200 on tissues | Molecular probes |
| Anti-Rat Alexa488 | 1/200 on tissues | Molecular probes |
| Anti-Rat Rhodamine Red-X | 1/200 on tissues | Jackson Laboratories |
| Anti-Rat HRP | 1/200 on tissues | Jackson Laboratories |
| Anti-Guinea pig Rhodamine LRSC | 1/200 on tissues | Jackson Laboratories |
| Anti-Mouse HRP | 1/200 on tissues<br>1/1000 on Western blots | Jackson Laboratories |
| Anti-Rabbit Cy3 | 1/200 on tissues | Jackson Laboratories |
| Anti-Rabbit HRP | 1/200 on tissues | Jackson Laboratories |
| Anti-Mouse biotin | 1/200 on tissues | Jackson Laboratories |
| Anti-streptavidin Alexa 488 | 1/200 on tissues | Molecular probes |

*2.2.5 Primers*

All primers were designed using PrimerExpress Version 1.0 (Applied Biosystems) across an intron-exon boundary and were purchased from Geneworks.

(all primers 5' to 3' )

ninaE5'- GCCGCCTGCTACAATCCA

ninaE3'- GCGATATTTCGGATGGCT

rp49F- ATCGATATGCTAAGCTGTCGCAC

rp49R- TGTCGATACCCTTGGGCTTG

## 2.3 Methods

Standard molecular genetic techniques were performed as described in (Sanbrook et al., 1989) or (Ausuble et al., 1994).

*2.3.1 Light and dark reared conditions for* Drosophila

The dark-reared flies were either grown in dark conditions from embryogenesis or placed in the dark during mid-pupal stages, before the onset of *ninaE* expression. The light-reared flies were grown in light conditions from embryogenesis.

*2.3.2 Sectioning*

*2.3.2.1 Tangential sectioning*

The adult head was dissected away from the body, the proboscis removed and the heads were cut in half. The heads were then fixed overnight in 2.5% gluteraldehyde in 0.1 M Na phosphate buffer (pH 7.2), washed in 0.1 M Na phosphate buffer and post fixed in $O_sO_4$. After washing with water and dehydration with acetone, the samples were mounted in epoxy resin and sectioned at 1 micron using an RMC Mt7 ultramicrotome and mounted onto slides. The slides were then stained with methylene blue and visualised on a Ziess Axiophot light microscope. Images were captured with a Fujix HC-1000 digital camera, and then processed in Adobe Photoshop 6.0.

*2.3.2.2 Adult head sectioning*

2.3.2.2.1 DAB staining

Adult heads were dissected away from the body and the proboscis removed. The heads were fixed in 2% formaldehyde in 0.05 % PBT for 1 hour. The samples were washed three times in 1X PBS then incubated overnight at 4°C in 12% sucrose. The sucrose was removed and the head orientated in OCT compound (Tissue-Tek) before being frozen on dry

ice. Sections were cut on a Leica cryostat machine at 10 microns thickness and placed on a poly-lysine coated slide. The slides were post-fixed in 0.2% formaldehyde/0.05% PBT for one hour. The slides were washed 3 times in 1 X PBS for five minutes followed by blocking in 5% BSA for 30 minutes. The primary antibody was then added and incubated at 4°C overnight. The slides were washed 3 times for 15 minutes each in 1X PBT and the HRP-conjugated secondary antibody was added and incubated for 2 hours at room temperature. The slides were washed 3 times for 15 minutes in PBT and then colour detection was performed with DAB. Once the colour reaction was completed, the slides were washed three times in 1X PBT for 5 minutes and twice in 1x PBS to stop the reaction. The slides were mounted in 80% glycerol in PBS and visualised under a Ziess Axiophot light microscope. Images were captured with the Fujix HC-1000 digital camera and processed in Adobe Photoshop 6.0.

2.3.2.2.2 Fluorescent staining

Adult heads were dissected and immersed immediately in OCT compound and frozen in the correct orientation on dry ice. The heads were sectioned on a Leica cryostat machine at 10 microns thickness and mounted on poly-lysine coated slides. The slides were post fixed in 4% formaldehyde for 10 minutes then washed three times in PBS. The slides were immersed in cytoskeletal buffer for 5 minutes and washed three times in 0.01% Saponin in PBS. The primary antibody was added and incubated overnight at 4°C. The primary antibody was removed by washing three times in 0.01% Saponin for 15 minutes each. The secondary antibody was added and incubated at room temperature for 2 hours then washed 3 times in 0.01% Saponin followed by two washes in 1 X PBS. The slides were then mounted in 80% glycerol in PBS and visualised under a Bio-rad confocal microscope. Images were processed in Adobe Photoshop 6.0.

### *2.3.3 Scanning electron micrograph*

Adult eyes were dehydrated progressively through an acetone series (25%, 50%, 75%, 100% acetone). Flies were air dried and mounted on EM studs. The flies were viewed without coating at 1mB accelerating voltage by filed emission scanning electron microscopy (Phillips, at CEMMSA, Adelaide University). Digital images were collected and analysed in Adobe Photoshop 6.0.

### *2.3.4 Antibody Staining*

Tissues were dissected in 1 X PBS and fixed immediately in 4% formaldehyde in 0.05% PBT and incubated at room temperature for 20 minutes. The tissues were washed

three times in PBT for 5 minutes and then blocked in 5% Goat serum for 1 hour. The primary antibody was diluted in 5% Goat serum and added to the tissue and incubated overnight at 4°C. The secondary antibodies were then added and incubated at room temperature at 2 hours. For the DAB staining a secondary HRP conjugated antibody was used, for fluorescent staining a secondary antibody conjugated to a chromophore was added. After two hours the samples were washed three times for 10 minutes. The fluorescent samples were mounted in 80% glycerol and stored at 4°C. For the HRP staining, DAB and hydrogen peroxide were added, and the colour reaction was allowed to proceed. If the signal was to be intensified then Nickel Chloride (8 µl of 8% stock solution) was added to the DAB Once the colour reaction had been completed the tissues were washed a further three times for 5 minutes in PBT stopped the reaction, the samples were then mounted in 80% glycerol and visualized on either Ziess Axiophot light microscope or Bio-rad confocal microscope. Images were processed in Adobe Photoshop 6.0.

### *2.3.5 Gel electrophoresis*

#### *2.3.5.1 RNase-free Agarose gel electrophoresis*

SeaKem LE grade agarose was used to prepare all agarose gels. The agarose was dissolved in 1X HEPES buffer and melted to give a final concentration of 1%. 10 mls of 1% agarose was poured onto a RNase-free glass slide and the combs were placed in the melted agarose to create the wells. The gel was placed in a RNase-free gel tank containing 1X HEPES buffer. An aliquot (1 µl) of RNA was boiled at 100°C for 2 minutes then placed immediately on ice. 2 µl of FOFAL loading buffer was added to the RNA and the RNA/load buffer samples were then loaded into the wells. The agarose gel underwent electrophoresis at between 70-90V until the bromophenol blue had run the required distance. The gel was then stained in RNase-free ethidium bromide and visualised under short wave UV light.

#### *2.3.5.2 SDS PAGE gel*

Glass plates, spaces, combs and the gel apparatus were thoroughly cleaned then assembled. For a 10% separating gel, the following components were added. 4 ml of $H_2O$, 2.5 mls of 1.5 M Tris pH 8.8, 100 µl of 10% SDS, 3.33 mls of 30% acrylamide, 50 µl of 25% APS and 10 µl of TEMED. The solution was mixed then added to the pre-prepared glass plates and allowed to set. Once set the 4% stacking gel, which consisting of 6.1 ml $H_2O$, 2.5 mls of 0.5M Tris pH 6.5, 100µl of 10% SDS, 1.33 ml of 30% acrylamide, 50 µl of 25% APS and 10 µl TEMED, was added on top of the separating gel and the combs positioned to form wells. Once set, the wells were removed and the gel was transferred to the gel tank.

*2.3.6 Western analysis*

The sample was dissected and placed directly into protein sample load buffer. The samples were either stored at –80°C or homogenized. Once homogenized the samples were boiled for 10 minutes. 10 µl of sample/load buffer were loaded directly onto a 10% SDS-PAGE gel. 10 µl of the pre-stained molecular markers were also loaded. The gel was run at 180 V for 40 minutes or until the lowest molecular markers were at the end of the gel. The gel, Whatman paper and nitrocellulose membrane was washed in Western transfer buffer before being arranged and transferred for 30 minutes on the BIORAD trans-blot SD semi-dry transfer cell. Once the transfer had been completed, the membrane was incubated in 5% blotto for 1 hour, then the primary antibody in fresh blotto was added before being incubated overnight at 4°C. The following day the membrane was washed 3 times for 5 minutes each in PBT, followed by a further 2 washes in PBT for 10 minutes. The appropriate HRP-conjugated secondary antibody was then added to the membrane and incubated for 2 hours at room temperature. The membrane was washed three times in PBT for 10 minutes each time, then exposed to ECL for 1 minute, blotted to remove excess liquid and exposed to autoradiograph film for between 2 seconds and 5 minutes.

*2.3.6.1 Semi-quantitative analysis from Western blots*

The autoradiographs were scanned and saved as a .tif files using a HP PrecisionScan scanner and software. The .tif file was opened on Quantity One quantitation software (BIO-RAD) version 4.2. The lanes from the image were defined and the background in the lanes subtracted. Each band was outlined and the background levels set. The Quantity One software analysed the volumes and provided the adjusted volume values where the adjusted volume = sum of the intensity of the pixels within the volume boundary x pixel area – background. The ratio between the Rh1 band and α-tubulin was determined.

*2.3.7 Collection of material for Real time PCR analysis*

Flies with the correct genotype (*eyFLP;FRT42D/FRT2R11.5cl*, or *eyFLP;FRTdri*$^{2}$*/FRT2R11.5cl*) were decapitated and the heads placed immediately onto dry ice. Between 100-400 heads were collected and stored at -80°C.

*2.3.8 Extraction of total RNA*

200 µl of the Tri-reagent (Sigma) was added to each sample, the samples homogenised and a further 800µl of Tri-reagent added. The volume of Tri-reagent was increase to 1 ml and the solution was incubated at room temperature for 5 minutes. 300 µl of chloroform was added, vortexed and centrifuged at 13 000 rpm for 15 minutes at 4 °C. The

upper phase was collected and an equal volume of 70% ethanol was added and vortexed. The solution was added to a RNeasy column (Qiagen). Manufactures instructions were followed except the product was eluted in 60µl of RNase-free $H_20$ and not Buffer EB.

The concentration of RNA was determined by spectrometry and the quality of the RNA determined via a RNase-free agarose gel (see section 2.3.3.1)

### *2.3.9 Real time PCR*

#### *2.3.9.1 cDNA synthesis*

Between 1-5 µg of RNA was used in each reaction, to which 2 µl of 50 ng/µl Random hexamer primers (GibcoBRL), 1 µl of 10mM dNTPs (GibcoBRL) and DEPC-treated $H_2O$ to a final volume of 13 µl, were added. The reaction was incubated at 65°C for 5 minutes then placed immediately on ice. To this 4 µl of 5x Transcription buffer, 2 µl of 0.1M DTT, and 1 µl of Superscript III (Invitrogen) was added and incubated at 25°C for 5 minutes then 50°C for 50 minutes. The reaction was stopped by heating at 70 °C for 15 minutes. The quantity of cDNA produced was determined by spectrometry.

The No Amplification Control (NAC) for each RNA sample was set up as above except that $H_2O$ was added instead of Superscript III. Likewise, the No Template control (NTC) had $H_2O$ added instead of RNA.

#### *2.3.9.2 Real time PCR*

The first experiments involved determining the amplification efficiency for each primer pair. This was achieved by serial dilutions (100ng, 50ng, 10ng, 5ng and 1ng) of the cDNA template. To the various starting templates, 1 µl of forward primer (180nM), 1 µl of Reverse primer (180nM), 5 µl of 2x Sybr-Green PCR mix (Applied Biosystems) and $H_2O$ to a final volume of 10 µl was added to each well of a 96 well plate and each reaction was performed in triplicate. The plate was mixed and centrifuged at 2000 rpm in a Beckman benchtop centrifuge. The Real time PCR was performed on an ABI 7000 Sequence Detection System (Applied Biosystems) and the PCR conditions were as follows: 50°C for 2 minutes once, 95°C for 10 minutes once followed by 95°C for 15 seconds then 60°C for 1 minute 40 times. A dissociation curve was performed on every plate. The results were initially analysed using the ABI Prism 7000 SDS program to determine the CT values. The slope for the serial dilutions was determined in Microsoft Excel. Then a detailed analysis was undertaken with the program Q-gene (Muller et al., 2002), which takes into account the PCR efficiency of each primer pair.

In the subsequent 3 experiments 1 µl of 50 ng cDNA, 1 µl Forward primer (450 nM), 1 µl Reverse primer (450 nM), 5 µl 2X SYBR-Green PCR master mix and 2 µl $H_2O$ was added to each well and each primer and template combination were performed in triplicate. The PCR conditions were as follows: 50°C for 2 minutes once, 95°C for 10 minutes once followed by 95°C for 15 seconds then 60°C for 1 minute 40 times and a dissociation curve was performed. The results were initially analysed using the ABI Prism 7000 SDS program then further analysed in Q-gene (Muller et al., 2002) to obtain the relative expression of each sample. A Mann-Whitney U-test was undertaken because of the low number of samples.

# Chapter 3: The expression of *dead ringer* in the eye

## 3.1 Introduction

The embryonic distribution of Dead ringer (Dri) has been well described, with ubiquitous nuclear distribution until germ band retraction followed by a specific temporally and spatially restricted pattern (Gregory et al., 1996) (see section 1.4). However, the expression and role of Dri during the later larval development stages has not been as extensively studied. The study of various larval tissues, notably the developing eye disc, has contributed enormously to our understanding of developmental regulatory mechanisms. Therefore, to gain insight into the role of Dri, I chose to characterise the pattern of Dri expression during eye development.

Differentiation of the cells that give rise to the adult eye begins during the third larval instar, with a wave of differentiation occurring across the developing eye disc (reviewed by Meinertzhagen and Hanson, 1993). Differentiation occurs in and behind an indentation in the eye epithelium, the morphogenetic furrow, which moves posterior to anterior across the eye disc. This results in the establishment of sets of cells that become the photoreceptor cells (also referred to as R cells), cone cells, pigment cells (including primary, secondary and tertiary) and bristle cells, all of which are required for normal vision in the adult fly. Dri had been observed to be expressed in the developing third larval instar eye disc, with expression beginning several rows behind the morphogenetic furrow, presumably in the R1-R6 photoreceptor cells plus either the R7 or R8 cells (T. Shandala personal communication, Figure 3.1 A-B). This chapter describes a detailed characterisation of the pattern of *dri* expression in the larval and pupal eye disc and adult eye.

## 3.2 Results

### *3.2.1* Dri *is expressed in R1-R6 and R8 cells during the third larval instar*

To distinguish which R cells expressed *dri*, the enhancer trap line (X64), which expresses β-galactosidase in R8, R2 and R5 cells, was used. Third larval instar eye discs from X64 larvae were dissected and immunohistochemistry was performed with antibodies raised against β-galactosidase and Dri (Figure 3.1 C-E). These two antibodies were detected in the same R cells. Therefore *dri* is expressed in the R8, R2 and R5 cells.

## Figure 3.1 Expression of Dri in eye development

(**A**) Anti-Dri staining of a wild type ($w^{1118}$) third larval instar eye imaginal disc. Staining begins several rows behind the morphogenetic furrow (arrow). (**B**) A higher magnification of (**A**), showing that seven of the eight photoreceptor cells express Dri (a-g). By position a, b, c, e, f, g are R1-R6 photoreceptor cell nuclei. d could be either an R7 or R8 photoreceptor cell nucleus.

(**C**) Anti-β-galactosidase staining of a third larval instar eye imaginal disc, from the enhancer trap X64, showing expression in R8, R2 and R5. (**D**) The same eye disc stained with the anti-Dri antibody. (**E**) A merge of (**C**) and (**D**) showing co-localisation of the β-galactosidase and Dri antibodies in R8, R2 and R5 cells.

(**F**) The posterior edge of a $w^{1118}$ third larval instar eye imaginal disc showing anti-Prospero staining localized in the nuclei of R7 cells. (**G**) The same eye disc stained with anti-Dri antibody staining. (**H**) merge of (**F**) and (**G**) showing no co-localisation between the Prospero and Dri antibodies, indicating the Dri is not expressed in R7 cells.

(**I**) The same eye disc as (**F**) but at a different focal plane, showing Prospero antibody staining in the cone cells. (**J**) The same eye disc as (**G**) showing anti-Dri staining (**K**) merge of (**I**) and (**J**) showing no co-localisation between Dri and Prospero antibodies in the cone cells.

In all images the morphogenetic furrow is the left.

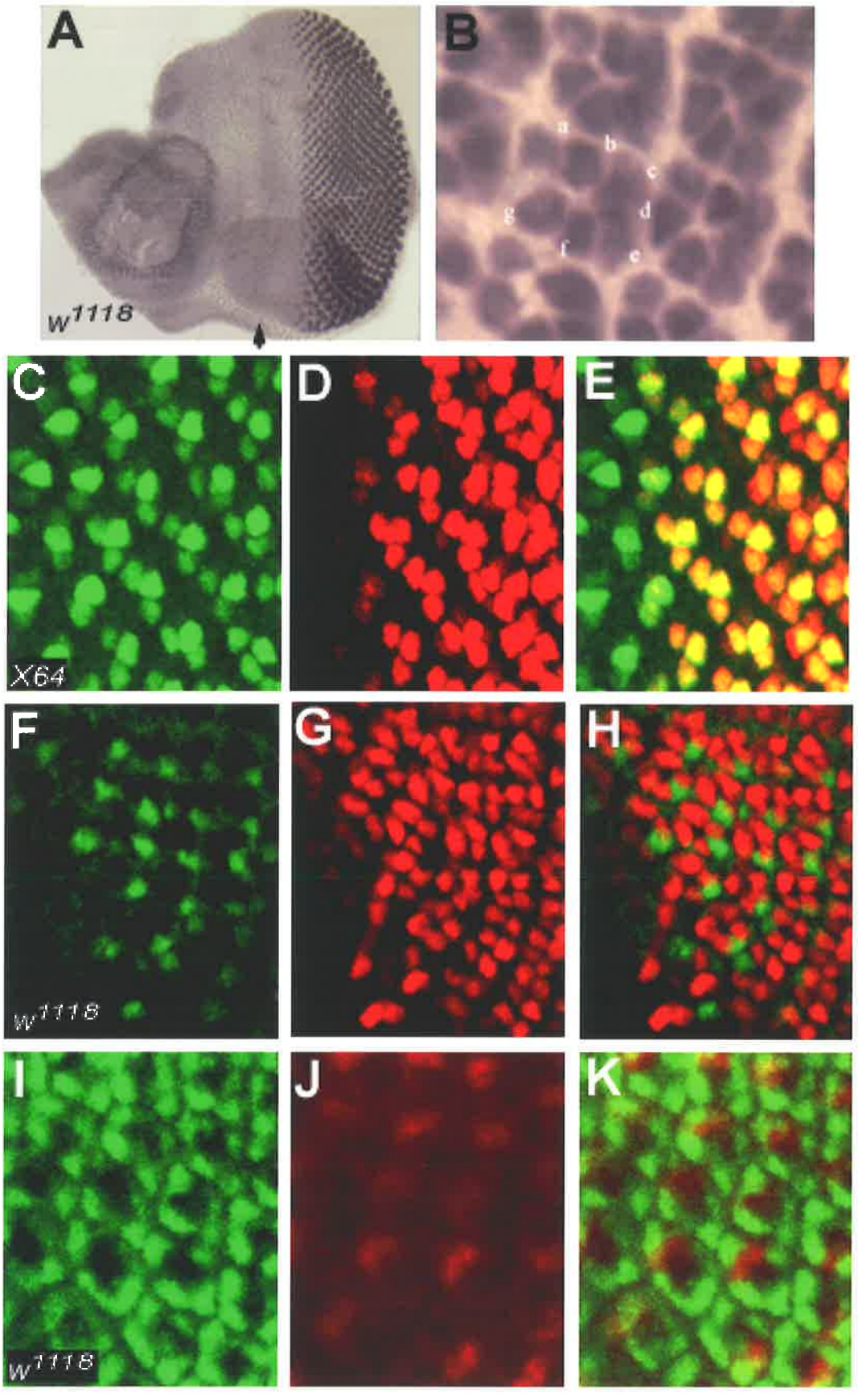
A
w1118
B
a
b
c
d
e
f
g
C
X64
D
E
F
w1118
G
H
I
w1118
J
K

Interestingly, expression begins in R8 cells then spreads to R2 and R5 cells. This pattern of expression mirrors the order in which these photoreceptor cells differentiate, even though *dri* is expressed well after the initial specification of these cells. To confirm that Dri was not expressed in R7 cells during third larval instar imaginal eye disc development, the co-localisation of Dri and Prospero, a protein specifically expressed in the R7 and cone cells, was investigated. Prospero and Dri did not co-localise in either the R cells or the cone cells (Figure 3.1 F-H, I-K). I conclude that Dri is not expressed in either R7 or the cone cells during the third larval instar, but that Dri is expressed in R8, R2, R5, R3, R4, R1 and R6 cells during third larval instar eye imaginal disc development.

### *3.2.2 Expression of* Dri *in pupal stages*

Although these observations show that Dri is expressed in photoreceptor cells during the third larval instar, it was unknown if expression continues into and during pupal stages. To answer this question, newly formed pupae were aged at 25°C for defined time periods, the retinas dissected and immunohistochemical staining performed with the anti-Dri antibody. At 6 hours after pupal formation (APF), Dri continued to be expressed in seven photoreceptor cells (Figure 3.2 A). However, when the patterning of the pupal retina had been completed by 42 hours APF, Dri expression had become restricted to six photoreceptor cells (Figure 3.2 D). Further examination showed that this downregulation of Dri in one cell had occurred by 24 hours APF (Figure 3.2 C). It was of interest to determine which photoreceptor cells were still expressing Dri at the later stages of pupal development, as it might provide an insight into a possible function for Dri. Because of its different developmental characteristics, the R8 cells were considered the most likely to undergo downregulation of *dri* expression. Therefore, retinas from the enhancer trap line X64 (utilized in identifying R8 cells in the larvae) were aged 24 hours APF. Although not reported in the literature, it was found that during pupal development, β-galactosidase from X64 animals was no longer restricted to R8, R2 and R5 cells, but was expressed in five-unidentified R cells (Figure 3.3 B and D). However, co-localisation of Dri and β-galactosidase did reveal that β-galactosidase was expressed in two photoreceptor cells that were not expressing Dri (Figure 3.3 D, as indicated by the black arrowheads). Based on the position of these two β-galactosidase only cells, it could be assumed that these cells were either R1 and R6 or R7 and R8 (Figure 3.3 A). To examine if Dri was expressed in R7 cells, the anti-Prospero antibody was used. As expected from the larval expression pattern, Dri and Prospero did not co-localise in retinas that were aged 24 hours APF (Figure 3.3 E-G).

## Figure 3.2 Expression of Dri during pupal stages

Retinas from wild type ($w^{1118}$) animals aged 6 (**A**), 21 (**B**), 24 (**C**) or 42 (**D**) hours after pupal formation were dissected and immunohistochemical staining performed with the anti-Dri antibody.

**(A)** At 6 hours APF Dri is observed in 7 photoreceptor cells.
**(B)** At 21 hours APF Dri is observed in either 6 (as indicated by the arrow) or 7 photoreceptor cells.
**(C)** At 24 hours APF, Dri is observed in 6 photoreceptor cells.
**(D)** At 42 hours AFP, Dri is observed in 6 photoreceptor cells.

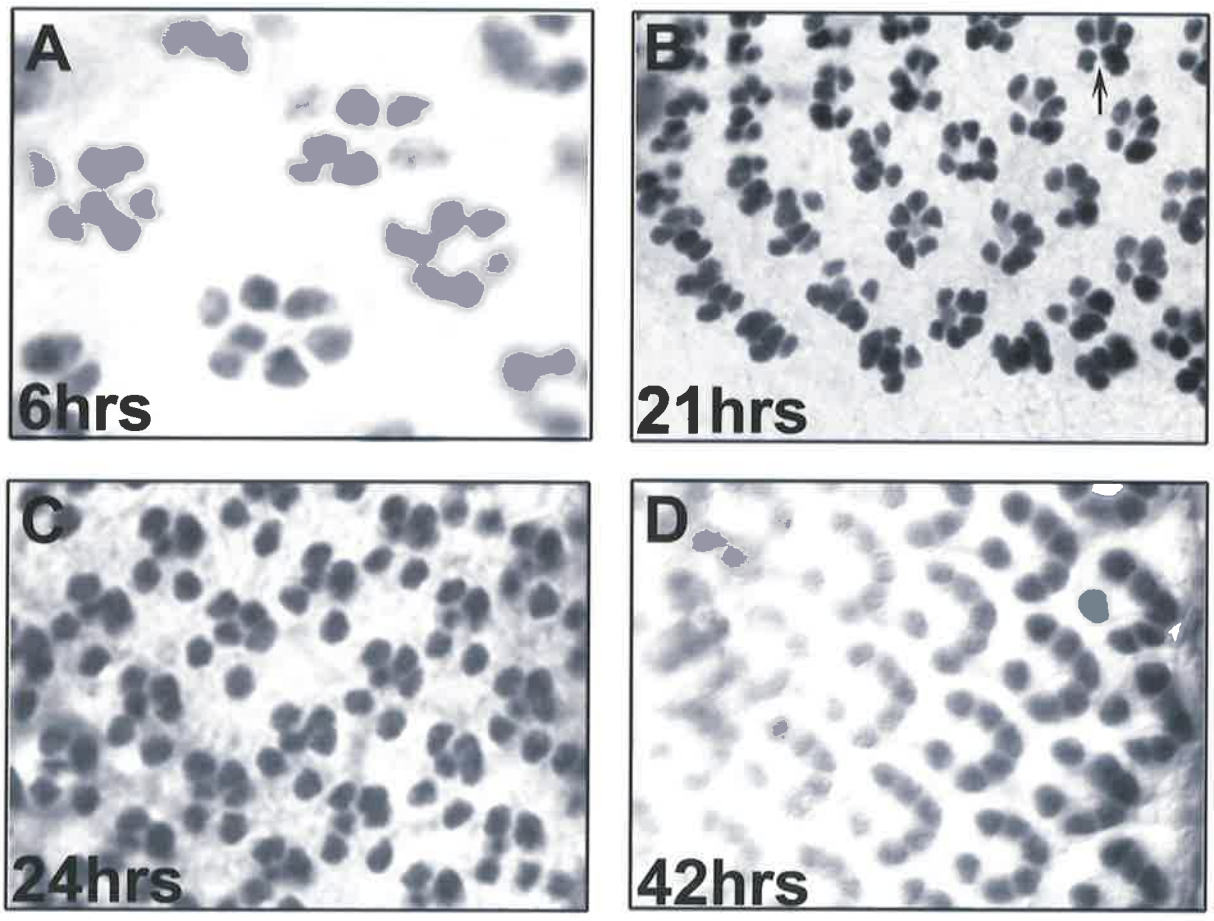
A
6hrs
B
21hrs
C
24hrs
D
42hrs

## Figure 3.3 Dri is down regulated in R8 cells during pupal development

(**A**) A schematic of the pupal retina showing the position of all of the cellular components within the retina. R1-R8: the photoreceptor cells 1-8. Cone: the cone cells. B: the Bristle cells, 1°, 2°, 3°: the three types of pigment cells.

(**B**) An X64 enhancer trap line retina, 24 hours APF, showing the β-galactosidase antibody observed in 5 unidentified R cells. (**C**) The same retina as (**B**) stained with the Dri antibody. Circles indicate the R cells in which Dri is observed. (**D**) A merge of (**B**) and (**C**) showing the two cells that do not express Dri but do express β-galactosidase (black arrowheads). Circles indicate the R cells in which Dri is observed.

(**E**) A $w^{1118}$ retina 24 hours APF, stained with the Prospero antibody showing staining in the R7 cells (arrow) and bristle cells. (**F**) The same retina as (**E**) stained with the Dri antibody. (**G**) A merge of (**E**) and (**F**) showing that Dri does not co-localise with Prospero in R7 cells as indicated by the white arrow.

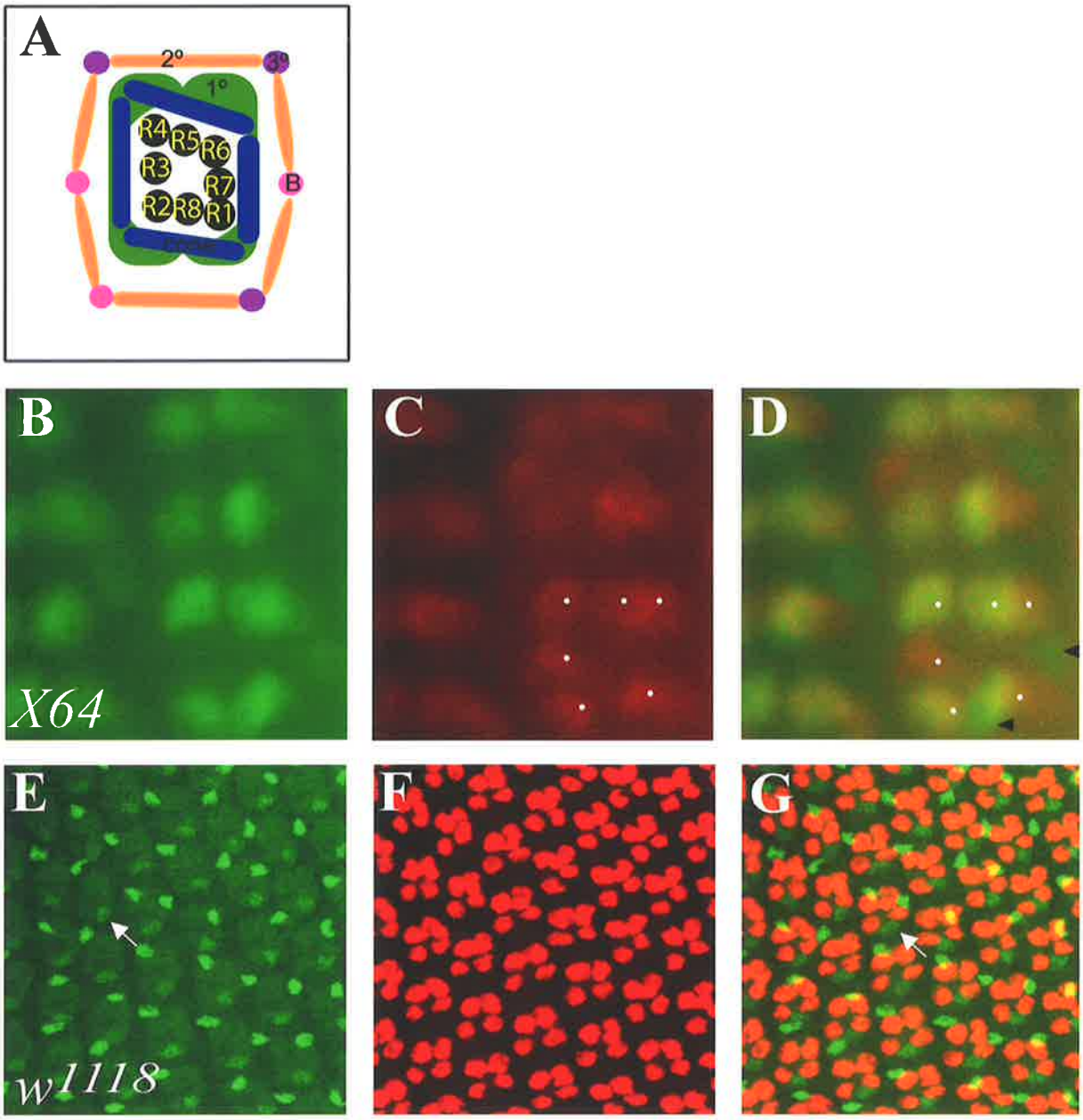
A
2°
3°
1°
R4
R5
R6
R3
R7
R2
R8
R1
B
B
X64
C
D
E
w1118
F
G

However, Dri did not co-localise with Prospero in this cell type (Figure 3.3 E-G). In summary, examination of the retinas from X64 showed that Dri was expressed in either R7 or R8 cells or R1 and R6 cells. However, staining for Prospero showed that Dri was not expressed in R7 cells. I conclude therefore, that Dri is expressed in R1-R6 cells and downregulated in R8 cells during pupal development. It is interesting to note that the expression of Dri in R8 cells, at 21 hours APF, is significantly downregulated when compared to 6 hours APF with some ommatidia no longer expressing Dri in R8 cells (compare Figure 3.2 A with Figure 3.2 B).

Dri expression was not observed in the nuclei of the developing cone, pigment and bristle cells, suggesting that this protein is not required for the specification of these non-neuronal cell types.

### *3.2.3 Adult expression of Dri*

The continued expression of Dri into late pupal development led to the possibility that the protein may be expressed in adult eyes. To test this possibility, horizontal sections through wild type ($w^{1118}$) heads, were stained with anti-Dri antibody and the neuronal nuclear marker, Elav (a neuron-specific spliceosome factor). This staining revealed that Dri was indeed expressed in the nuclei of the adult eye and that it was not expressed in all photoreceptor cells (Figure 3.4 A-C, cells not expressing Dri indicated by arrows). In order to determine which nuclei were expressing Dri, the yeast Gal4-UAS system was utilized (Brand and Perrimon, 1993). This system involves expressing the Gal4 transcription factor in the desired tissue. The Gal4 protein then binds to a UAS site upstream of the construct, resulting in the expression of the construct in the desired cell type. In this case, Rhodopsin 1 *(Rh1)-Gal4*, in which Gal4 is expressed in R1-R6 cells, was used to drive a *UAS-nlacZ* construct so that the nuclear-targeted β-galactosidase was expressed in the nuclei of R1 to R6 cells. Horizontal sections through adult heads that contained both the *Gal4* and *UAS* constructs were generated followed by immunohistochemical staining with anti-Dri and anti-β-galactosidase antibodies. Dri and β-galactosidase were observed to co-localise in R1-R6 cells (Figure 3.4 D-F), showing that the pupal expression of Dri extended into adult life. In order to verify that Dri was not being expressed in R7 cells, anti-Prospero and anti-Dri antibodies were used to stain horizontal sections through wild type ($w^{1118}$) heads. As expected, Dri and Prospero did not co-localise (Figure 3.4 G-I). Therefore, Dri is not expressed in R7 cells during adulthood. To examine if Dri was expressed in R8 cells, *Rh6-Gal4* was utilised to express *UAS-nlacZ* in approximately 70 percent of R8 cells (Huber et al, 1997).

## Figure 3.4 Adult expression of Dri

(**A**) A $w^{1118}$ eye section stained with anti-Elav antibody showing all R cell nuclei. (**B**) The same section as (**A**) stained with the anti-Dri antibody. (**C**) Merge of (**A**) and (**B**) showing that Dri and Elav co-localise in some but not all photoreceptor nuclei. Arrows indicate cells that Dri is not observed in. The insert is a higher magnification view of the boxed region in (**C**).

(**D**) A *Rh1Gal4;UASnlacZ* eye section stained with anti-β-galactosidase antibody showing staining in R1-R6 nuclei. (**E**) The same eye section as (**D**) stained with anti-Dri antibody. (**F**) Merge of (**D**) and (**E**) showing that the Dri and β-galactosidase antibodies co-localise in R1-R6 cells. The insert is a higher magnification view of the boxed region in **F**.

(**G**) A $w^{1118}$ eye section stained with anti-Prospero antibody showing all R7 cells. (**H**) The same section as (**G**) stained with the anti-Dri antibody. (**I**) Merge of (**G**) and (**H**) showing that the Dri and Prospero antibodies do not co-localise (as indicated by the arrow) indicating that Dri is not expressed in R7 cells. The insert is a higher magnification view of the boxed region in **I**.

(**J**) A *Rh6Gal4;UASnlacZ* eye section stained with anti-β-galactosidase antibody showing approximately 70 percent of R8 nuclei. (**K**) The same section as (**J**) stained with the anti-Dri antibody. (**L**) Merge of (**J**) and (**K**) showing that the Dri and β-galactosidase antibodies do not co-stain R8 cell nuclei (arrow).

In all images the apical edge is to the left.

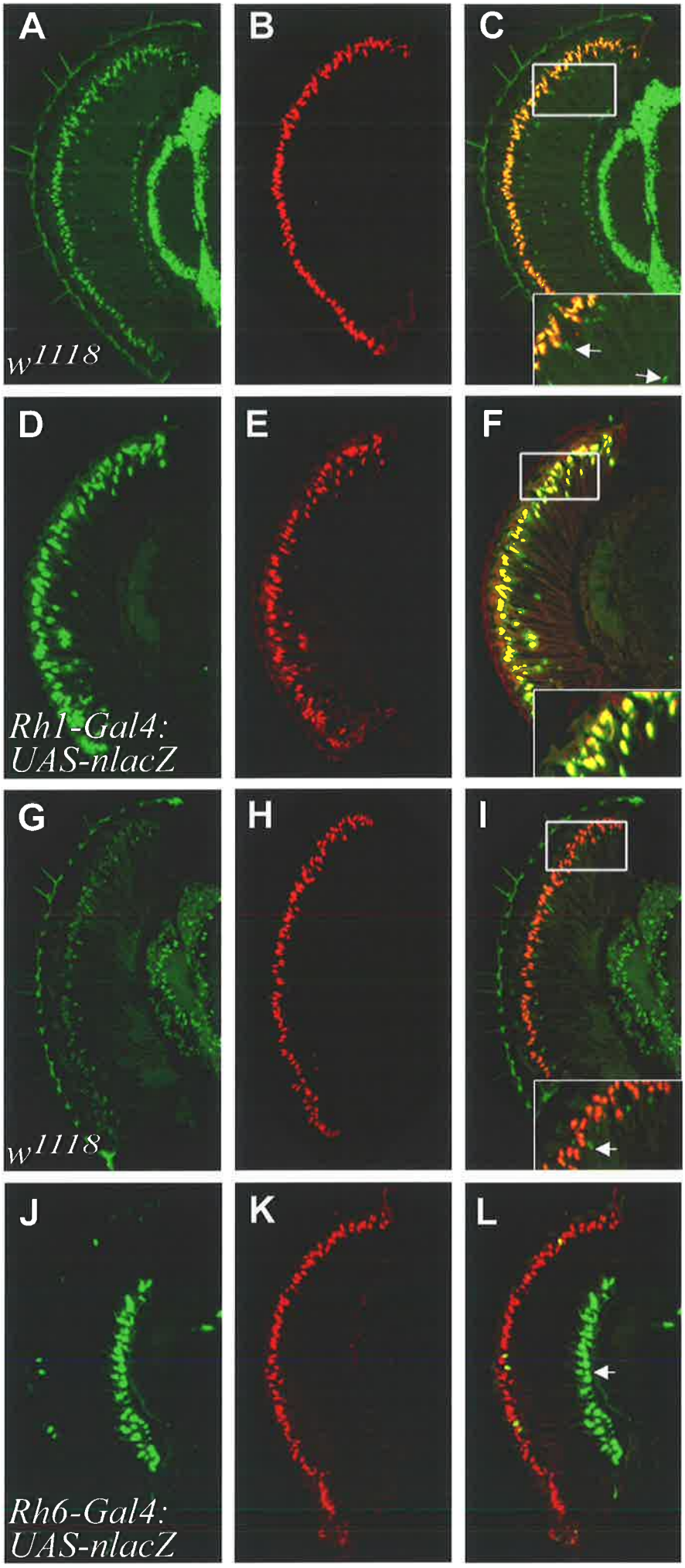
A
B
C
w1118
D
E
F
Rh1-Gal4:
UAS-nlacZ
G
H
I
w1118
J
K
L
Rh6-Gal4:
UAS-nlacZ

Horizontal sections through the *UAS-nlacZ;Rh6-Gal4* animals, stained with the anti-Dri and anti-β-galactosidase antibodies, showed that Dri did not co-localise with the β-galactosidase positive cells in the basal section of the adult eye. In the adult eye, the R8 rhabdomere is positioned directly below the R7 rhabdomere, so it follows that R8 cell nuclei will be in the basal section of the eye and closest to the optic lobe (Figure 3.4 L, indicated by an arrow). Dri was not observed in these nuclei (Figure 3.4 J-L). Therefore, as expected, Dri is not found in R8 cells. Unexpectedly, some nuclei were stained with β-galactosidase and Dri in the apical half of the eye at the level of the R1-R6 and R7 nuclei. The reason for this staining is not known.

The work described in this section established that Dri expression occurs in a cell-type-restricted manner, not only during the larval and pupal developmental stages but also in the adult eye.

## 3.3 Discussion

### *3.3.1 The expression of* Dri *during the third larval instar*

The pattern of Dri expression occurs not only during embryonic development but also at later stages in the larval, pupal and adult eye. These observations are consistent with a later role for *dri* in development. During the course of this PhD, Jasper et al., (2002) also showed that Dri was expressed in the eye several rows behind the morphogenetic furrow. Expression of Dri begins in a subset of photoreceptor cells and increases until seven of the eight photoreceptor cells are expressing the protein. The work presented in this chapter establishes that Dri is expressed in R8 cells and not R7 cells. It is unclear at this stage why Dri expression would be restricted to seven of the eight photoreceptor cells and, in particular, why Dri would never be expressed in R7 cells.

### *3.3.2 Expression of* Dri *during pupal and adult stages*

The expression of Dri during pupal development becomes restricted to six photoreceptor cells, (R1 to R6 cells). Examination of Dri expression at 21 hours APF revealed that some ommatidia continue to express Dri in R8 cells, although at a lower level, while others do not, indicating that the downregulation of Dri in R8 cells is a gradual process. The timing of this downregulation as yet provides no insight into the possible function of Dri in eye development.

Dri expression was found to continue into adulthood in the nuclei of photoreceptor cells R1 to R6. This probably means that Dri expression in R1-R6 cells is maintained throughout pupal development. This expression pattern is noteworthy as it suggests that Dri may not only be important during eye development but also during eye function.

### *3.3.3 The expression patterns and possible* Dri *function*

The restriction of Dri expression to the nuclei of neuronal photoreceptor cells and not the cone cells, pigment or bristle cells contrasts with the expression of Dri during embryonic central nervous system (CNS) development. In the CNS, Dri expression is restricted mainly to a subset of longitudinal glial cells (Shandala et al., 2003) and in *dri* mutant embryos those glial cells fail to migrate correctly, resulting in a mild axonal fasciculation defect (Shandala et al., 2003). This indicates that Dri is playing different roles during CNS and eye development.

Expression of Dri in the developing eye begins several rows behind the morphogenetic furrow, suggesting that Dri is not involved in the specification of the photoreceptor cells but may be important for later differentiation events and/or maintaining cell fate once specified. If so, R7 cells would require a different mechanism from R1-R6 and R8 cells for later differentiation and/or maintenance of cell fate. Dri expression continues throughout pupal development where expression in R8 cells is downregulated, perhaps suggesting that genes regulated by Dri are no longer required in the R8 cell, or alternatively, genes that were repressed by Dri are now required.

Dri is expressed in R1 to R6 in the adult eye. These photoreceptor cells are required for the visualisation of blue light (Scavarda et al, 1983; Zuker et al, 1985; Feiler et al, 1988; O'Tousa et al, 1989). Rhodopsins are G-coupled receptor proteins, which are responsible for sensing light. There are 5 rhodopsin proteins that are expressed in the adult eye in a non-overlapping pattern. Rhodopsin 1 (Rh1), which is encoded by the *ninaE* gene, is expressed exclusively in R1-R6 cells. One possibility is that Dri may be involved in regulating transcription of *ninaE*, a possibility that is considered further in Chapter 5. An argument against this possibility is that during larval stages, *ninaE* is expressed in the Bolwig nerve (Zuker et al., 1985b; Pollock and Benzer, 1988) a cell type in which Dri is not expressed.

The dynamic expression pattern of Dri during the different stages of eye development suggests that Dri may be regulating different genes at different stages of eye development. To investigate this hypothesis further, Chapter 4 describes an investigation of the role of *dri* in

eye development during the third larval instar stage and Chapter 5 describes analyses of the role of *dri* in the adult eye.

# Chapter 4: Role of *dead ringer* in the developing eye

## 4.1 Introduction

In Chapter 3 it was established that Dri is restricted to the nuclei of R1-R6 and R8 cells during the third larval instar stage of eye development. Dri expression begins several rows behind the morphogenetic furrow with expression mirroring the order of differentiation of the R cells. This expression pattern, however, gave little insight into a possible function for Dri.

Mutations within the *dri* gene result in embryonic lethality (Shandala et al., 1999) so determining the role of this gene in the development of later tissues, such as the eye, is difficult. However, a recently developed system that uses mitotic recombination to create a mosaic animal, mutant for a gene of interest specifically in the eye, has been used to overcome this problem (Stowers and Schwarz, 1999; Newsome et al., 2000a). In order to produce somatic eye clones, an enhancer region of the early expressing gene, *eyeless*, is used to express the yeast *FLP recombinase* (*FLP*) gene in the developing eye (Newsome et al., 2000a). FLP induces site-specific recombination between *FRT* sequences. In the system used here, one *FRT* chromosome carried a mutation in the *dri* gene while the homologous chromosome contained a *FRT* sequence proximal to a recessive cell lethal (*cl2R11.5*). In the presence of *eyFLP*, recombination between the *FRT* sites on non-sister chromatids, followed by mitotic segregation, can result in one cell being homozygous for the mutation in *dri* while the sister cell is homozygous for the recessive cell lethal, *cl2R11.5* (Figure 4.1). The cell that contains the recessive cell lethal undergoes apoptosis. The end result of many such events is that cells homozygous for the mutation in the *dri* gene constitute between 80 and 95 percent of the adult eye (Newsome et al., 2000a) (Figure 4.1). This chapter discusses the phenotypes that result from the loss of Dri during eye development.

## 4.2 Results

### *4.2.1 The loss of Dri in the eye results in blindness*

The external morphology of *dri* mutant eye mosaics appeared normal, indicating as expected from the expression pattern that *dri* is not required for eye formation. To determine if Dri had a more subtle role in eye development, the function of the differentiated organ, vision in the adult fly, was examined.

## Figure 4.1 Creating somatic mutant clones that spanned the entire eye

The enhancer region of *eyeless* is utilised to express *FLP*. The FLP protein causes double stranded breaks at *FRT* sites. These double stranded breaks can lead to recombination between the chromatids of homologous chromosomes. One chromosome carries a mutation in *dri* (*FRT42Ddri*$^{2}$) while the other chromosome carries a recessive cell lethal (*FRT42Dcl2R11.5*). Recombination between the chromatids can result in a cell that is homozygous for *dri* and a twin spot that is homozygous for *cl2R11.5*. The cell that is homozygous for *dri* becomes a part of the adult eye. The cell that is homozygous for the *cl2R11.5* chromosome will undergo apoptosis. Those cells that are heterozygous will be progressively lost in further rounds of recombination until between 80 and 95 percent of the adult eye is mutant for *dri*.

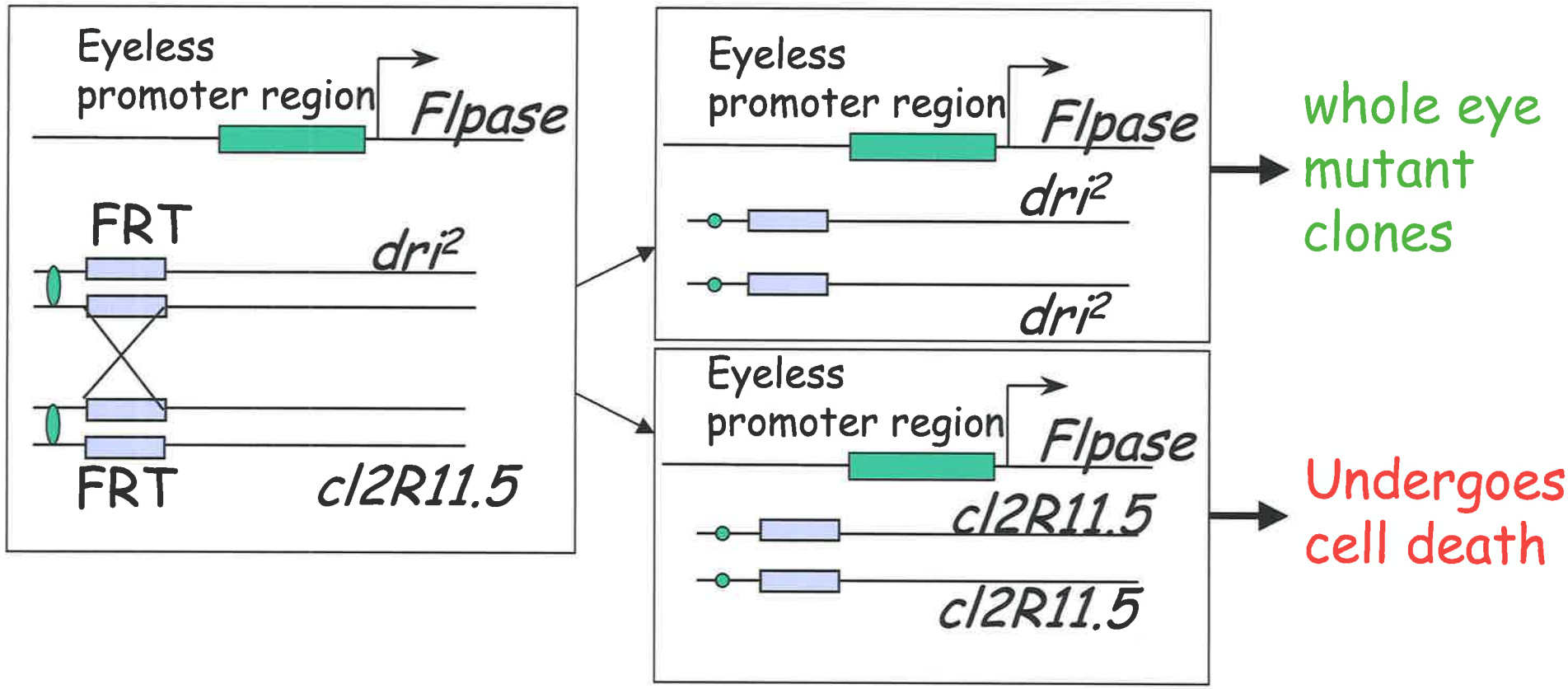
Eyeless
promoter region
Flpase
FRT
dri2
FRT
cl2R11.5
Eyeless
promoter region
Flpase
dri2
dri2
whole eye
mutant
clones
Eyeless
promoter region
Flpase
cl2R11.5
cl2R11.5
Undergoes
cell death

Vision was analysed by exposing the flies to a pulse of light, and measuring the subsequent electrical current between electrodes in the eye and thorax of the fly to generate an electroretinogram (Wes et al., 1999). The electroretinograms were performed by Dr Len Kelly of the University of Melbourne. The light causes modification of the Rhodopsins (G coupled receptors of light) within the membrane of the rhabdomeres, activating the light pathway, resulting in an influx of calcium into the cell (see section 1.7.2 for further details). The influx of calcium causes depolarisation of the cell, which sends a signal down the axons to the monopolar neurons, the synaptic partners of the R cell axons. This depolarisation leads to a current being produced that is represented in the electroretinograms. When comparing the difference in electroretinograms between one-week old *FRT42D* control flies and one-week old flies with eye clones of two different mutant alleles of *dri*, the off-transients (the depolarisation observed when the light is switched off) in the *dri* mutant eye mosaics flies were significantly reduced (Figure 4.2 A, B and C). Loss of the off-transient indicates that Dri is essential for visualisation of white light. This conclusion was confirmed using a behavioural test, the optomotor response test. This involves a rotating drum with black and white stripes, which is illuminated from the outside. If the eye is functional then the flies will fly in the direction of the rotating drum, however *dri* mutant eye mosaics failed to exhibit this phenomenon (L. Kelly, personal communications) and therefore *dri* is vital for vision in the *Drosophila* eye. Blindness due to the lack of Dri protein could result if components of the visual system were not differentiated correctly. At the third larval instar stage, differentiation of the R cells and the monopolar neurons occurs and the R cell axons are targeted from the eye disc to the optic lobe. If any of these processes are disrupted then it could lead to the blindness observed in *dri* mutant eye mosaic flies. These processes were therefore investigated further.

### *4.2.2 The loss of Dri does not affect the differentiation or fate of the photoreceptor cells*

Firstly, I examined whether the loss of Dri in the developing eye affected the specification of the photoreceptor cells. To investigate whether the normal array of photoreceptor cells occurred, the pattern of Elav, a neural marker expressed in the nuclei of all photoreceptor cells, was investigated in eye imaginal discs from *FRT42D* controls that contained no mutation and from *dri* mutant eye mosaics. The results showed that all of the photoreceptor cells appear to form correctly in the absence of Dri (Figure 4.3 A and B). To ensure that all the photoreceptor cell types within the ommatidium were forming, the expression of marker genes for the first and last differentiated photoreceptor cells was investigated.

## Figure 4.2 *dri* mutant eye mosaic animals are blind

Electroretinograms of (**A**) *FRT42D* control (*eyFLP;FRT42D/FRT42lcl2R11.5*) flies, (**B**) $dri^1$ mutant eye mosaic (*eyFLP;FRT42Ddri*$^1$*/FRT42Dcl2R11.5*) flies and (**C**) $dri^2$ mutant eye mosaic (*eyFLP;FRT42Ddri*$^2$*/FRT42Dcl2R11.5*) flies. The average off-transient amplitude (indicated by the arrow) for the *FRT42D* control animals was 3.8mV (**A**). The average off-transient amplitudes of two *dri* alleles were 0.68 and 1.32mV respectively (**B** and **C**), indicating that the vision of the *dri* mutant eye mosaic animals is impaired. Note that the scale for the Y-axis for $dri^2$ (**C**) is different from the *FRT42D* control.

**A**

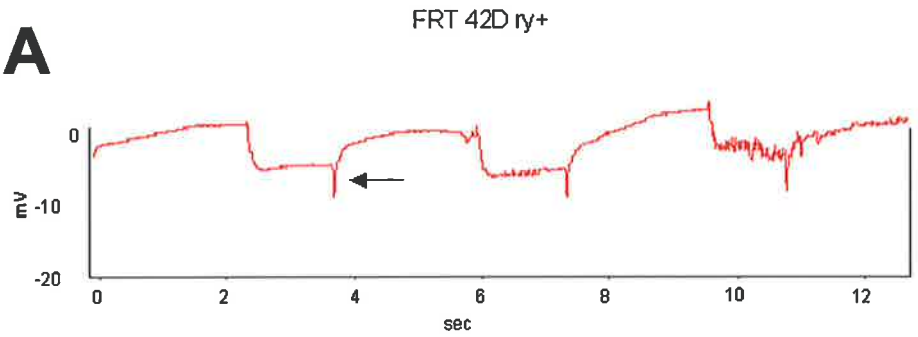


**Average off-transient amplitude = 3.8mV**

**B**

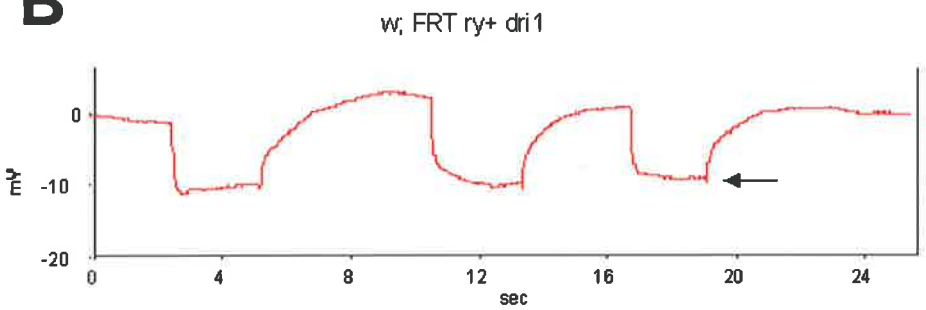


**Average off-transient amplitude = 0.68mV**

**C**

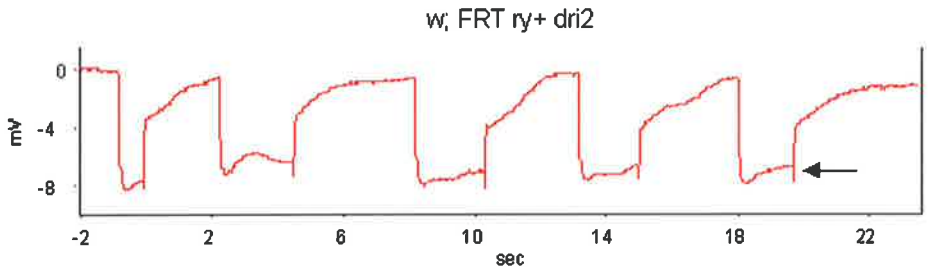


**Average off-transient amplitude = 1.32mV**

## Figure 4.3 The R cells are specified normally in *dri* mutant eye mosaics

(**A**) A *FRT42D* control (*eyFLP;FRT42D/FRT42Dcl2R11.5*) third larval instar eye imaginal disc stained with anti-Elav (in green) and anti-Dri (in red) antibodies, showing that Elav is expressed in all photoreceptor cells (as indicated by the arrow). (**B**) A *dri* mutant mosaic eye imaginal disc (*eyFLP;FRT42Ddri*$^{2}$*/FRT42Dcl2R11.5)* stained with anti-Elav (in green) and anti-Dri (in red) antibodies. All photoreceptor cells are specified correctly in cells not staining with the Dri antibody (as indicated by the arrow). (**C**) A *FRT42D* control third larval instar eye disc stained with anti-Boss (in green) (as indicated by the arrow) and anti-Dri (in red) antibodies, showing that Boss is expressed in R8 cells in a regular pattern. (**D**) A *dri* mutant eye mosaic eye imaginal disc stained with anti-Boss (in green) (as indicated by the arrow) and anti-Dri (in red) antibodies showing that, like the control, R8 cells are present in a regular pattern even in the most posterior ommatidia. (**E**) A *FRT42D* control third larval instar eye disc stained with anti-Prospero (in green) and anti-Dri (in red) antibodies, showing that Prospero is expressed in R7 cells (arrow) in a regular pattern. (**F**) A *dri* mosaic eye imaginal disc stained with anti-Prospero (in green) and anti-Dri (in red) antibodies, showing that R7 cells are specified correctly (as indicated by the arrow) and their fate maintained in the absence of Dri.

In all images the morphogenetic furrow is to the left hand side of the image.

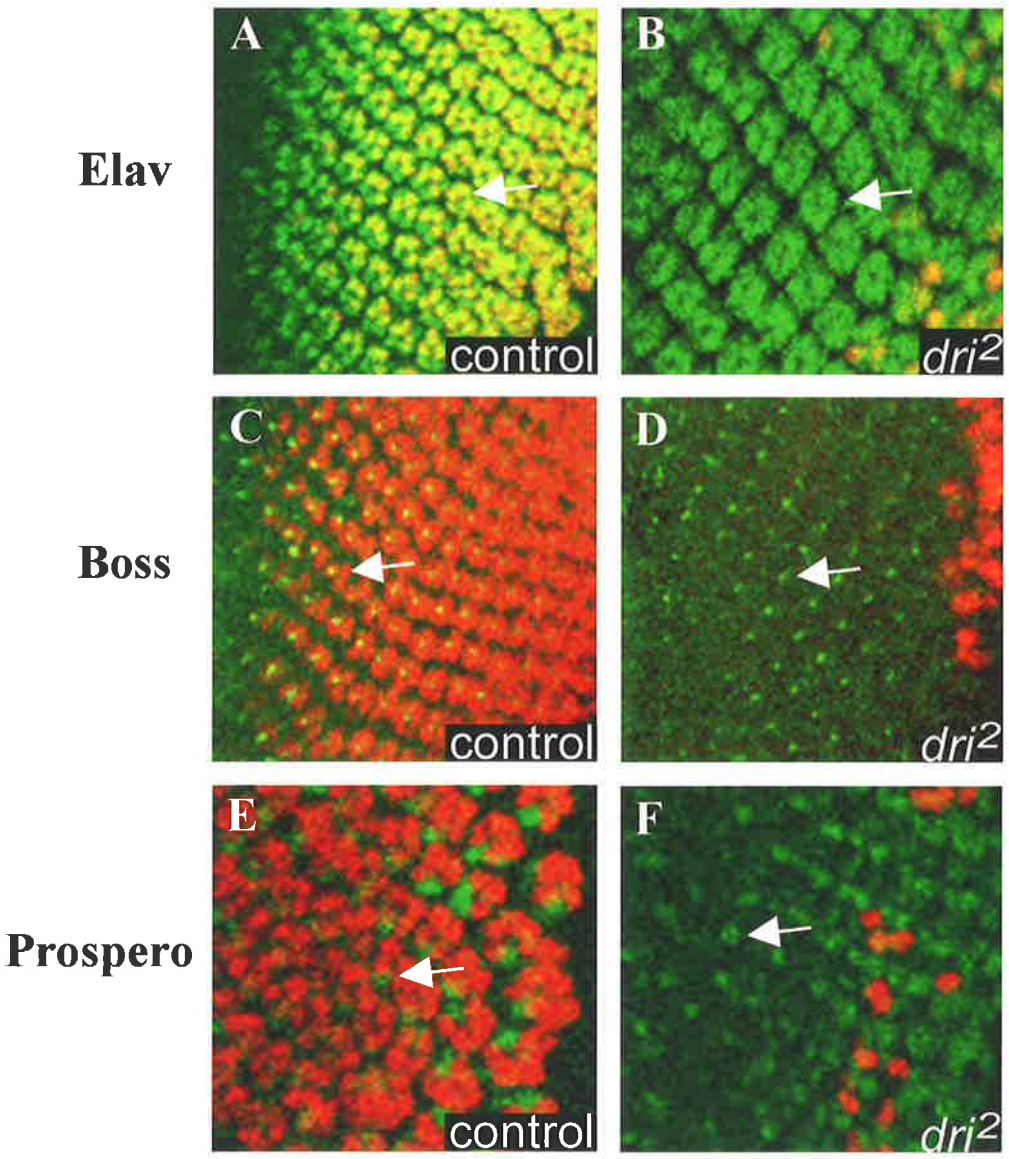
Elav
Boss
Prospero
A
control
B
dri2
C
control
D
dri2
E
control
F
dri2

Boss is a seven trans-membrane domain-containing protein that is expressed solely in R8 cells, the first R cell differentiated (Hart et al., 1990; Kramer et al., 1991), and therefore is an appropriate marker for this cell type. Immunofluorescence staining of third larval instar eye imaginal discs with anti-Boss and anti-Dri antibodies showed that Boss was expressed in both the *FRT42D* controls and *dri* mutant eye mosaics. I conclude, therefore, that R8 cells form correctly in *dri* mutant eyes (Figure 4.3 C and D). Similarly, when the pattern of R7 cells (the last photoreceptor cell differentiated) was examined, using anti-Prospero and anti-Dri antibodies, no difference was observed between the *FRT42D* control and *dri* mosaic mutant eye imaginal discs. Thus, R7 cells also formed normally in the absence of Dri (Figure 4.3 E and F). Given that the differentiated first and last photoreceptor cells appear to have formed correctly and the R cell cassette, as determined by Elav staining, appears normal, it is likely that R1-R6 cells also form in the absence of *dri*. Since Prospero is also expressed in the developing cone cells, differentiation of this non-neuronal cell type could also be examined with the anti-Prospero antibody. As expected, given that *dri* is not expressed in this cell type (see chapter 3.2.1), the normal array of cone cells was present in *dri* mutant eye mosaics (data not shown). Thus the R cells and cone cells appear to form correctly in the absence of Dri.

The fact that Dri is not required for the specification of photoreceptor cells during the third larval instar stage is consistent with *dri* expression initiating several rows behind the morphogenetic furrow. Furthermore, the continued expression of *dri* into the pupal and adult stages (see section 3.2.1) is consistent with Dri having a later role, such as maintaining cell fate or regulating later aspects of R cell differentiation. Given that the cells that are in the most posterior region of the eye disc are older than the cells directly behind the morphogenetic furrow, they could be examined to see if *dri* was important for maintaining cell fate. The spacing of the R8 cells in the posterior of the eye disc in *dri* mutant eye mosaics indicated that this cell type maintained its fate (Figure 4.3D). Likewise, R7 cells appeared to maintain their fate in the absence of Dri (Figure 4.3 F).

To observe in more detail any effects of loss of Dri on eye morphology, the external morphology and the internal structure of the ommatidia of adult mutant eyes were examined. The external morphology of the eye was examined by scanning electron microscopy (SEM). There was no distinguishable difference in external morphology between the adult eyes of *dri* mutant eye mosaics or *FRT42D* control animals (Figure 4.4 A and B), adding further support to the observation that differentiation of the eye had occurred normally in the absence of Dri. However, examination of the ommatidial structure at eclosion via tangential sections of the eye revealed minor defects.

## Figure 4.4 The structure of the *dri* mosaic adult eye is relatively normal

(**A-B**) Scanning electron microscopy of adult eyes (A) A *FRT42D* control (*eyFLP;FRT42D/FRT42Dcl2R11.5*) eye showing a regular array of ommatidia. (**B**) An adult *dri* mutant mosaic eye (*eyFLP;FRT42Ddri*$^{2}$*/FRT42Dcl2R11.5*) is indistinguishable from control flies with the same regular array of ommatidia. (**C**) Schematic representation of an ommatidium within the adult *Drosophila* eye. The left hand fissure shows a longitudinal section of an ommatidium. Rh: rhabdomere. PP, SP and TP: primary, secondary and tertiary pigment cells. CC: cone cells. L: lens, B: bristle cell, A: photoreceptor cell axon M: basal membrane. On the right hand side are cross sections at three positions along the apical-basal axis of the ommatidium. AC, PC, EQC and PCL referred to the position of the cone cells (AC is the anterior cone cell, PC is the posterior cone cell, EQC is the equatorial cone cell and PLC is the polar cone cell. The second cross section is through the apical part of the R cell region of the ommatidium. The R7 rhabdomere (in green) is positioned between the R1 and R6 rhabdomere (in pink). In the more basal section the R8 rhabdomere (in red) lies between R1 and R2 (in pink). (Image reproduced from Dickson and Hafen, 1993) (**D**) Tangential section through an adult eye of a *FRT42D* control fly. The R8 rhabdomeres (arrow) are present in all ommatidia in this focal plane. (**E**) Tangential section through an adult *dri* mosaic eye. Both R7 and R8 rhabdomeres are observed within the one ommatidium (indicated by the arrows). (**F**) A tangential section through an adult *FRT42D* control eye. The orientation of each ommatidium is marked with magenta lines and all ommatidia are pointing in the same direction. (**G**) Tangential section through an adult *dri* mosaic mutant eye. The orientation of the ommatidia within the *dri* mosaic eye is marked with magenta lines and the arrowhead indicates a slightly mis-orientated ommatidium.

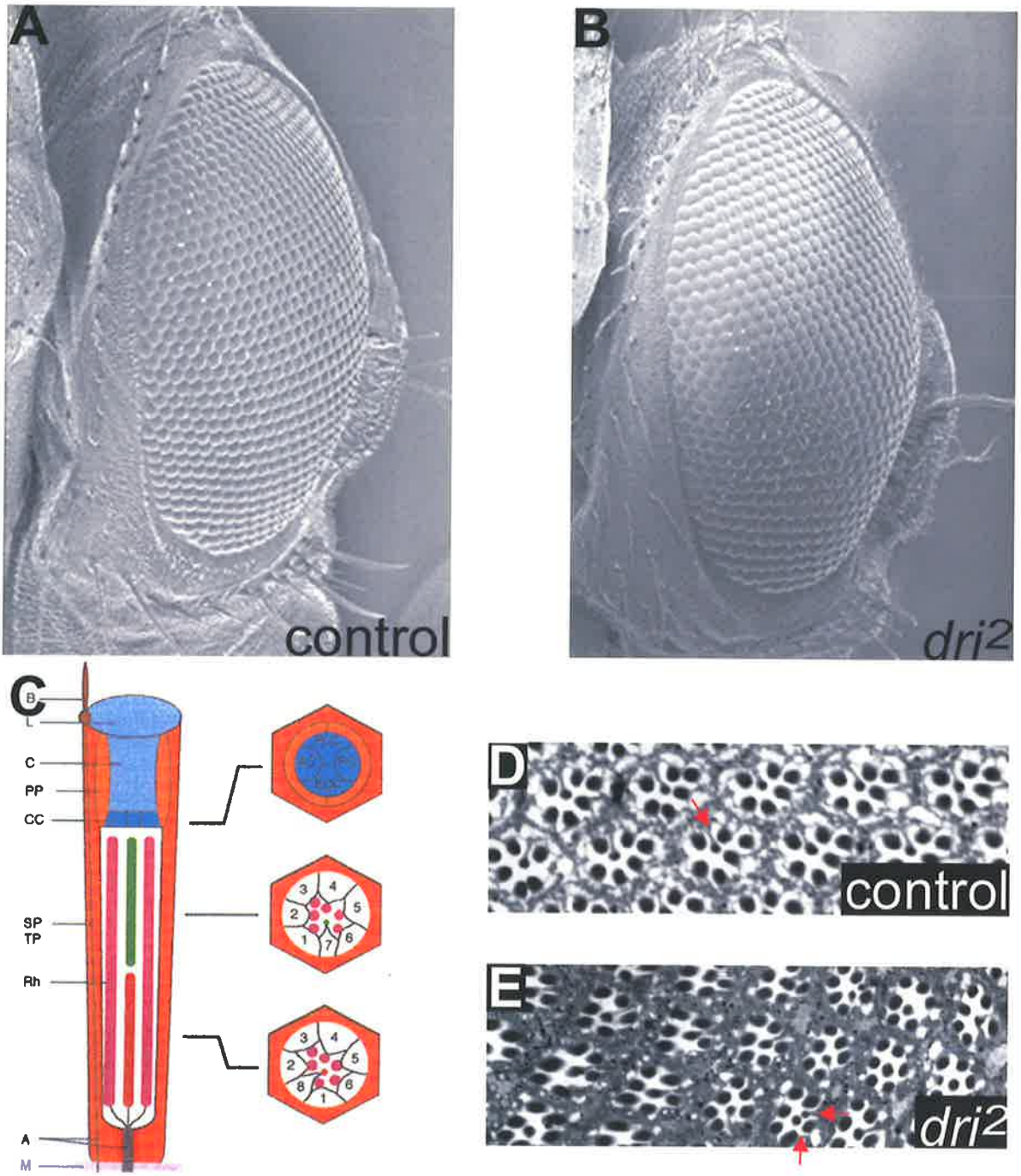
A
control
B
dri2
C
B
L
C
PP
CC
SP
TP
Rh
A
M
1
2
3
4
5
6
7
8
D
control
E
dri2
F
control
G
dri2

In wild type sections, each ommatidium exhibits six outer rhabdomeres (R1 to R6) and either the R7 or R8 rhabdomere depending on the plane of sectioning (Figure 4.4 C). In apical sections, the smaller R7 rhabdomere is located between the R1 and R6 cells (Figure 4.4 C). In basal tangential sections, the R8 rhabdomere is located between the R1 and R2 cells, forming a different trapezoidal arrangement (Figure 4.4 C and D). However, in *dri* mutant eye mosaics, approximately 20 percent of the ommatidia (82 out of the 354 ommatidium scored) showed two inner R cells at the same focal plane (Figure 4.4 E). These rhabdomeres were smaller than those of the outer R cells and the position of these rhabdomeres were consistent with these two cells corresponding to R7 and R8 cells. A mild orientation defect was also observed in a small number of ommatidia in tangential sections from *dri* mutant mosaics eyes (Figure 4.4 F and G). However, both the occasional abnormal inner R cell within an ommatidium and the orientation defect are unlikely to result in blindness of *dri* mutant eye mosaic flies.

### *4.2.3 The monopolar neurons are differentiated in the absence of Dri*

The monopolar neurons are located in the lamina and receive the light signal from the R1-R6 cell axons. If this cell type is not formed, the adult fly will be blind. At the third larval instar stage of development, the differentiation of the monopolar neurons is dependent on the innervation of the R cell axons (Huang et al., 1998). A Hedgehog signal is carried on the R cell axons, which induces the lamina precursor cells to undergo their final division. This event corresponds with the expression of Dachshund, so that these cells can be visualised with an anti-Dachshund antibody (Huang et al., 1998/ Figure 4.5 A). A subset of these neuronal precursor cells will differentiate to form the monopolar neurons, and therefore express the neural specific protein, Elav (Huang et al., 1998/ Figure 4.5 A). In the absence of Dri the lamina precursor cells expressed Dachshund and a subset of those cells became the monopolar neurons as visualised with anti-Elav antibody staining (Figure 4.5 B). Therefore I conclude that the monopolar neurons formed correctly in the absence of Dri and this cannot be the reason for the blindness observed in *dri* mutant eye mosaic flies.

### *4.2.4 Axon projections are disrupted in the absence of Dri*

Vision requires R cell axons to innervate the correct layer of the optic lobe. The possibility that the loss of Dri may be disrupting this connection was investigated in collaboration with Dr B. Dickson and Dr K-A. Senti. The results presented here are my own data.

## Figure 4.5 The specification of the monopolar neurons is unaffected in the absence of Dri

(**A-B**) A third larval instar brain stained with anti-Dachsund (green), which stains the lamina precursor cells (LPC), and anti-Elav (red), which stains cells that have differentiated into neuronal cells. (**A**) The normal pattern of LPCs and neuronal cells in a *FRT42D* control (*eyFLP;FRT42D/FRT42Dcl2R11.5*) brain. (**B**) A *dri* mutant eye mosaic (*eyFLP;FRT42Ddri$^{2}$/FRT42Dcl2R11.5*) brain showing the normal distribution of Dachsund and Elav-expressing cells.

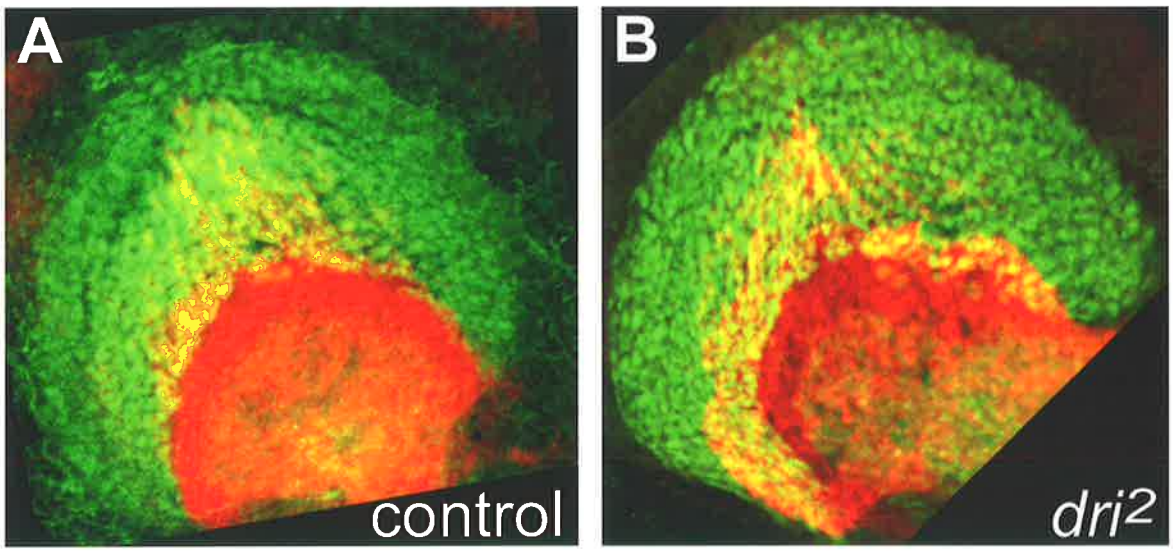
A
control
B
dri2

At the third larval instar stage, axons from the newly differentiated photoreceptor cells bundle at the basal surface of the eye disc and innervate the optic lobe via the optic stalk (reviewed by Meinertzhagen and Hanson, 1993) (Figure 4.6 A). The R8 axons, which are the first axons to innervate the optic lobe, terminate in the second ganglion, the medulla. R1 to R6 axons enter next and terminate in the first optic ganglion, the lamina, thus creating the lamina plexus (Figure 4.6 A as indicated by the black brackets). To investigate whether axon innervation was occurring normally in *dri* mutant eye mosaic animals, third larval instar eye-brain complexes were immunohistochemically stained with the monoclonal antibody mAb 24B10, which recognises the R8 and R1-R6 axons at this stage. The staining revealed that in *dri* mutant eye mosaics, the lamina plexus was not as well defined as in wild type (compare Figure 4.6 A, B and C) with gaps appearing in the lamina plexus, as indicated by the arrows, and some axons terminating prematurely, as indicated by the arrowhead. The severity of this phenotype varies between alleles. In Figure 4.6 C the eye-brain complex was from an earlier stage than shown in Figure 4.6 B, but nevertheless has a more severe phenotype. Therefore, during the third larval instar stage of eye development, Dri plays a role in the innervation of the optic lobe by axons from the eye.

### *4.2.5 R8 axons are targeted to the correct layer in the absence of Dri*

To gain a more precise description of the *dri* mutant eye mosaic phenotype, R8 axons were visualised by expressing a fusion of a Myc peptide and the microtubule-binding protein, Tau (τ), specifically in R8 cells using an enhancer region of the R8-specific gene *atonal* (Senti et al., 2003). Immunofluorescence staining with the anti-Myc antibody on *dri* mutant eye mosaic eye-brain complexes revealed that the R8 axons terminated in the correct layer, the medulla, but did not appear to have attached correctly to the target area (Figure 4.7 B and B'). In the *FRT42D* control eye-brain complexes, the growth cones of the R8 axons formed an "inverted Y" shape (Figure 4.7 A and A'), but in the absence of Dri this structure is not formed correctly and in some cases not formed at all (Figure 4.7 B and B'). This phenotype was also seen when a *lacZ* marker was expressed in all the R cell axons using a *glass* enhancer region (Newsome et al., 2000a). In the wild type axons, R8 formed the "inverted Y" shape (Figure 4.7 C and C'), but in *dri* mutant eye mosaic brains, β-galactosidase accumulated abnormally at the growth cones of the R cell axons and the "inverted Y" shape was not observed (Figure 4.7 D and D'). In the adult optic lobe the R8 axons terminate in the M3 layer of the medulla (Figure 4.7 E). These axons were visualised by expressing the *UAS τlacZ* construct in approximately 70 percent of R8 cells using a Rhodopsin 6 enhancer region to express Gal4 (Senti et al., 2003). The Gal4 transcription factor in these R8 cells binds to the UAS site and induces expression of the *τlacZ* construct.

## Figure 4.6 R cell axon targeting in *dri* mutant eye mosaics is disrupted

Third larval instar eye-brain complexes were dissected from (**A**) a *FRT42D* control animal (*eyFLP;FRT42D/FRT42Dcl2R11.5*), (**B**) a $dri^2$ mutant eye mosaic (*eyFLP;FRT42Ddri*$^2$*/FRT42Dcl2R11.5*) animal and (**C**) a $dri^3$ mutant eye mosaic (*eyFLP;FRT42Ddri*$^3$*/FRT42Dcl2R11.5*) animal and immunohistochemical staining was performed with anti-mAb24B10 antibody. The lamina plexus, indicated by brackets, is disrupted in both (**B**) and (**C**). The arrows indicate gaps within the lamina plexus and the arrowheads show axons that have terminated before the lamina plexus. os: optic stalk, me: medulla.

The $dri^3$ allele was isolated in Dr. Barry Dickson's laboratory.

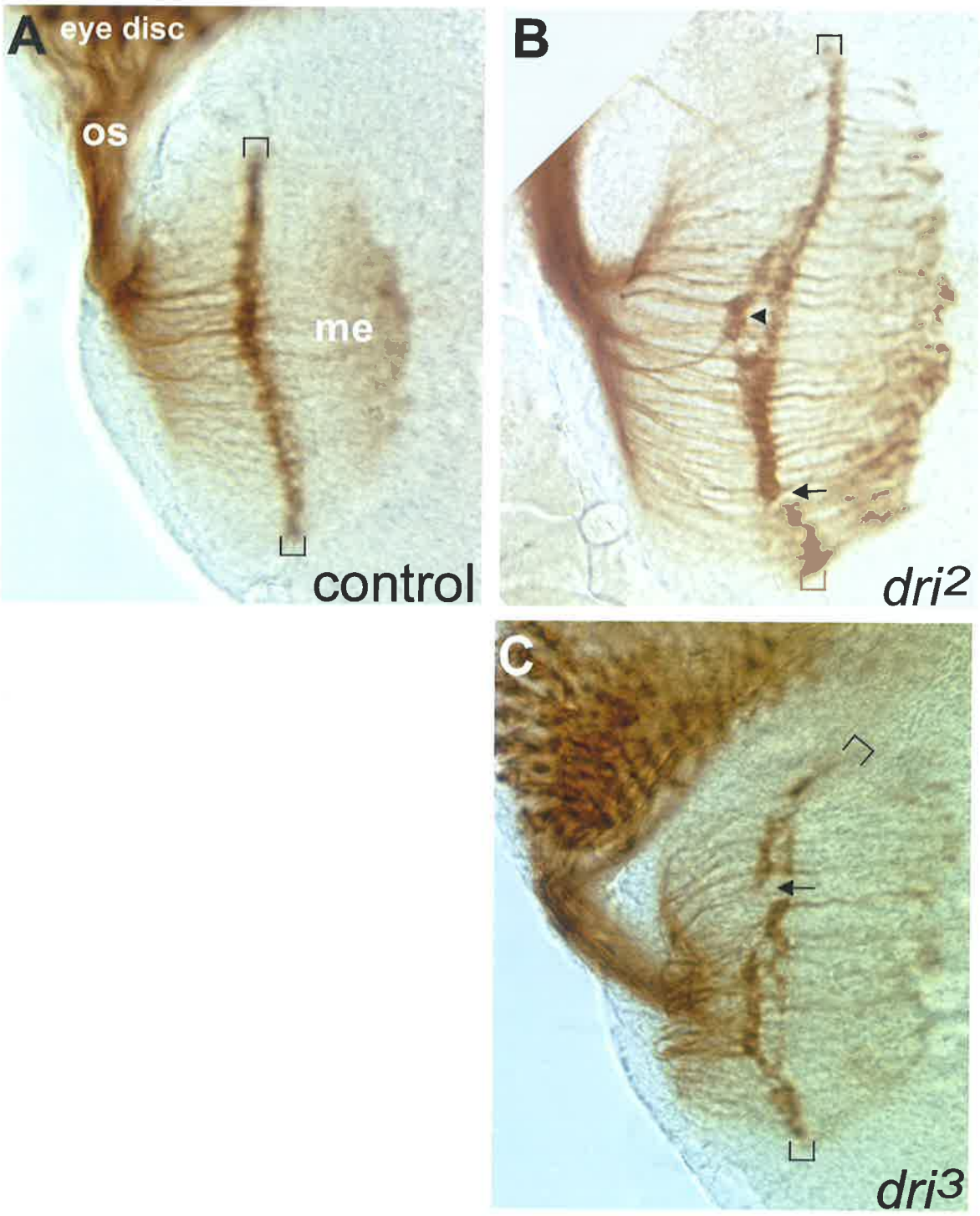
A
eye disc
os
me
control
B
dri2
C
dri3

## Figure 4.7 R8 axon growth cone shape is disrupted in *dri* mutant eye mosaics

(**A-B**) Third larval instar eye-brain complexes in which the *atonal* enhancer drives the expression of a Myc-τ fusion protein in R8 cells. τ is a microtubule binding protein. The fusion protein is stained with anti-MYC antibodies to highlight all R8 cells (Senti et al, 2003) (**A**) In a *FRT42D* (*eyFLPatoτmyc;FRT42D/FRT42Dcl2R11.5*) control brain, R8 axons terminate at the medulla and the growth cones form an "inverted-Y" shape (arrow). (**A'**) A higher magnification of the boxed region in **A**. (**B**) In a *dri* mutant eye mosaic (*eyFLPatoτmyc;FRT42Ddri*$^{2}$*/FRT42Dcl2R11.5*) the R8 axons terminate in the medulla but many growth cones do not form this "inverted-Y" shape correctly, and some not at all, as indicated by the arrow. (**B'**) A higher magnification view of the boxed region in **B**.

(**C-D**) The *glass* enhancer region was utilised to express *lacZ* in all R cell axons, which were visualised using an anti-β-galactosidase antibody. (**C**) A *FRT42D* control (*eyFLP glass-lacZ;FRT42D/FRT42Dcl2R11.5*) brain complex showing that the growth cones of R8 axons form an inverted-Y shape (arrow) when terminated. (**C'**) A higher magnification view of the boxed region in **C**. (**D**) A *dri* mutant eye mosaic (*eyFLP glass-lacZ;FRT42Ddri*$^{2}$*/FRT42Dcl2R11.5*), showing that the R8 cell growth cones are misshaped (arrow). (**D'**) A higher magnification view of the boxed region in **D**.

The lamina plexus is indicated by the brackets, ed: eye disc, os: optic stalk, me: medulla.

(**E-F**) Horizontal sections through adult heads expressing a *τlacZ* marker gene in the Rh6 expression pattern, visualised by staining with anti-β-galactosidase (in green) antibody and the mouse monoclonal antibody 22C10, which highlights all axons (in red). (**E**) A section of a *FRT42D* control (*eyFLP;FRT42D/FRT42Dcl2R11.5;Rh6-Gal4/UASτlacZ*) adult head showing that the R8 axons terminate in the M3 layer of the medulla (indicated by the arrowhead). (**F**) A section of a *dri* mutant mosaic eye (*eyFLP;FRT42Ddri*$^{3}$*/FRT42Dcl2R11.5;Rh6-Gal4/UASτlacZ*) showing that the R8 axons terminate in the M3 layer of the medulla (indicated by the arrowhead) but the array of R8 axons is slightly disrupted.

la: lamina, me: medulla. M3 and M6 layers of the medulla are indicated by arrows.

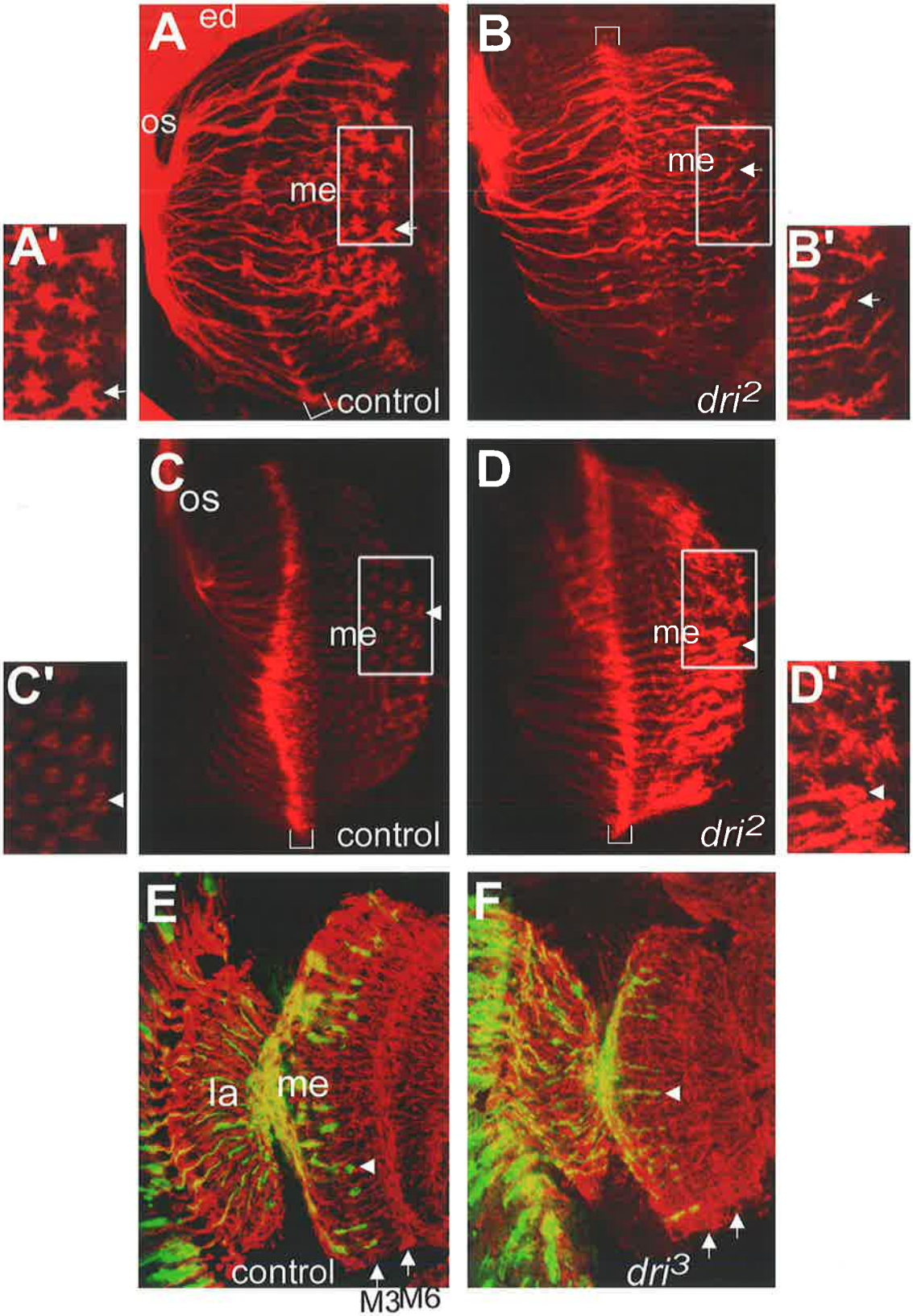
A
ed
os
me
control
B
me
dri2
A'
B'
C
os
me
control
D
me
dri2
C'
D'
E
la
me
control
M3
M6
F
dri3

In *dri* mutant eye mosaic animals the R8 axons attached to the M3 layer of the medulla (Figure 4.7 F). It appears that the initial incorrect growth cone shape of the R8 cells had no affect on the position of these axons. However, it is unknown if the R8 axons are able to function normally in *dri* mutant eye mosaic animals.

### *4.2.6 R1-R6 axons pass through to the medulla in* dri *mutant eye mosaics*

To further characterise the axonal defects observed at the lamina plexus in Figure 4.6, the targeting of R1-R6 axons in *dri* mutant eye mosaics was investigated. A subset of R1 to R6 axons was visualised using *τlacZ* expressed under the control of the *rough* enhancer region (Garrity et al., 1999; Senti et al., 2000). Rough is expressed in the R2 and R5 photoreceptor cells (Kimmel et al., 1990), so the axons of these R cells were visualised using immunofluorescence staining with anti-β-galactosidase antibody. Unlike *FRT42D* control R1-R6 axons (Figure 4.8 A), in the absence of Dri a subset of these axons did not terminate in the correct layer, the lamina, but passed through to the medulla (Figure 4.8 B). Therefore Dri is required for the R1-R6 axons to terminate in the lamina.

### *4.2.7 Glial cell migration is not the reason for the R1-R6 targeting defects in* dri *mutant eye mosaics*

Under normal conditions the R1-R6 axons terminate in the lamina plexus, which also contains the lamina glial cells and monopolar neurons. It has been established that disruption in the migration of the lamina glial cells will result in a disruption of the R1-R6 axons terminating in the lamina (Perez and Steller, 1996; Huang et al., 1998; Poeck et al., 2001; Suh et al., 2002). Interestingly, Suh and colleagues (2002) have shown that a signal from the R cells is required for the migration of the lamina glial cells. Dri is expressed in a subset of longitudinal glial cells in the *Drosophila* embryo and *dri* mutant embryos exhibit defects in glial cell migration and formation of the axon tract in the CNS (Shandala et al., 2003). Although Dri expression could not be detected in the lamina glial cells in the larval brain (Shandala et al., 2002) (Figure 4.9 A and B), it was important to identify if a signal from the R cells was disrupted in *dri* mutant eye mosaics, resulting in the lamina glial cells not migrating to the lamina plexus and, consequently, leading to the R1-R6 axon pass-through phenotype. Therefore the migration of the lamina glial cells was investigated using an anti-Repo antibody, which stains glial cells. In *dri* mutant eye mosaics, like *FRT42D* controls, the lamina glial cells migrated to the lamina plexus (Figure 4.9 C and D). Thus *dri* is not required for the migration of the lamina glial cells to the lamina plexus and this was not the reason for the aberrant termination of R1-R6 axons.

## Figure 4.8 A subset of R1-R6 axons terminate in the medulla

(**A-B**) Third larval instar eye-brain complexes expressing the marker gene *lacZ* fused to the microtubule binding protein *tau*, expressed in the R2 and R5 cells using a *rough* enhancer. Anti-β-galactosidase antibody stains the R2 and R5 axons (in green). Monoclonal antibody 24B10 stains all R cell axons (in red). The lamina is indicated by the bracket. os: optic stalk, me: medulla. (**A**) A *FRT42D* control (*eyFLP;FRT42D/FRT42Dcl2R11.5;ro-lacZ*) eye-brain complex showing R2 and R5 axons terminating in the lamina. (**B**) A *dri* mutant eye mosaic (*eyFLP;FRT42Ddri$^{3}$/FRT42Dcl2R11.5;ro-lacZ*) eye-brain complex showing a subset of R2 and R5 axons passing through to the medulla..

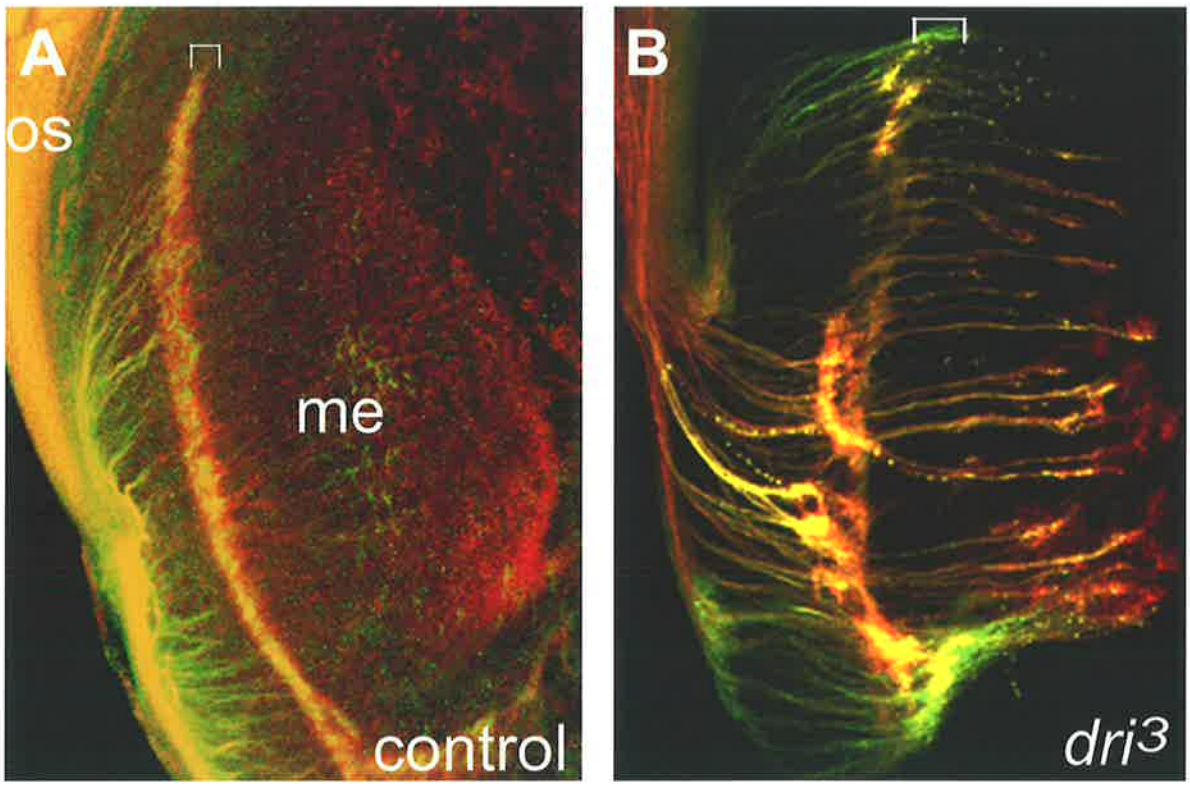
A
os
me
control
B
dri3

## Figure 4.9 Lamina glial cell migration occurs normally in the absence of Dri

(**A-B**) A third larval instar brain from a *FRT42D* control (*eyFLP;FRT42D/FRT42Dcl2R11.5*) animal dissected and immunohistochemically stained with anti-Dri antibody. (**A**) Dri is not located in the optic lobe where the axons innervate the brain. The arrows indicate the lamina plexus. (**B**) At a deeper focal plane than (**A**) showing a subset of cells in which Dri is found (arrow).

(**C-D**) Third larval instar eye-brain complexes were dissected and immunofluorescence staining performed with an anti-Repo antibody (in green), to stain the lamina glial cells, and mAB22C10 antibody (in red) to highlight the R cell axons. (**C**) A control *FRT42D* (*eyFLP;FRT42D/FRT42Dcl2R11.5*) eye-brain complex showing the migration of the lamina glial cells to the lamina plexus (arrow). (**D**) A *dri* mutant eye mosaic (*eyFLP;FRT42Ddri*$^{2}$*/FRT42Dcl2R11.5*) eye-brain complex showing that lamina glial cells migrate normally into the lamina plexus (arrow).

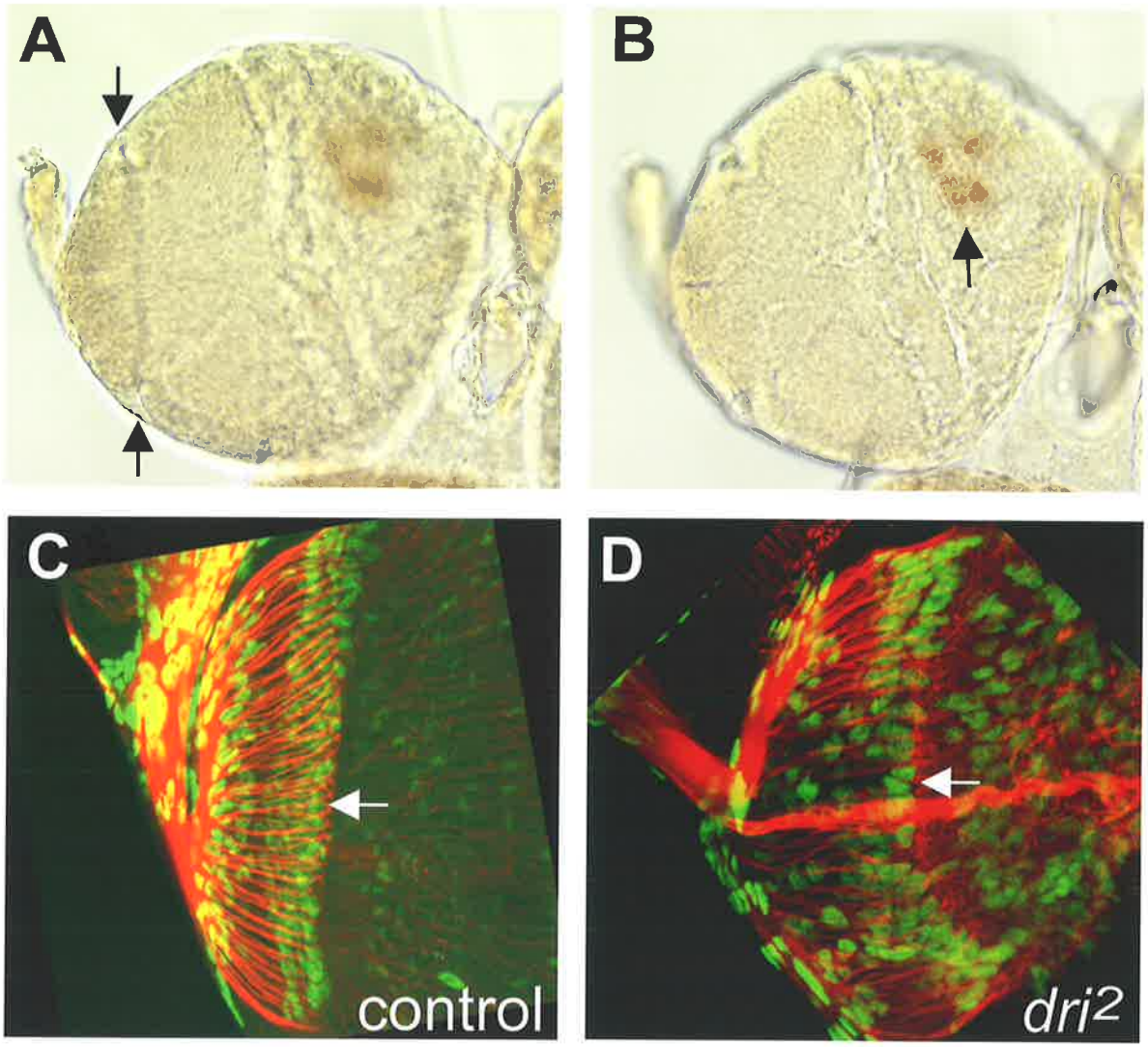
A
B
C
control
D
dri2

### *4.2.8 Dri does not regulate runt expression*

Recently, a transcriptional hierarchy has been identified that is required for R1-R6 axons to terminate in the correct layer of the optic lobe. The *dri* mutant eye mosaic R1-R6 phenotype is similar to that of the zinc-finger nuclear factor, *brakeless* (*bks*), which is also required for the correct targeting of R1-R6 axons to the lamina (Rao et al., 2000; Senti et al., 2000). It has been demonstrated that the role of *bks* is to repress the expression of *runt* (*run*) in R2 and R5 cells (Kaminker et al., 2002). Run is a transcription factor (Kania et al., 1990; Canon and Banerjee, 2000), which is expressed exclusively in R7 and R8 cells (Kaminker et al., 2002, Figure 4.10 B). Misexpression of *run* in R2 and R5 cells results in all R1-R6 axons terminating in the medulla (as R2 and R5 axons are the lamina pioneering axons) (Kaminker et al., 2002). Given the similarity of phenotype between *bks* and *dri*, *dri* could be acting as a co-factor with *bks*, to suppress *runt* expression in R2 and R5 cells (Figure 4.10 A). Examination of Run expression, with an anti-Runt antibody, in *dri* mutant eye mosaics showed that this was not the case (Figure 4.10 B and C), indicating that the role of *dri* is not to suppress *run* expression in R2 and R5 cells. However, *dri* could be acting downstream of *run*, in which case the loss of Bks would derepress *run* expression in R2 and R5 cells, and result in the repression of *dri* in these cells (Figure 4.10 D). However, *bks* mutant eye mosaic imaginal eye discs stained with the anti-Dri antibody showed the normal *dri* pattern, including expression in seven R cells (Figure 4.10 E and F), indicating that *dri* is not downstream of Run. Therefore, I conclude that *dri* is involved in a different, but as yet unidentified, pathway to *bks* and *run*.

### *4.2.9 The adult axonal defects are mild in* dri *mutant mosaic eyes*

For the axonal defects that are observed in the larvae to be responsible for the blindness observed in *dri* mutant eye mosaic adult flies, these axonal defects must continue into the adult fly. The pattern of the adult axons was investigated using the *glass* enhancer region to express a marker gene, *lacZ*, in all R cell axons (Newsome et al., 2000a). Horizontal sections through both *FRT42D* control and *dri* mutant eye mosaic heads, followed by immunohistochemical staining with the anti-β-galactosidase antibody, were performed. In the adult eye the structure of the optic lobe is different from the third larval instar optic lobe. During pupal development, the lamina extends and the R8 and R7 axons terminate in different layers of the medulla. R8 axons terminate in the layer closest to the lamina, the M3 layer, while R7 axons terminate in the M6 layer of the medulla (Figure 4.11 A, indicated by arrows).

## Figure 4.10 *runt* expression is unaffected by the loss of Dri

(**A**) A schematic of the Brakeless-Runt pathway in R2 and R5 cells showing a possible function of Dri (grey arrows) co-operating with Bks to repress the expression of *run*.

Third instar eye imaginal discs were dissected and immunofluorescence staining was performed with anti-Runt (in green) and anti-Dri (in red) antibodies. (**B**) A *FRT42D* control (*eyFLP;FRT42D/FRT42Dcl2R11.5*) eye disc showing that Runt is expressed in R7 and R8 cells (arrows) and Dri is expressed in R8 but not R7 cells. (**C**) A *dri* mutant eye mosaic (*eyFLP;FRT42Ddri$^{2}$/FRT42Dcl2R11.5*) eye disc, showing that Runt continues to be expressed in R7 and R8 cells (arrows).

(**D**) A schematic diagram showing the possible repression of *dri* by Runt in R2 and R5 cells.

Third instar eye imaginal discs were dissected and immunohistochemical staining was performed with anti-Dri antibodies. (**E**) A *FRT42D* control (*eyFLP;FRT42D/FRT42Dcl2R11.5*) eye disc showing the normal *dri* pattern, with Dri found several rows behind the morphogenetic furrow (MF). (**F**) A *bks* mutant eye mosaic (*eyFLP;FRT42Dbks$^{2}$/FRT42Dcl2R11.5*) eye disc, showing that Dri, as in control, is expressed several rows behind the MF. The insert shows that Dri is found in seven R cells, which are indicated by the stars.

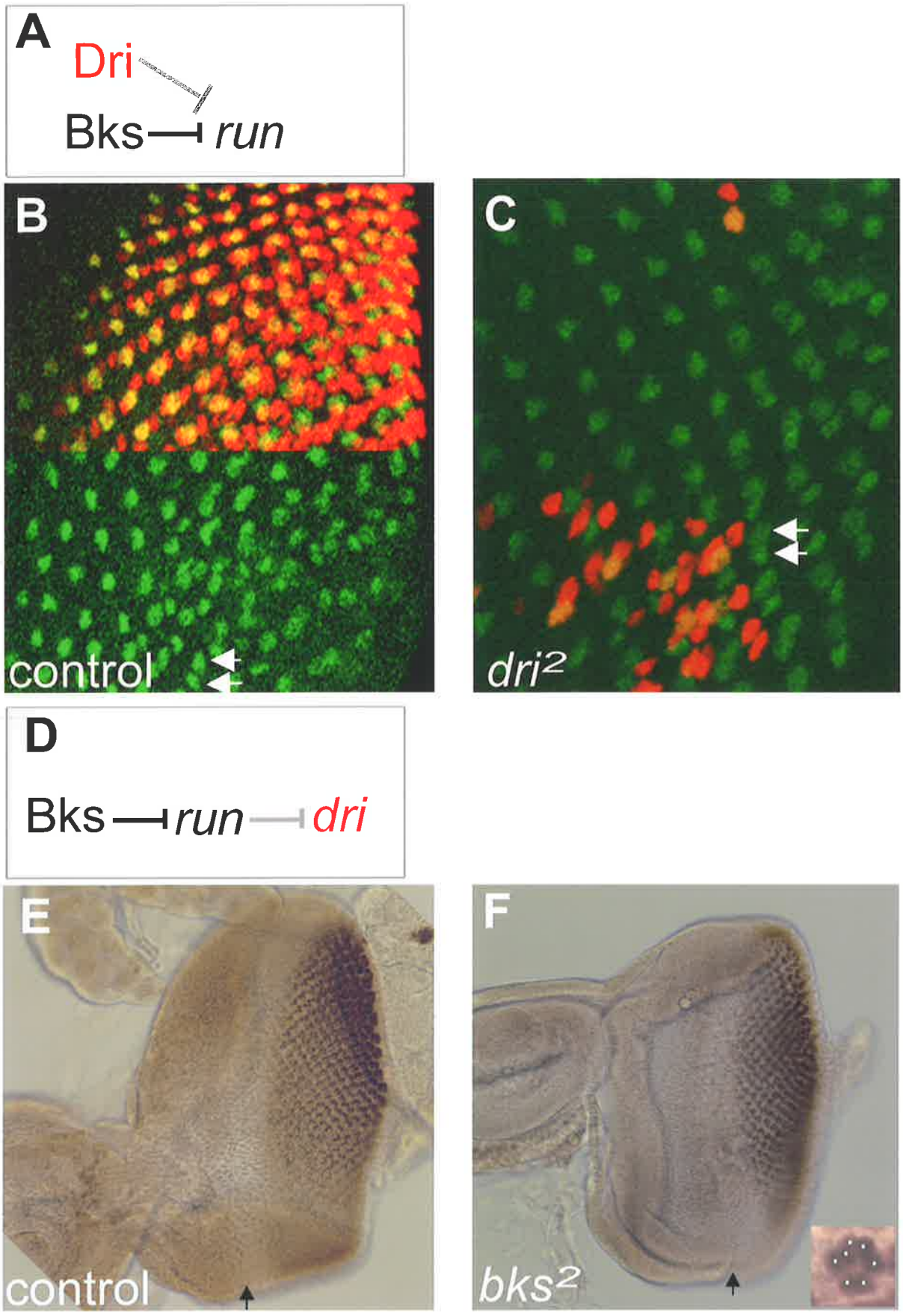
A
Dri
Bks
run
B
control
C
dri2
D
Bks
run
dri
E
control
F
bks2

## Figure 4.11 Loss of Dri results in mild adult axonal defects

(**A-B**) A horizontal section through adult heads that express *lacZ* driven by a *glass* enhancer region in all R cells stained with anti-β-galactosidase antibody. (**A**) A *FRT42D* control (*eyFLPglass-lacZ;FRT42D/FRT42Dcl2R11.5*) head showing the position of the lamina (as indicated by the arrowhead) and the medulla. The R8 axons terminate in the M3 layer, closest to the lamina while the R7 axons terminate in the M6 layer of the medulla (as indicated by the arrows). (**A'**) A higher magnification view of the boxed region in **A**. (**B**) A *dri* mutant eye mosaic (*eyFLPglass-lacZ;FRT42Ddri$^{3}$/FRT42Dcl2R11.5*) head showing that the M3 and M6 layers of the medulla are mildly disrupted. (**B'**) A higher magnification view of the boxed region in **B**. (**C-D**) Horizontal sections through adult heads where R1-R6 cells are expressing the τ-LacZ fusion protein driven by a Rh1 enhancer region. Anti-β-galactosidase (in green) antibody detects the R1-R6 axons while the monoclonal 22C10 antibody (in red) highlights all the axons in the brain. (**C**) A *FRT42D* control (*eyFLP Rh1-τLacZ;FRT42D/FRT42Dcl2R11.5*) head showing that the R1-R6 axons terminate in the lamina. (**C'**) A higher magnification view of the boxed region in **C**. (**D**) A *dri* mutant eye mosaic (*eyFLP Rh1-τlacZ;FRT42Ddri$^{1}$/FRT42Dcl2R11.5*) head showing that some R1-R6 axons terminate in both the M3 and M6 layers of the medulla (as indicated by the arrowheads). (**D'**) A higher magnification view of the boxed region in **D**. (**E-F**) Horizontal sections through adult heads where 70 percent of R7 cells are expressing the τ-LacZ fusion protein, driven by the Rh4 enhancer region. Anti-β-galactosidase antibody stains of the R7 axons and the anti-mAb22C10 antibody highlights all axons. (**E**) A control (*eyFLP;Rh4-τlacZFRT42Ddri$^{3}$/CyO*) head showing the R7 axons terminating in the M6 layer of the medulla (as indicated by the arrowhead). (**E'**) A higher magnification view of the boxed region in **E**. (**F**) A *dri* mutant eye mosaic (*eyFLP;Rh4-τlacZFRT42Ddri$^{3}$/FRT42Dcl2R11.5*) head showing all R7 axons terminating in the correct layer of the medulla (indicated by the arrowhead), although the topographical map of these axons is mildly disrupted. (**F'**) A higher magnification view of the boxed region in **F**.

la: lamina, me: medulla. M3 and M6 layers of the medulla are indicated by arrows.

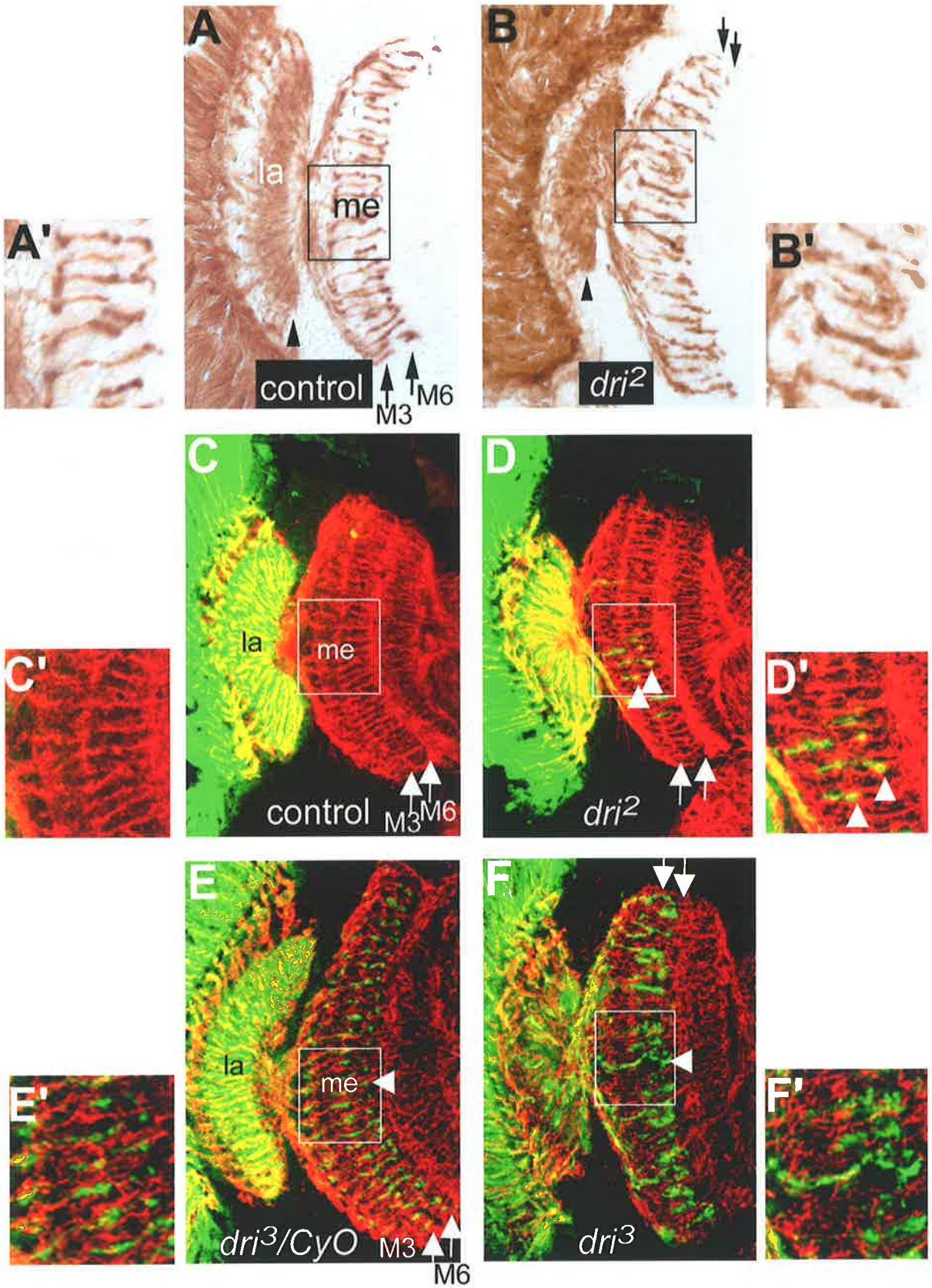
A
la
me
control
M3
M6
B
dri2
A'
B'
C
la
me
control
M3
M6
D
dri2
C'
D'
E
la
me
dri3/CyO
M3
M6
F
dri3
E'
F'

In the *dri* mutant eye mosaic optic lobe, the medulla organisation was mildly disrupted with the distinct layers of the medulla being difficult to distinguish (Figure 4.11 B). To investigate the mild disruption of the axons, the different classes of axons were examined. The *rh1* enhancer region was utilised to express a marker gene, *lacZ*, fused to the microtubule binding protein, *tau* ($\tau$) to visualise the R1-R6 axons (Newsome et al., 2000a). Horizontal sections and immunohistochemical staining with an anti-β-galactosidase antibody and the monoclonal antibody 22C10 that visualised all the axons within the adult head, were performed. In a *FRT42D* control optic lobe, R1-R6 axons terminated in the lamina (Figure 4.11 C), however in a *dri* mutant eye mosaic optic lobe, some of the R1 to R6 axons terminated in both layers of the medulla (Figure 4.11 D). The R7 axons were visualised by expressing *tlacZ* in the Rh4 pattern of expression (in approximately 70 percent of R7 cells) (Newsome et al., 2000a) (Figure 4.11 E). In *dri* mutant eye mosaic optic lobes, the R7 axons terminated in the correct layer, although the topographical map was slightly disrupted, possible due to aberrant R1-R6 axons terminating in the incorrect layer (Figure 4.11 F). The R8 axons also terminated in the correct layer of the medulla in *dri* mutant eye mosaics and the same disruption observed with the R7 axons was also seen with the R8 axons (Figure 4.7 F). These axonal defects were relatively mild and unlikely to result in blindness.

## 4.3 Discussion

### *4.3.1 Dri is required for R1-R6 axons to terminate in the lamina*

This chapter describes the phenotypes associated with the loss of *dri* expression specifically in the eye during the third larval instar stage of development. Dri expression begins several rows behind the morphogenetic furrow in R8, R1-R6 cells (Chapter 3.2.1). In order to identify if *dri* had a role in the *Drosophila* eye, *dri* mutant somatic clones that spanned the majority of the eye, were generated and the vision of the mosaic adult flies examined. Interestingly, as determined by electroretinograms and optomotor response tests, *dri* mutant eye mosaic flies were blind, confirming that *dri* was required in the eye. Blindness of the *dri* mutant eye mosaic flies could potentially be explained by the incorrect formation of R cells or of monopolar neurons or by the incorrect targeting of the R cell axons from the eye to the optic lobe. Analysis of third larval instar *dri* mutant eye mosaics when R cells extend their axons, revealed that although the R cells and monopolar neurons appeared to form correctly in the absence of Dri, a subset of R1-R6 axons did not terminate in the lamina, but passed through to the medulla. Glial cells have been shown to be vital for R1-R6 axon termination within the lamina (Perez and Steller, 1996; Huang et al., 1998; Poeck et al., 2001; Suh et al., 2002), but glial formation and migration was found to occur normally in *dri* mutant eye mosaics.

The R8 axons, which normally express Dri, targeted appropriately to the medulla in the absence of Dri, suggesting that *dri* was not required for the guidance of these axons. However, growth cone formation in R8 axons was disrupted in third larval instar *dri* mutant eye mosaic optic lobes, although this had no effect on the adult position of the R8 axons. It is unclear at this time if the R8 axons can function normally in the absence of Dri.

### *4.3.2 Possible targets for Dri transcriptional regulation*

Recently, the nuclear factor *brakeless* (*bks*), which is also expressed in R cells and is required for the targeting of R1-R6 axons (Rao et al., 2000; Senti et al., 2000), has been shown to repress *runt* expression in R2 and R5 cells (Kaminker et al., 2002). Run is normally expressed in R7 and R8, but the mis-expression of *run* in R2 and R5 cells results in all the R cell axons terminating in the medulla, a phenotype more severe than *bks* mutant eye mosaics. Therefore I investigated whether *dri* was also suppressing *runt* expression within R1-R6 cells. However, Dri was found not to regulate *run* expression. In addition, *dri* expression was unaffected in a *bks* mutant eye mosaic, showing that *dri* does not act downstream of Runt. Therefore, *dri* is acting in a different pathway to *bks*.

*run* mosaics have no phenotype suggesting that there may be functional redundancy between two *run*-related proteins in targeting R7 and R8 axons to the medulla (Kaminker et al., 2002). Little is known about the *run*-related proteins. Although Dri plays no role in *run* repression in R1-R6 cells it remains possible that Dri represses one of the *run*-related proteins in R1 to R6.

A number of proteins including signalling molecules (Dreadlocks, Pak, Misshapen, Bifocal), receptors (LAR, PTP69D and N-Cadherin) and nuclear factors (Brakeless) have been found to be important for R1-R6 axon termination in the lamina (Garrity et al., 1996; Garrity et al., 1999; Newsome et al., 2000a; Newsome et al., 2000b; Rao et al., 2000; Senti et al., 2000; Clandinin et al., 2001; Lee et al., 2001; Maurel-Zaffran et al., 2001). However, LAR, N-cadherin, PTP69D, Pak and Dock are also required in R7 axons for correct termination in the medulla. Dri is not expressed in R7 cells throughout development of the eye and therefore many of these genes are not good candidate genes for Dri regulation. Two genes identified so far, *misshapen* (*msn*), which encodes a Ste-20 kinase (Treisman et al., 1997a; Su et al., 1998; Su et al., 2000) and *bifocal* (*bif*), which interacts with Msn and re-organises F-actin (Ruan et al., 2002), are potential candidate genes because both are required for R1-R6 axon targeting (Ruan et al., 1999; Ruan et al., 2002). Furthermore, somatic clones mutant for *msn* have both an ectopic inner R cell and a mis-orientation defect, similar to

somatic *dri* mutant clones (Treisman et al., 1997a; Paricio et al., 1999). *bif* somatic mutant clones do not have ectopic inner R cells but do have misshaped rhabdomeres similar to *dri*. Furthermore, the loss of *bif* from R7 cells has no effect on the targeting of R7 axons (Bahri et al., 1997; Ruan et al., 2002), indicating that either *bif* is not expressed in R7 cells, which is consistent with the *dri* expression pattern, or *bif* is redundant in R7 cells. Hence, Dri may be regulating one or more factors, including some of the known genes, such as *msn* and/or *bif*, that are important for the termination of R1-R6 axons within the lamina. Although all of these genes represent possible *dri* targets, perhaps the best approach to identify genes that are under Dri regulation may be a genomic-based approach, such as microarray analysis, as this approach should identify all genes whose expression is altered in *dri* mutant eye discs.

### *4.3.3 Conclusions*

In this chapter I have demonstrated a role for *dri* in R cell axon guidance and behaviour in the developing eye-brain. However, this role is unlikely to be the sole reason for blindness in *dri* mutant eye mosaic flies because in the adult optic lobe most R1-R6 axons terminate in the correct layer, suggesting that *dri* may also play a role in correct synapse formation between the R cell axons and the monopolar neurons. Dri expression in the eye continues into adulthood where it may play a later role. To investigate this possibility, the role of Dri in the adult eye will be examined and described in the next chapter.

# Chapter 5: The role of *dead ringer* in the visual system

## 5.1 Introduction

During larval development, Dri is present in the nuclei of R1-R6 and R8 cells and is required to regulate one or more factors that are essential for the R1-R6 axons to terminate in the correct layer of the optic lobe, the lamina (Chapter 4.2.6). In Chapter 3 I showed that Dri expression continued in the adult eye with expression restricted to the R1-R6 nuclei (Chapter 3.2.3). This observation suggests that Dri may be important in the regulation of one or more factors that are required in the adult eye. The component of the photoreceptor cell that responds to light is the rhabdomere. The tightly packed stacks of microvilli within the rhabdomeres contain the light-sensing receptor molecule Rhodopsin. The actin-based cytoskeleton, termed the rhabdomere terminal web (RTW) inhibits the rhabdomere from collapsing into the photoreceptor cytoplasm (Kumar and Ready, 1995b). Organisation of the RTW is dependent on Rhodopsin (Chang and Ready, 2000). Consequently, if individuals are homozygous for a mutation within the Rhodopsin-encoding gene, the rhabdomeres collapse and the photoreceptor cells degenerate (Kumar and Ready, 1995a; Kumar and Ready, 1995b; Kurada and O'Tousa, 1995; O'Tousa et al., 1995; Bentrop, 1998; Chang and Ready, 2000).

Six Rhodopsins have been identified in *Drosophila*, and are expressed in a non-overlapping pattern in R cells. Rh1 (the protein product of *ninaE*) is expressed in R1-R6 cells (Scavarda et al., 1983; Zuker et al., 1985a; Feiler et al., 1988; OTousa et al., 1989), an expression pattern similar to *dri*. Rh3 and Rh4 are expressed in R7 cells, Rh5 and Rh6 are expressed in R8 cells, while Rh2 is ocellar specific (Cowman et al., 1986; Zuker et al., 1987; Montell et al., 1987; Fryxell and Meyerowitz, 1987; Pollock and Benzer, 1988; Feiler et al., 1988; Feiler et al., 1992; Huber et al., 1997; Salcedo et al., 1999;). Different Rhodopsins detect different wavelengths of light. Rh3 and Rh4 detect UV light (Fryxell and Meyerowitz, 1987; Montell et al., 1987; Zuker et al., 1987; Feiler et al., 1992), Rh5 and Rh6 detect green-blue light (Huber et al., 1997; Salcedo et al., 1999), Rh1 detects blue light, while Rh2 detects violet light. The Rhodopsin receptors are activated by a photon of light which leads to the isomerization of Rhodopsin to Metarhodopsin, which in turn activates the Gα protein and the visual transduction pathway, resulting in an influx of calcium into the cell (see Chapter 1.7.2 for further detail and Figure 5.7). The influx of calcium into the cell depolarises the R cells,

leading to a signal being sent to the optic lobe of the brain where it is processed. The signalling pathway activated by light must be inactivated (see Chapter 1.7.3 for details) or light-dependent degeneration of the photoreceptor cells will occur.

This chapter examines the role of *dri* in the adult eye, utilising the previously described whole eye clones (Chapter 4.1, Figure 4.1).

## 5.2 Results

### *5.2.1 The Rh1 protein level is significantly reduced in* dri *mutant eye mosaics*

As shown in Chapter 3, Dri is found in the nuclei of the R1-R6 cells in the adult eye. Rh1, encoded by the *ninaE* gene, is the only visual transduction pathway member whose expression is restricted to R1-R6 cells. To test the hypothesis that *dri* regulates *ninaE* expression, the Rh1 protein levels in *dri* mutant eye mosaics were investigated. If Dri is regulating *ninaE* transcription then Rh1 protein levels will be significantly reduced in the *dri* mutant eye mosaic compared to *FRT42D* controls. Total protein extracts from *FRT42D* control and *dri* mutant eye mosaic heads, aged for approximately two weeks, were separated by SDS-Page, blotted onto a membrane support and probed with anti-Rh1 antibody. Anti-α-tubulin antibody staining was used as a load control. Two different *dri* alleles, $dri^2$ and $dri^3$ showed a significant reduction in Rh1 protein levels in comparison to *FRT42D* control and wild type ($w^{1118}$) heads (Figure 5.1). These results show that in the absence of Dri, Rh1 levels are decreased, indicating that Dri is required for the expression of *ninaE*.

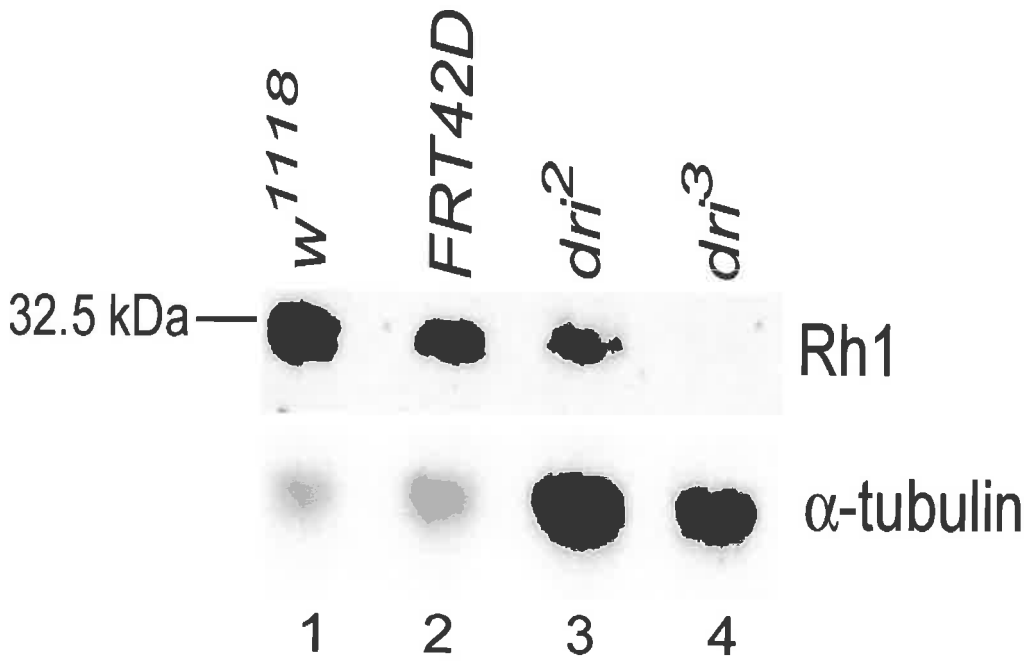


**Figure 5.1 Rh1 protein levels are reduced in *dri* mutant eye mosaic flies**

Western analysis of $w^{1118}$ (lane 1), *FRT42D* (*eyFLP;FRT42D/FRT42lcl2R11.5*) control (lane 2), $dri^2$ (*eyFLP;FRT42D*$dri^2$*/FRT42Dcl2R11.5*) mutant eye mosaic (lane 3) and $dri^3$ (*eyFLP;FRT42D*$dri^3$*/FRT42Dcl2R11.5*) mutant eye mosaic (lane 4) heads probed with anti-Rh1 and anti-α-tubulin antibodies. In *dri* mutant eye mosaic heads less Rh1 protein is present.

### *5.2.2 Dri does not directly regulate ninaE transcription*

If *dri* directly regulates *ninaE* transcription then there will be different transcript levels of *ninaE* in *dri* mutant mosaic eyes compared to *FRT42D* control eyes. The levels of *ninaE* transcripts were determined by real time PCR. RNA was extracted from adult *FRT42D* control and *dri* mutant eye mosaic heads followed by cDNA synthesis. Primers were designed across an exon-intron boundary of *ninaE* and *ribosomal protein 49* (*rp49*) genes to discriminate against any amplification of contaminating genomic DNA present in the RNA samples. Additionally, real time PCR was performed on RNA samples to which no reverse transcriptase was added to the cDNA synthesis reaction. No genomic contamination was found in either the *FRT42D* control or *dri* mutant eye mosaic RNA samples (data not shown). *rp49* was utilised as the reference gene for this experiment as this gene encodes a ribosomal subunit that should not be regulated by *dri*. The real time PCR was performed with Sybr-Green fluorescent dye, which binds to the newly synthesised DNA. The absorbance levels of the Sybr-Green fluorescence were measured and a reading, within the linear phase of the PCR, was utilised to determine at what cycle the samples reached an arbitrary threshold (the CT value), which was above background fluorescence levels (Appendix A). Dissociation curves were performed on all samples to determine if specific products were produced, one peak was observed for each sample indicating specific amplification of the *ninaE* or *rp49* genes. Serial dilution of the cDNA was performed to determine the amplification efficiency of each RNA sample with both primers utilised in these experiments and the experiment was repeated three times. The relative expression of *ninaE* compared to *rp49* for each group (Table 1) was determined using the Q-gene program (Appendix A). Statistical analysis of the relative expression levels using the Mann Whitney U test (performed by the SPSS program) showed that there was not a significant difference in the levels of *ninaE* expression in *FRT42D* control and *dri* mutant eye mosaic heads. Therefore, I conclude that the transcription factor Dri does not directly regulate *ninaE* transcription or RNA stability.

**Table 1: The relative expression of *ninaE* mRNA compared to *rp49* in *dri* mutant eye mosaic heads compared to *FRT42D* control.**

| | ***FRT42D* control** | ***dri*$^2$** |
|---|---|---|
| **#1** | 1.01 ± 0.067 NEU | 0.67 ± 0.0288 NEU |
| **#2** | 1.16 ± 0.0818 NEU | 0.907 ± 0.0304 NEU |
| **#3** | 1.44 ± 0.0827 NEU | 1.19 ± 0.0851 NEU |
| **Scores from Mann-Whitney U test** | | *FRT42D* vs. *dri*$^2$ P>0.05 |

Note: A Mann-Whitney U test score lower than P< 0.05 is considered significant.
NEU stands for normalised expression units.

### *5.2.3 Rhabdomeres in* dri *mutant eye mosaics degenerate in an age- and light-dependent manner*

Although *dri* is not directly regulating the expression of *ninaE* it may be regulating a gene that is required for the maturation of Rh1. *ninaA* and *rab6* have been identified as genes that are required for the folding and transport of Rh1 from the golgi apparatus to the surface of the microvilli (Colley et al., 1995; Shetty et al., 1998). Mutations in these genes result in the incorrect folding or localisation of Rh1 (Colley et al., 1995; Shetty et al., 1998) and presumably disruption of the actin-based cytoskeleton, the RTW, leading to the degeneration of the photoreceptor cells independent of the activation of the light pathway. I investigated whether degeneration of R cells occurred in *dri* mutant eye mosaic flies and, if so, whether degeneration occurred in a light-independent or dependent manner. At two-week intervals, heads from both *FRT42D* control and *dri* mutant eye mosaic adult flies were dissected and tangential sections performed. At eclosion, mild defects in the ommatidial structure were observed in *dri* mutant eye mosaic sections from both light- and dark-reared flies (Figure 5.2 D and G, Table 2). Approximately 19% to 25% of ommatidia examined had either missing or misshaped rhabdomeres (Table 2, Figure 5.2 C, Figure 5.2 C' and Figure 5.3). The remaining ommatidia were classed as either containing the normal seven-rhabdomere complement or as containing both R7 and R8 rhabdomeres within the one ommatidium (Table 2).

**Table 2: The phenotypes of ommatidia scored in *FRT42D* control and *dri* mutant eye mosaics at newly eclosed, 4 and 6 weeks of age from flies reared in both light and dark conditions.**

| | | Ommatidial phenotype | | | |
|---|---|---|---|---|---|
| **Age of flies and rearing conditions** | | **7 Rhabdomeres** | **Two inner R cells in one ommatidium** | **Missing or misshaped ommatidia** | **Total no. of ommatidia scored** |
| **Light/Dark** | Newly eclosed (n=4) | 331<br>96.86 % ± 1.34 | 3<br>1 % ± 0.86 | 7<br>2.13 % ± 0.89 | 341 |
| ***FRT42D* control** | 4 week old (n=4) | 467<br>93.15 % ± 3.11 | 1<br>0.15 % ± 0.15 | 34<br>6.7 % ± 3.1 | 502 |
| | 6 week old (n=5) | 362<br>92.27 % ± 1.43 | 1<br>0.48 % ± 0.31 | 29<br>7.25 % ± 1.37 | 392 |
| **Dark-reared** | Newly eclosed (n=5) | 284<br>46.94 % ± 2.36 | 208<br>33.75 ± 6.11 | 113<br>19.31 % ± 7.09 | 605 |
| ***FRT42D dri* mutant mosaic** | 4 week old (n=6) | 315<br>56.54 % ± 4.39 | 131<br>22.38 % ± 1.83 | 137<br>21.07 % ± 6.02 | 583 |
| | 6 week old (n=6) | 314<br>46.03 % ± 1.4 | 53<br>19.96% ± 0.48 | 326<br>46.38 % ± 1.36 | 693 |
| **Light-reared** | Newly Eclosed (n=5) | 274<br>59.47 % ± 2.42 | 72<br>15.96 % ± 2.9 | 116<br>24.57 % ± 2.79 | 462 |
| ***FRT42D dri* mutant mosaic** | 2week old (n=7) | 261<br>49.19 % ± 3.1 | 113<br>22.34 % ± 2.93 | 155<br>28.47 % ± 4.4 | 529 |
| | 4 week old (n=5) | 153<br>32.52 % ± 1.66 | 74<br>15.67 % ± 2.2 | 238<br>51.81 % ± 3.47 | 465 |
| | 6 week old (n=6) | 161<br>27.42 % ± 3.01 | 49<br>8.56% ± 1.33 | 365<br>64.01% ± 3.62 | 575 |

## Figure 5.2 R cells undergo age- and light-dependent degeneration in *dri* mutant eye mosaics

Tangential sections of adult eyes from flies that were newly eclosed or had aged 4 or 6 weeks. (**A-C**) Sections of *FRT42D* (*eyFLP;FRT42D/FRT42lcl2R11.5*) control eyes showing the normal seven-rhabdomere complement and trapezoidal arrangement from (**A**) a newly eclosed fly, (**B**) a 4-week old fly, (**C**) a 6-week old fly. The sections presented here are representative of both dark- and light-reared *FRT42D* control eyes. (**D**) A section of a light-reared *dri* mutant eye mosaic (*eyFLP;FRT42Ddri*$^{2}$*/FRT42Dcl2R11.5*) eye from a newly eclosed fly. The arrow indicates an ommatidium that is missing one rhabdomere. (**D'**) shows an ommatidium that contains a rhabdomere that is misshaped (arrow). (**D''**) shows an ommatidium with two inner-R cell rhabdomeres (arrows). (**E**) A section from a light-reared 4 week-old *dri* mutant mosaic eye showing early ommatidial degeneration. The trapezoidal arrangement of the seven-rhabdomere complement is disrupted (black arrow) and the *dri* mutant ommatidium (red arrowhead) is smaller than the *dri* heterozygous ommatidium (red arrow). (**F**) Section from a 6-week old *dri* mutant eye showing that the *dri* mutant ommatidium (red arrowhead) is smaller than the *dri* heterozygous ommatidium (red arrow). (**G**) A dark-reared *dri* mutant eye mosaic (*eyFLP;FRT42Ddri*$^{2}$*/FRT42Dcl2R11.5*) eye section from a newly eclosed fly. The tangential sections from light- and dark-reared flies are indistinguishable. (**H**) A section from a dark reared *dri* mutant mosaic eye that was aged 4-weeks. The red arrow indicates a *dri* heterozygous ommatidium and the red arrowhead shows an ommatidium mutant for *dri*. Note that sizes of the ommatidia are approximately equal. (**I**) A section from a dark-reared *dri* mutant mosaic eye aged 6 weeks. The *dri* heterozygous ommatidium (red arrow) is slightly larger than the *dri* mutant ommatidium (as indicated by red arrowhead). (**J**) A graph showing the percentage of ommatidia with misshaped or missing rhabdomeres at newly eclosed, 4 and 6 weeks in light and dark reared flies. The number of misshaped and missing ommatidia was unchanged at newly eclosed and 4-week-old control flies. In 6-week-old control flies there is an increase in the number of missing or misshaped ommatidia. Light-reared *dri* mutant eye mosaic flies that were 4 weeks of age showed an increase in the percentage of ommatidia with misshaped and missing rhabdomeres The percentage of aberrant rhabdomeres continued to increase at 6 weeks of age for light-reared *dri* mutant mosaic eyes. In dark reared *dri* mutant mosaic eyes, there was no increase in the percentage of misshaped or missing rhabdomeres at 4 weeks of age compared to newly eclosed dark reared flies. At 6 weeks of age the percentage of missing or misshaped rhabdomeres in dark-reared *dri* mutant eye mosaic flies had increased but the percentage was less than the percentage of aberrant rhabdomeres from 4-week-old light-reared flies.

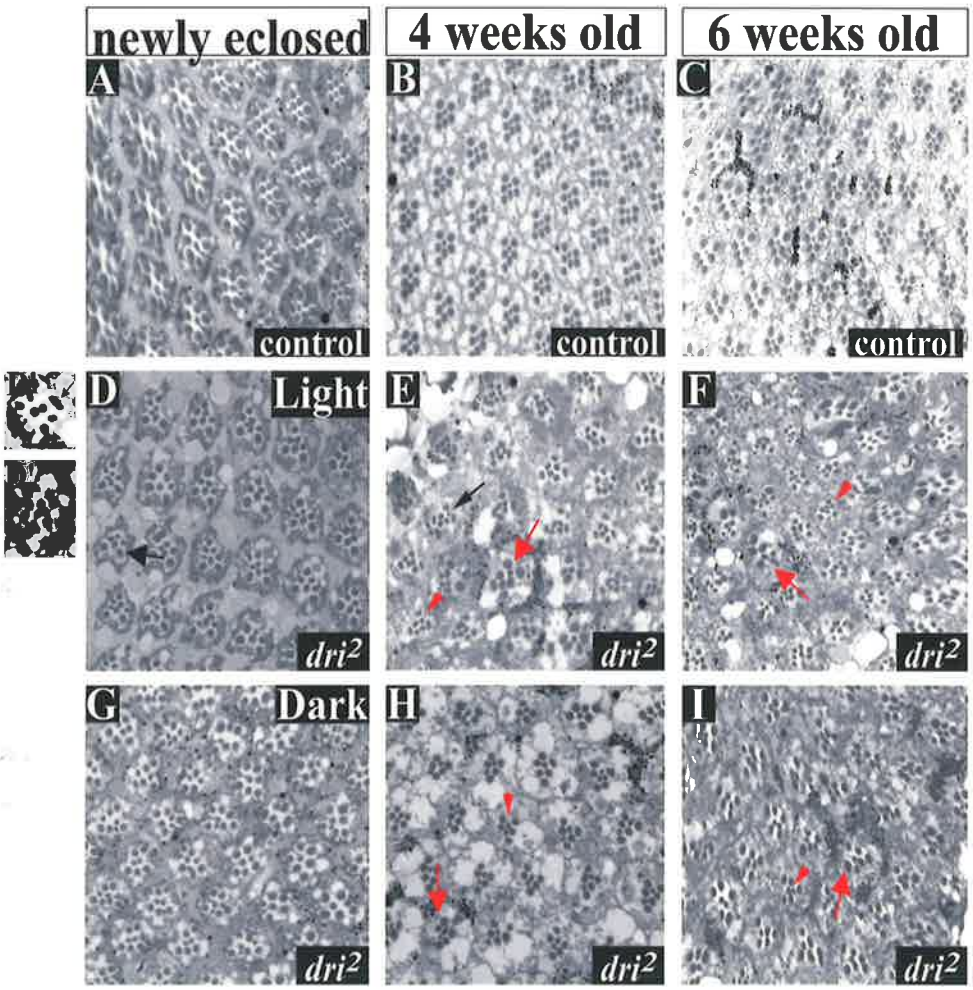
newly eclosed
4 weeks old
6 weeks old
A
control
B
control
C
control
D
Light
dri2
E
dri2
F
dri2
G
Dark
dri2
H
dri2
I
dri2

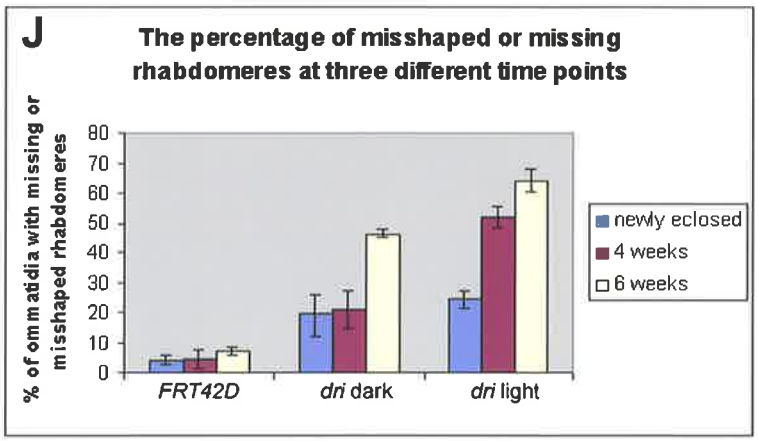
J
The percentage of misshaped or missing rhabdomeres at three different time points
% of ommatidia with missing or misshaped rhabdomeres
80
70
60
50
40
30
20
10
0
FRT42D
dri dark
dri light
newly eclosed
4 weeks
6 weeks

**Figure 5.3 R cells degenerate in an age- and light-dependent manner in *dri* mutant mosaic adult eyes**

**(A)** A graph showing the percentage of ommatidia within light-reared newly eclosed and light-reared 4-week-old *dri* mutant mosaic eyes. The ommatidia were classified into three groups, ommatidia that contained the normal seven-rhabdomere complement, ommatidia with R7 and R8 rhabdomeres within the same ommatidium and ommatidia where the rhabdomeres were either misshaped or missing. The number of ommatidia where both R7 and R8 photoreceptor cells were observed within one ommatidium was unchanged at the newly eclosed and 4-week-old stages.

**(B)** A graph showing the percentage of ommatidia with misshaped or missing rhabdomeres at newly eclosed, 2, 4 and 6 weeks in light-reared *dri* mutant eye mosaic flies. At two weeks of age there is a trend towards an increase in the number of missing and misshaped rhabdomeres. At 4 weeks of age there is an increase in the number of missing and misshaped rhabdomeres compared to newly eclosed and 2-week old flies. At 6 weeks of age the trend towards the increase in the number of missing or misshaped rhabdomeres continues.

**A**

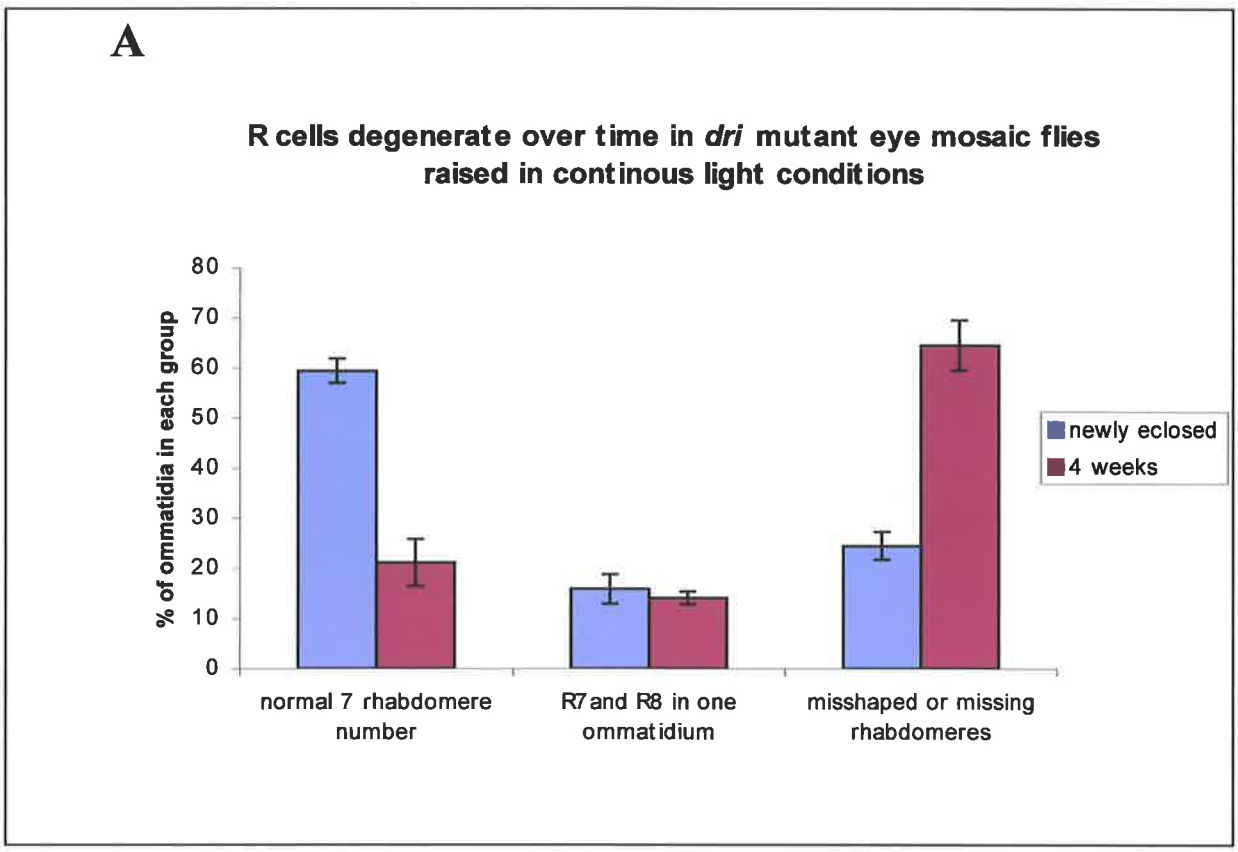
R cells degenerate over time in dri mutant eye mosaic flies raised in continous light conditions
% of ommatidia in each group
80
70
60
50
40
30
20
10
0
normal 7 rhabdomere number
R7 and R8 in one ommatidium
misshaped or missing rhabdomeres
newly eclosed
4 weeks

**B**

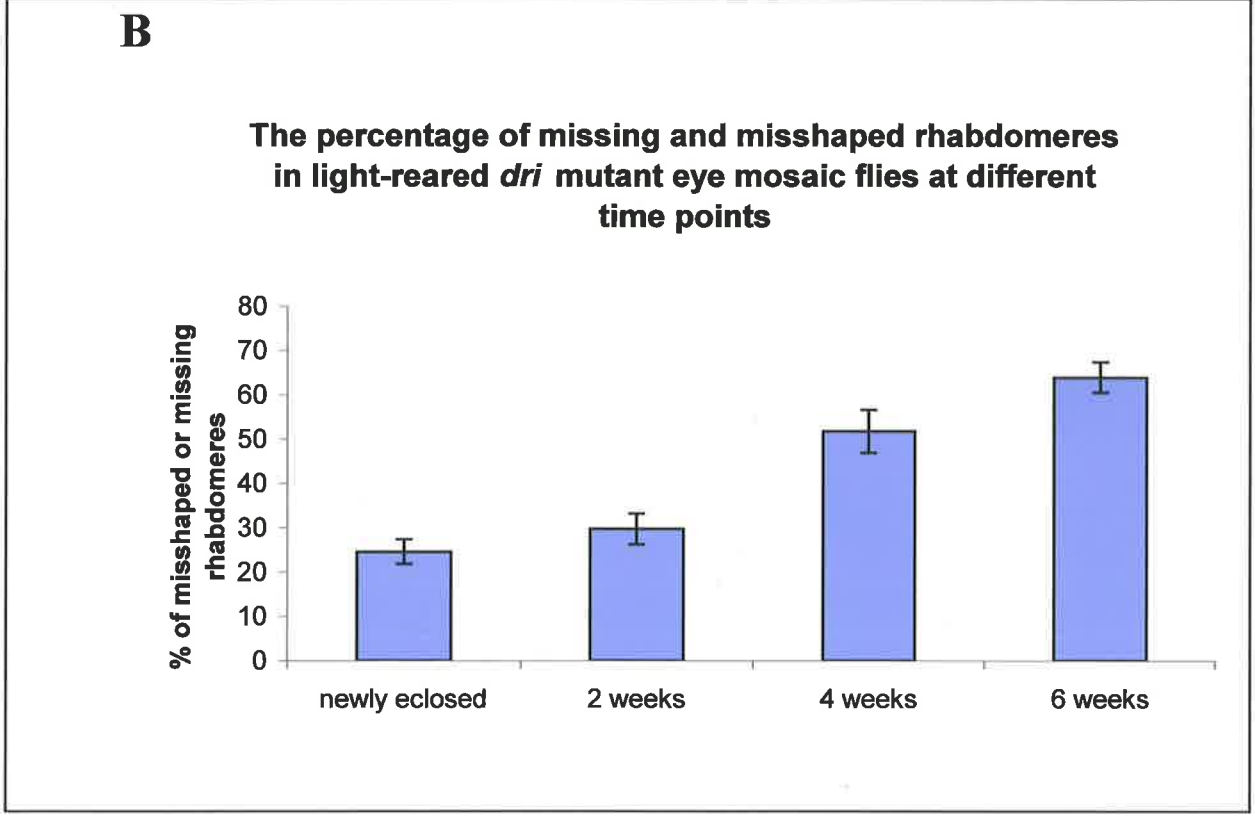
The percentage of missing and misshaped rhabdomeres in light-reared dri mutant eye mosaic flies at different time points
% of misshaped or missing rhabdomeres
80
70
60
50
40
30
20
10
0
newly eclosed
2 weeks
4 weeks
6 weeks

*5.2.3.1* FRT42D *control flies*

Greater than 96 percent of the ommatidia in tangential sections from *FRT42D* control flies that were newly eclosed showed the normal seven rhabdomere complement, with the other ommatidia showing either misshaped, missing or ectopic rhabdomeres (Table 2 and Figure 5.3 B). At 4 weeks of age the number of missing or misshaped rhabdomeres increased to 6% and by 6 weeks of age the number of misshaped or missing rhabdomeres had increased to 7.5%, indicating that the ommatidia degenerated with age (Table 2 and Figure 5.2 J). The levels of Rh1 present within the *FRT42D* control flies remained constant until 4 weeks of age (Figure 5.4 A).

*5.2.3.2 Dark-reared* dri *mutant eye mosaic flies*

The expression of *ninaE* begins during the later stages of pupal development (Kumar and Ready, 1995b) and some mutations in the *ninaE* gene result in the ablation of R1-R6 rhabdomeres at eclosion (Kumar and Ready, 1995a; Kurada and O'Tousa, 1995; O'Tousa et al., 1995; Bentrop, 1998), therefore the number of missing and misshaped rhabdomeres that were observed at eclosion in both light- and dark-reared flies may be due to light-independent degeneration (Table 2). However, in dark-reared *dri* mutant eye mosaic sections that were aged 4 weeks, no increase in the number of misshaped or missing rhabdomeres was observed when compared to the newly eclosed stage (Table 2 and Figure 5.2 J). Furthermore the trapezoidal arrangement of the ommatidia in 4-week-old dark reared flies was preserved (Figure 5.2 H). When utilising the whole eye mutant clone system, between 80-95 percent of the cells are mutant (Newsome et al., 2000a). The cells that were heterozygous for *dri* could be visualized by the presence of pigment cells. At 4 weeks of age, the size of the mutant rhabdomeres was preserved, suggesting that further retinal degeneration has not occurred. Retinal degeneration was observed in sections from 6-week old dark-reared *dri* mutant mosaic eyes, as the number of missing or misshaped rhabdomeres increased from those observed at 4 weeks (Table 2, Figure 5.2 I and Figure 5.2 J). Also at 6 weeks of age a slight decrease in the size of the mutant ommatidia was observed (Figure 5.2 I). The levels of Rh1 from dark-reared flies that were either newly eclosed or 4 weeks old were determined by Western analysis. α-tubulin was utilised as a load control and the ratio between Rh1 and α-tubulin was determined. In *dri* mutant eye mosaic flies there was less Rh1 protein produced compared to *FRT42D* controls but the level of Rh1 did not decrease between the newly eclosed and 4-week old *dri* mutant flies (Figure 5.4 A).

*5.2.3.3 Light-reared* dri *mutant eye mosaic flies*

The number of ommatidia with missing or misshaped rhabdomeres increased in light-reared *dri* mutant eye mosaic flies as they aged (Table 2 and Figure 5.3 B). At 4-weeks of age there were significantly more ommatidia that displayed missing or misshaped rhabdomeres compared to either newly eclosed or 2 week old light-reared *dri* mutant mosaic retinas (Table 2 and Figure 5.3 A, B). In 4-week old eyes, the sizes of heterozygous ommatidia (Figure 5.2 E, red arrow) were greater than the sizes of *dri* mutant ommatidia (Figure 5.2E red arrowhead), indicating that *dri* mutant ommatidia were degenerating. Furthermore, some mutant ommatidia with normal seven-rhabdomere complements no longer formed the normal trapezoidal arrangement (Figure 5.2 E, black arrow) observed in sections from *FRT42D* control flies of the same age. Examination of tangential sections from 6-week old light-reared *dri* mutant mosaic eyes showed that degeneration of the rhabdomeres continued, with an increase in the proportion of ommatidia that were missing or had misshaped rhabdomeres and a decrease in the size of the ommatidia (Table 2 and Figure 5.2 F, J and Figure 5.3 B). The levels of Rh1 protein in *dri* mutant eye mosaic and *FRT42D* control flies at 1, 2, and 3 weeks, were determined by Western analysis as the ratio of Rh1 to α-tubulin, which was utilised as a load control. As in dark-reared *dri* mutant eye mosaic flies, there was less Rh1 produced in *dri* mutant eye mosaic flies reared in the light across all ages examined (Figure 5.4 B) and the level of Rh1 decreased as the flies aged (Figure 5.4 B)

Interestingly, in light-reared *dri* mutant mosaic eyes, approximately the same percentage of ommatidia contained both R7 and R8 rhabdomeres within one ommatidium at eclosion and 4 weeks of ages, even though the ommatidia were degenerating (Table 2 and Figure 5.3 A), suggesting that the additional inner rhabdomere in a section is not an intermediate step of degeneration, but a separate defect associated with the loss of Dri.

In sections from *dri* mutant eye mosaics that were raised in continuous light and aged 7 weeks, there were regions within the sections that were missing ommatidia, indicating that all of the rhabdomeres in that region had degenerated (Figure 5.5 B). Although there were some ommatidia present, it appeared as if most were in the process of degenerating, whereas in the *FRT42D* control flies that were raised in similar conditions and also aged 7 weeks, the majority of ommatidia still contained the normal seven-rhabdomere complement (Figure 5.5).

## Figure 5.4 Rh1 proteins do not change in light or dark reared conditions

(**A**) Western analysis of dark-reared *FRT42D* (*eyFLP;FRT42D/FRT42lcl2R11.5*) control heads dissected from newly eclosed (lane 1), 4 week old (lane 3) flies, and $dri^2$ (*eyFLP;FRT42D*$dri^2$*/FRT42Dcl2R11.5*) mutant eye mosaic heads from newly eclosed (lane 2) and 4 week old (lane 4) heads probed with anti-Rh1 and anti-α-tubulin antibodies. The ratio between the bands for Rh1 and α-tubulin is displayed. In *dri* mutant eye mosaic heads less Rh1 protein is present but the amount of Rh1 did not vary with age.

(**B**) Western analysis of light-reared *FRT42D* (*eyFLP;FRT42D/FRT42lcl2R11.5*) control heads dissected from 1 week old (lane 1), 2 week old (lane 3) and 3 week old (lane 5) flies and $dri^2$ (*eyFLP;FRT42D*$dri^2$*/FRT42Dcl2R11.5*) mutant eye mosaic heads from 1 week old (lane 2), 2 week old (lane 4) and 3 week old (lane 6) flies probed with anti-Rh1 and anti-α-tubulin antibodies. The ratios between the bands for Rh1 and α-tubulin are displayed. In *dri* mutant eye mosaic heads less Rh1 protein is present compared to the controls at each stage and the amount of Rh1 in *dri* mutant eye mosaic flies decreases over time.

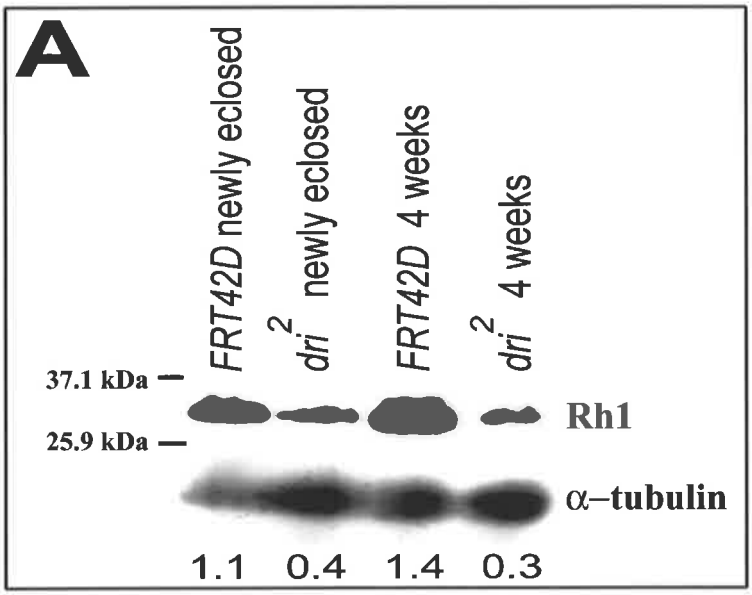
A
FRT42D newly eclosed
dri2 newly eclosed
FRT42D 4 weeks
dri2 4 weeks
37.1 kDa
25.9 kDa
Rh1
α–tubulin
1.1 0.4 1.4 0.3

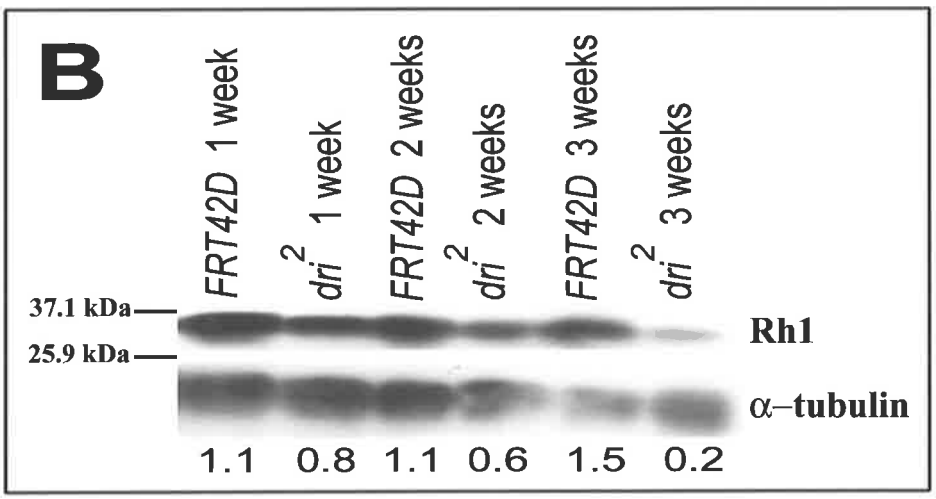
B
FRT42D 1 week
dri2 1 week
FRT42D 2 weeks
dri2 2 weeks
FRT42D 3 weeks
dri2 3 weeks
37.1 kDa
25.9 kDa
Rh1
α–tubulin
1.1 0.8 1.1 0.6 1.5 0.2

## Figure 5.5 R cells degenerate in an age- and light-dependent manner in *dri* mutant eye mosaic adult eyes

Tangential sections of adult eyes from 7-week old light-reared flies. (**A**) A section through a *FRT42D* (*eyFLP;FRT42D/FRT42lcl2R11.5*) control adult eye showing that ommatidia are present. (**B**) A section through a *dri* mutant mosaic (*eyFLP;FRT42Ddri*$^{2}$*/FRT42Dcl2R11.5*) eye showing that some ommatidia have degenerated resulting in regions where no ommatidia are present (indicated by the arrow).

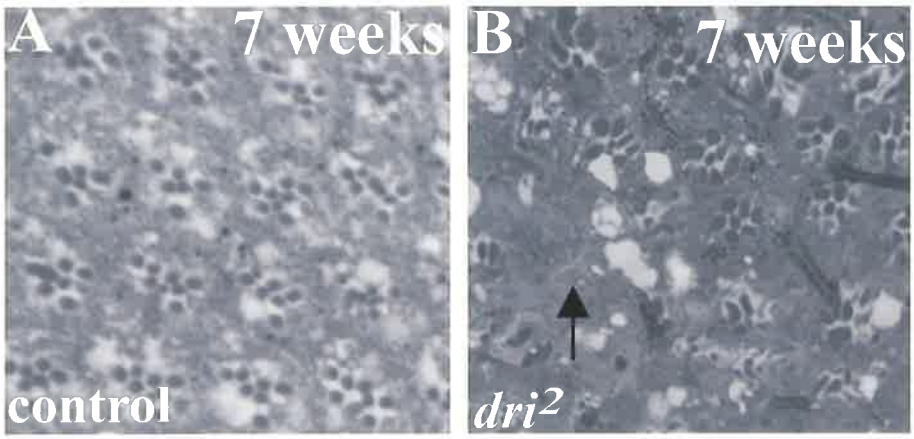
A
7 weeks
control
B
7 weeks
dri2

Tangential sections of *dri* mutant eyes viewed at lower magnification revealed that holes began to be observed at 4 weeks of age and became progressively more severe with age (Figure 5.6). This is in contrast to sections through *FRT42D* control eyes where the structure of the eye appeared normal until 7 weeks when a small number of holes were apparent (Figure 5.6). Thus, in *dri* mutant eye mosaics, R cells degenerate in an age- and light-dependent manner.

## 5.3 Discussion

### *5.3.1* dri *is required for normal Rh1 levels and for normal rhabdomere structure and stability*

Strikingly, much less Rh1 protein is produced in *dri* mutant eye mosaic flies than in *FRT42D* control flies at all stages and in all conditions examined in this study. A lower level of Rh1 present in photoreceptor cells has been shown to be associated with blindness (Shetty et al., 1998), although this effect could not explain the blindness observed in *dri* whole eye mutant flies, as depolarization still occurs in these younger, but still blind, flies. A substantial proportion of mutant photoreceptor cells were found to be abnormal in newly eclosed flies and to degenerate in an age-dependent manner, a process that was accelerated in the presence of light. The fact that retinas of dark-reared *dri* mutant eye mosaic flies do not begin to degenerate until 6 weeks of age, even though less Rh1 was produced at eclosion, suggests that enough Rh1 was produced in *dri* mutant eye mosaic flies to prevent the RTW from collapsing into the photoreceptor cell.

A substantial proportion of misshaped or missing rhabdomeres were present in *dri* mosaic mutant eyes at eclosion in both light- and dark-reared flies. This defect may be due to light-independent degeneration, as *ninaE* expression begins before eclosion (Kumar and Ready, 1995b). Alternatively, the number of missing and misshaped rhabdomeres may be due to defects in morphogenesis of the eye during pupal development. Mutations in genes such as *misshapen*, one of the potential target genes for *dri* regulation during eye development, has both misshaped and missing rhabdomeres in the adult eye (Treisman et al., 1997a; Paricio et al., 1999). The observation that degeneration proceeded very slowly after eclosion in dark-reared flies is more consistent with developmental defects being the explanation for the phenotype at eclosion than retinal degeneration. An attempt to rescue the missing and misshaped rhabdomere phenotype by expression of *dri* specifically in the late pupal and adult stages using the *Rh1-Gal4* construct, would discriminate between these two possibilities.

**Figure 5.6 Degeneration holes appear in *dri* mutant eye mosaic sections.**

Low magnification image of tangential sections (**A**, **C**, **E**, **G**, **I**) of *FRT42D* (*eyFLP; FRT42D/FRT42lcl2R11.5*) control eyes and (**B**, **E**, **F**, **H**, **J**) *dri* mosaic mutant eyes (*eyFLP; FRT42Ddri*$^{2}$*/FRT42Dcl2R11.5*) from (**A-B**) newly eclosed, (**C-D**) 2 week old (**E-F**) 4 week old (**G-H**) 6 week old, (**I-J**) 7 week old flies. In a 4-week old *dri* mutant eye mosaic section (**F**) degeneration holes have begun to appear. In a 6-week old *dri* mutant eye mosaic section (**G**) a greater number of degeneration holes are observed. (**I**) A 7-week old *FRT42D* control section shows that a few degeneration holes have began to appear. (**J**) A 7-week old *dri* mutant eye mosaic section shows that the number of degeneration holes has further increased.

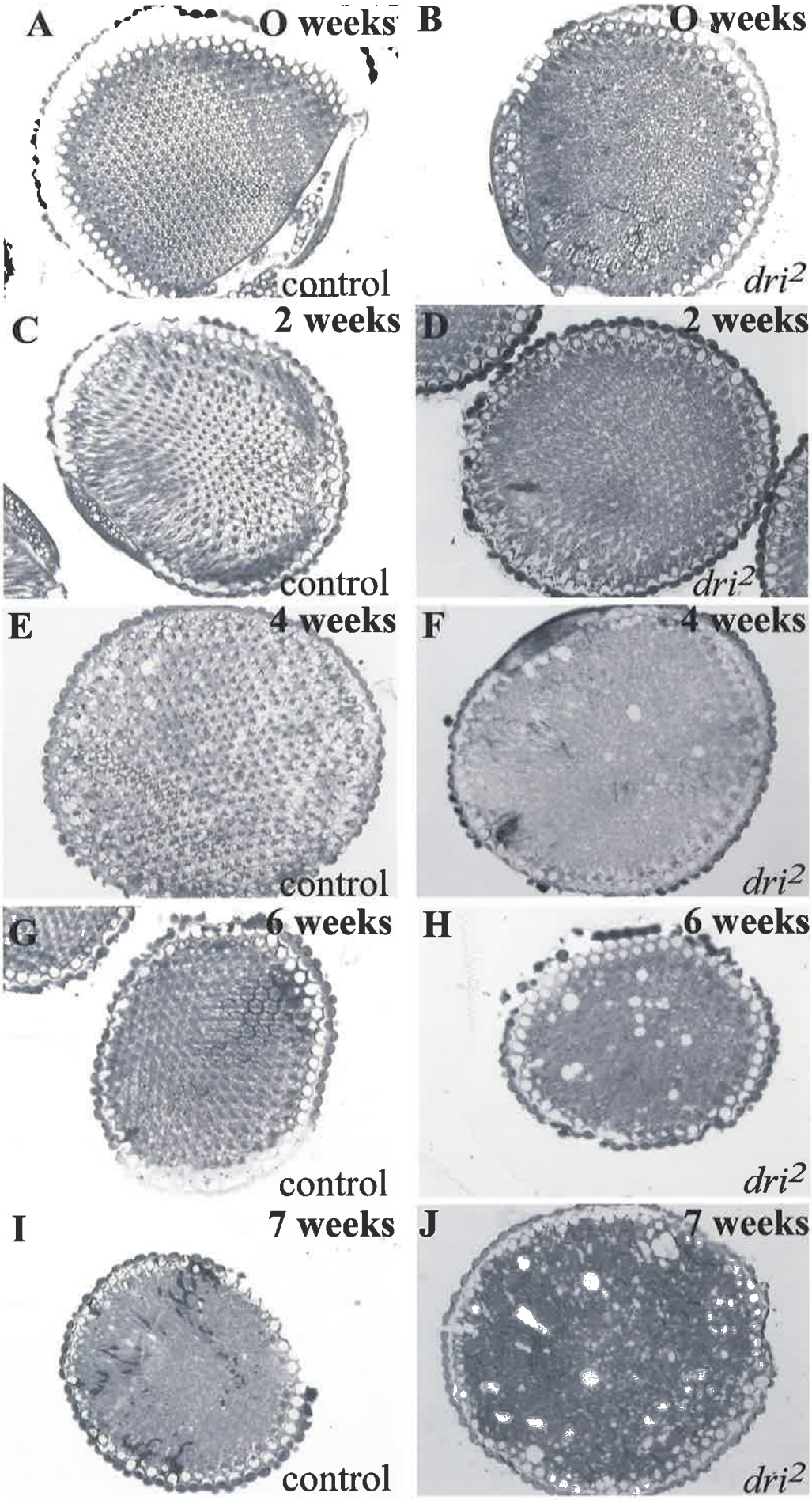
A
0 weeks
control
B
0 weeks
dri2
C
2 weeks
control
D
2 weeks
dri2
E
4 weeks
control
F
4 weeks
dri2
G
6 weeks
control
H
6 weeks
dri2
I
7 weeks
control
J
7 weeks
dri2

Rescue of the phenotype would indicate that degeneration due to low Rh1 levels was the cause, while failure to rescue would support the idea that the phenotype observed at eclosion were due to defects in morphogenesis during pupal development.

The work presented in this chapter has shown that Dri is not directly regulating *ninaE* transcription, despite the fact that Rh1 protein levels are reduced at all rearing conditions and ages examined. I conclude that Dri must regulate a factor required for the processing or stability of Rh1.

In light conditions, photoreceptor cells lacking Dri degenerate more rapidly than dark-reared *dri* mutant eye mosaic flies, indicating that light-dependent degeneration was occurring. This light-dependent degeneration could result from an enhanced decrease in the already limiting levels of Rh1 over time in the presence of light. Alternatively, *dri* could be regulating genes encoding light pathway members, mutations in which can lead to the loss of Rh1, presumably without the transcription of *ninaE* being affected (Alloway and Dolph, 1999; Alloway et al., 2000; Kiselev et al., 2000). In these cases, stable Rhodopsin-Arrestin complexes form, leading to the internalisation of this protein complex through the endocytic pathway, and activation of the apoptotic pathway (Alloway and Dolph, 1999; Alloway et al., 2000; Kiselev et al., 2000). It is unclear at this stage how the Rhodopsin-Arrestin complex, once internalized, triggers the apoptotic pathway. However, by inhibiting either the endocytic pathway via the introduction of the dynamin mutant, *shibire*, or inhibiting the apoptotic pathway by the introduction of *p35*, resulted in the inhibition of previously observed light-dependent retinal degeneration (Alloway et al., 2000; Kiselev et al., 2000). To examine whether the loss of Rh1 observed in *dri* mutant eye mosaic flies is due to the formation of stable Rhodopsin-Arrestin complexes, *shibire* or *p35* could be introduced to a *dri* mutant background to observe if it inhibits the light-dependent retinal degeneration. The possibility that Dri regulates one or more factors that operates within or in association with the light pathway is explored in the next sections.

### *5.3.2 At which stage in the termination of the visual transduction pathway could* dri *act?*

Members of the light pathway, which has been extensively studied, constitute some of the potential target genes for *dri* regulation. The visual transduction pathway is activated by a photon of light, which leads to the isomerization of Rhodopsin (Rh) to Metarhodopsin (M) and the activation of the $G_{\alpha}$ signalling pathway. Metarhodopsin becomes phosphorylated by Rhodopsin Kinase (Figure 5.7) (Hardie and Raghu, 2001), which allows the binding of

Arrestin1 (Arr1) or the predominant form, Arr2, to M thus disrupting the interaction between Metarhodopsin and $G_\alpha$ and inactivating the signalling pathway (Hardie and Raghu, 2001). This is one potential point of the visual transduction pathway on which Dri may be acting. For example, if Dri activates the expression of *arr1* or *arr2*, then in *dri* mutant eye mosaics less Arr protein will be available to bind to M resulting in the continual activation of the light pathway, which has been shown to lead to necrosis of R cells (Davidson and Steller, 1998; Alloway et al., 2000). Arr2 also acts as a clathrin adaptor to mediate endocytosis of stable Arrestin-Rhodopsin complexes (Kiselev et al., 2000). The loss of *arr2* results in a decrease in the level of Rh1 protein (Acharya et al., 2003), a phenotype similar to *dri*. RdgC, the phosphatase that removes the phosphate moiety from M and Rh (Figure 5.7) (Lee and Montell, 2001), is another potential target for Dri regulation, as retinas lacking *rdgC* undergo light-dependent degeneration. It has also been shown that this retinal degeneration can be partially suppressed by the introduction of a mutation in a member of the clathrin-mediated endocytosis pathway (Alloway et al., 2000), indicating that a stable Rhodopsin-Arrestin complex, which has been shown to lead to apoptosis of the R cells, was formed in *rdgC* mutants (Alloway and Dolph, 1999; Alloway et al., 2000; Kiselev et al., 2000). If *rdgC* expression is altered in *dri* mutant eye mosaics, then presumably a stable Arrestin-Rhodopsin complex could form, leading to the light-dependent retinal degeneration observed in *dri* mutant eye mosaic flies.

Once the signalling pathway has been inactivated, the second messages must be recycled, another potential process within the visual transduction pathway which *dri* may be regulating. NorpA, the phospholipase C, is activated by $G_\alpha$ and converts the second messages, $PIP_2$ to DAG and $InsP_3$ (Figure 5.7) (Hardie and Raghu, 2001). Interestingly, hypomorphic mutations in *norpA* result in the light-dependent degeneration of the rhabdomeres, even though the light pathway is not active (Alloway et al., 2000). Alloway and colleagues (2000) showed that in *norpA* mutants stable Rhodopsin-Arrestin complexes were formed and that the retinal degeneration observed in *norpA* mutants could be overcome by the reduction of Rh1. As the retinas of *norpA* mutant flies degenerate in a light-dependent manner, *norpA* is also a candidate target for Dri regulation. The mechanism by which degeneration occurs in *norpA* mutants is unresolved. Alloway and colleagues (2000) have shown that in *norpA* mutant retinas, neighbouring cells exhibit a hallmark of apoptosis and phagocytose R1-R6 photoreceptor cells. Furthermore retinal degeneration was partially overcome by the introduction of a temperature sensitive *shibire* allele, which reduces vesicle endocytosis, and by expression of the apoptotic inhibitor, *p35* (Alloway et al., 2000). However, subsequent studies, in which *p35* and other inhibitors of the apoptotic pathway

were introduced into a *norpA* mutant background, have found that retinal degeneration in *norpA* mutants was only mildly affected (Hsu et al., 2004), suggesting that retinal degeneration through the programmed cell death pathway is minor.

One of the second messengers, DAG is converted back to $PIP_2$ by a number of proteins, RdgA, a DAG-kinase, converts DAG to PA (Figure 5.7) (Hardie, 2003). RdgA is not a candidate for Dri regulation because mutations in this gene result in light-independent retinal degeneration (Harris and Stark, 1977; Matsumoto et al., 1988). PA is converted to CDS-DAG by Cds then to PI in the submicrovilli cisternae (SMC), which is a specialized smooth endoplasmic reticulum (Figure 5.7) (Hardie, 2003). Like *rdgA*, *cds* is an unlikely candidate for Dri regulation because in *cds* mutants Rh1 does not appear to decrease over time (Lee et al., 2003b). RdgB transports PI and Arrestin back to the microvilli (Figure 5.7) (Hardie, 2003), and may be a candidate for Dri regulation because mutations in *rdgB* result in rhabdomere degeneration in a light-dependent manner and a decrease in Rh1 levels over time is observed (Lee et al., 2003b). Furthermore RdgB is required for the correct localization of Arrestin and NorpA (Lee et al., 2003b). Alloway and colleagues (2000) have shown that a stable Rhodopsin-Arrestin complex is formed in the absence of RdgB and the loss of *arr2* can partially overcome the retinal degeneration observed in an *rdgB* mutant background (Alloway et al., 2000). Therefore, disruption of *rdgB* expression due to the loss of Dri would lead to stable Rhodopsin-Arrestin complexes forming, inducing apoptosis of the R cells.

The presence of DAG and $InsP_3$ leads to an influx of calcium into the cell. NorpA, which converts $PIP_2$ to DAG (Hardie and Raghu, 2001), is also associated with the signalplex (Figure 5.7) (Huber et al., 1996b; Shieh et al., 1997), a group of proteins that are important for the rapid termination of the light pathway. INAD, a PDZ protein, interacts with many of the proteins associated with the signalplex, including the TRP channels (Figure 5.7) (Huber et al., 1996b). INAD and TRP appear unlikely to be candidates for Dri regulation because in one-week old *trp* and *inad* mutant adult eyes the levels of Rh1 appear to be unaffected.

## Figure 5.7 Potential Dri targets in the light pathway

1) Light activates the Rhodopsin protein leading the isomerization of the receptor become Metarhodopsin. 2) The associated G protein $G_{\alpha\beta\gamma q}$-GDP is activated ($G_{\alpha q}$) which in turn activates PLC to hydrolyse $PIP_2$ into the secondary messengers, $InsP_3$ and DAG. 3) Calcium enters the cells via the TRP and TRPL channels leading to excitation of the photoreceptor cell.

The response is terminated by 4) the recycling of the second messengers: DAG is converted to PA by RdgA in the SMC, PA is converted to CDP-DAG via Cds, which becomes PI via PI synthase and is transported back to the microvilli by RdgB. In the microvilli PI is phosphorylated and becomes $PIP_2$. 5) After the activation of Rh to M, M becomes phosphorylated by rhodopsin kinases (RK). Arrestin 2 binds to the phosphorylated M and interferes with the interaction between M and $G_{\alpha q}$. M-P is dephosphorylated by RdgC and can be converted back to Rh by exposure to 580nm wavelength light. 6) The signalplex consists of the adaptor protein INAD, PKC, PLC, CaM, TRP and NinaC. INAD interacts with NinaC, a myosin III protein that interacts with actin and is required for the fast termination of the light response. INAD is also vital for the localization of PKC, PLC and TRP.
Image modified from Hardie 2003

The green stars indicate potential target genes for Dri regulation.

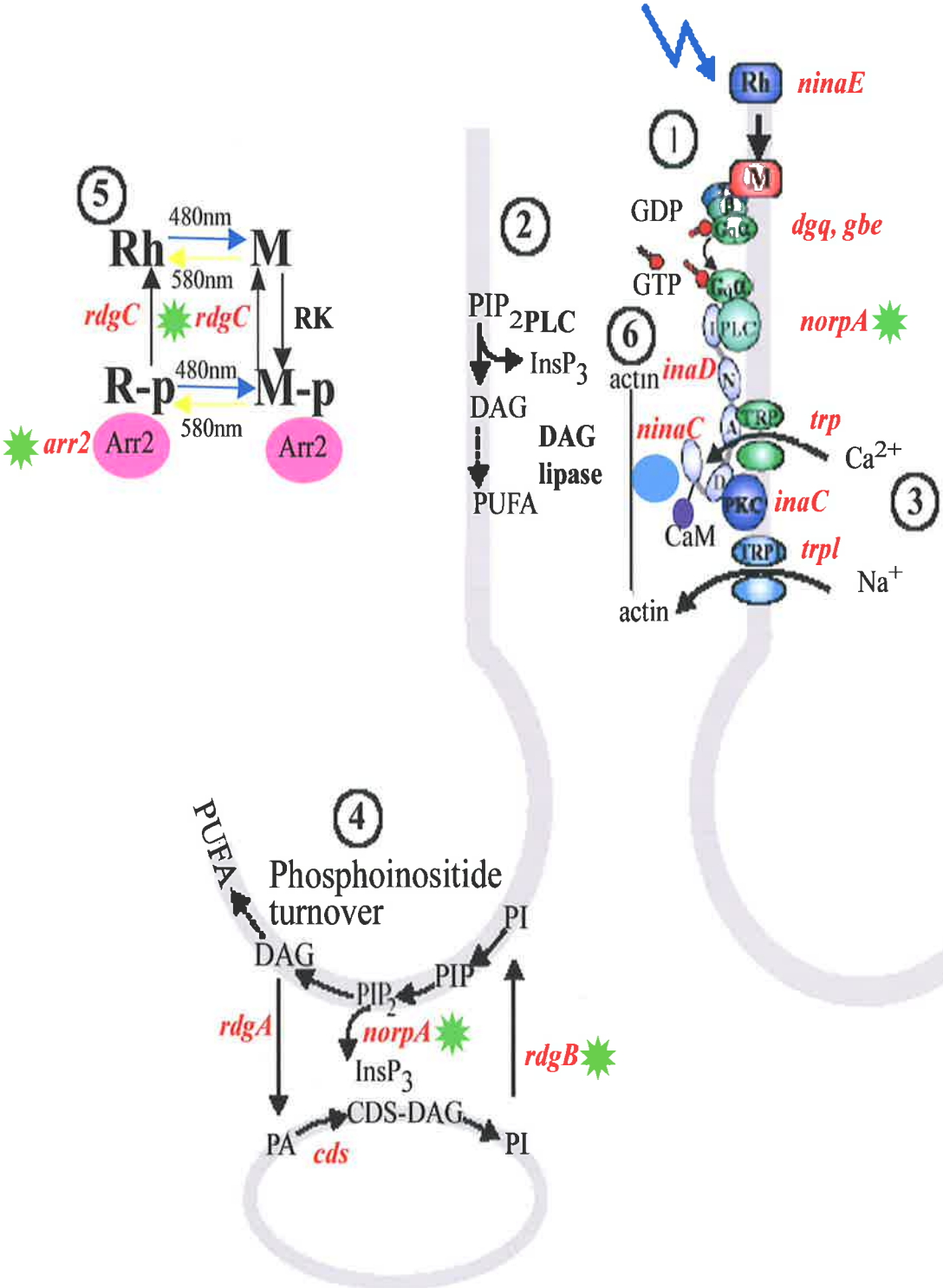
5
480nm
Rh
M
580nm
rdgC
rdgC
RK
480nm
R-p
M-p
580nm
arr2
Arr2
Arr2
2
PIP2
PLC
InsP3
DAG
DAG
lipase
PUFA
Rh
ninaE
1
M
GDP
GTP
dgq, gbe
norpA
6
actin
inaD
ninaC
trp
Ca2+
3
PKC
inaC
CaM
TRPL
trpl
Na+
actin
4
PUFA
Phosphoinositide
turnover
PI
DAG
PIP
PIP2
rdgA
norpA
rdgB
InsP3
CDS-DAG
PA
cds
PI

INAD also interacts with InaC, a $Ca^{2++}$/Calmodulin activated eye-specific protein kinase C (Figure 5.7) (Huber et al., 1996b), which has been shown to phosphorylate INAD and TRP (Liu et al., 2000). It is unknown at this time if mutations in InaC lead to light-dependent degeneration, so it is unclear if *inaC* is a potential candidate for Dri regulation. Calmodulin, the calcium sensor protein, is also a member of the signalplex (Figure 5.7) (Porter et al., 1993; Porter et al., 1995) and associates with as many as 13 other proteins, including INAD, Calcineurin, TRP and TRPL, dUNC-13, RdgC and NINAC (Scott et al., 1997; Xu et al., 1998b). Dri may be regulating Calmodulin, as the loss of this protein would result in the inability to terminate the light response, and presumably, retinal degeneration. NINAC, a myosin III, is one of the proteins that interacts with calmodulin (Porter et al., 1993; Porter et al., 1995), and is the connecting protein between the signalplex and the actin-based cytoskeleton (Wes et al., 1999). Subsequently, NINAC is vital for the termination of the visual transduction pathway (Figure 5.7) (Wes et al., 1999). Dri is unlikely to be regulating *ninaC* as the electroretinograms (ERG) produced from *ninaC* mutant flies have a latent off-transient peak, which is not evident in ERGs produced from *dri* mutant eye mosaic flies. Of all the proteins that are known to be involved in the visual transduction pathway, the best potential candidate genes for Dri regulation are therefore *norpA*, *arr2*, *rdgB* and *rdgC* (Figure 5.7).

Mutations in *crumbs*, a gene required for cell polarity, that does not have a direct role in the light pathway, have been shown to lead to degeneration in a light-dependent manner (Johnson et al., 2002) and therefore *crumbs* is also a potential candidate gene for Dri regulation. However it is unknown at this time if Rh1 levels decrease over time in *crumbs* mutants. Recently, Xu and colleagues (2004) have identified *sunglasses* (*sun*), the lysosomal tetraspanin, as being important for the turnover of Rh1 when exposed to continuous light (Xu et al., 2004). Mutations in *sun* lead to light- and age-dependent degeneration of the rhabdomeres (Xu et al., 2004). Dri is unlikely to be activating the expression of *sun*, as a mutation in *sun* reduces the turn over of Rh1 leading to an increase in Rh1, the opposite to the *dri* phenotype. However, Dri may be regulating, either by activation or repression, a factor that accelerates the turnover of Rh1, resulting in the loss of Rh1 from the cell. Interestingly, the overexpression of ceramidase, a member of the sphingolipid biosynthesis pathway that has been implicated in endocytic membrane trafficking, accelerated Rh1 turnover only in light conditions (Acharya et al., 2004) and may be a target for *dri* regulation. The findings reported here highlight the fact that although a lot is known about the visual transduction pathway in *Drosophila*, there are still some aspects that remain to be explored. In this case an unbiased approach, such as microarray analysis, may be the best way of

elucidating the role of *dri* in the adult eye. Alternatively, a genetic screen could be undertaken utilising the degeneration observed in *dri* mutant eye mosaics as a means of identifying enhancers and suppressors that genetically interact with *dri*.

### *5.3.3 Other possible roles for* dri

The expression of *dri* in R1-R6 cells may be associated with other regulatory activities that were not addressed in this thesis. For example, *dri* may repress Rh2, Rh3, Rh4, Rh5, or Rh6 expression, which are excluded from these cells. Immunohistochemical staining with the anti-Rh2 Rh3, Rh4, Rh5 and Rh6 antibodies would show if any of these genes are misexpressed in *dri* mutant eye mosaics flies. To determine if any de-repression of these genes in R1-R6 cells is directly due to *dri*, real time PCR analysis could be performed. However, if *dri* does repress expression of the other Rhodopsins, this would not account for the retinal degeneration observed in *dri* mutant eye mosaic flies. Other organisms are known to express more than one Rhodopsin within the one cell without deleterious effects (Townson et al., 1998; Applebury et al., 2000; Briscoe et al., 2000; Kitamoto et al., 2000). This is also true for *Drosophila*, as the loss of the transcription factor, *orthodenticle*, results in the expansion of *rh6* expression, which is normally restricted to a subset of R7 cells, into R1-R6 cells without inducing degeneration (Vandendries et al., 1996; Tahayato et al., 2003).

### *5.3.4 Conclusions*

This chapter has established that the loss of *dri* results in ommatidial defects at eclosion and an age-dependent degeneration of the rhabdomeres that is strongly enhanced by light. Despite the fact that *dri* is expressed exclusively in R1-R6 cells in the adult eye and the loss of *dri* results in a reduction of Rh1, *dri* does not regulate *ninaE* transcription or mRNA stability. Rather, *dri* must be regulating one or more factors required for Rh1 post-transcriptional processing or stability.

The analysis of *dri* mutant phenotypes in the adult eye presented in this chapter has established that *dri* is required for the integrity of the rhabdomeres, particularly upon light exposure, and that in addition to Rh1, *dri* may be regulating, either directly or indirectly, one or a number of genes required in the termination of the light pathway.

# Chapter 6: Final Discussion

## 6.1 Introduction

The research reported in this thesis has addressed the question: what biological role does the transcription factor *dead ringer* (*dri*) play in the *Drosophila* eye? Firstly a detailed analysis of the expression pattern of *dri* during eye development was undertaken. Following this, an analysis of the biological role of *dri* in eye development during the third larval instar stage and in eye function in the adult was undertaken.

## 6.2 Dri expression at different stages of eye development

An initial study of the expression pattern of *dri* in third larval instar eye imaginal discs had established that Dri was expressed several rows behind the morphogenetic furrow (Jasper et al., 2002) in 7 photoreceptor cells, including the R1-R6 cells (T. Shandala, personal communications), but it was unclear if Dri was localised in R7 or R8 cells. This thesis has established that *dri* is expressed in R8 cells during the third larval instar stage. The order of *dri*-expressing R cells was found to mirror the order of differentiation of the R cells. During pupal development, expression of *dri* in R8 cells is gradually downregulated, while the expression in R1-R6 cells continues into adulthood. Dri expression was not observed in R7 cells at any of the stages examined. This expression pattern suggested pleiotropic roles for *dri* in the *Drosophila* eye but gave little insight into what those roles may be. To elucidate the different roles of *dri* in the eye the work presented in this thesis focused on *dri* function in eye development during the third larval instar stage and on the function of *dri* in the adult eye.

## 6.3 The role of *dri* during the third larval instar stage

Somatic clones mutant for *dri*, that span the entire eye were produced in order to identify the role of *dri* during eye development. Tests for normal visual function in these eyes revealed that the loss of Dri resulted in flies that were blind (L. Kelly, personal communications), suggesting that *dri* plays one or more important roles in eye development. The possible reasons for the blindness associated with the loss of Dri were then investigated. This thesis established the monopolar neurons, which are the synaptic partners of the R cells that receive the light-induced neuronal signal, differentiated correctly in the absence of Dri. However, the axonal connections from the eye to the brain were not formed correctly in the

*dri* mutant eye mosaics. Further investigation revealed that the R1-R6 axons, which normally terminate in the lamina, pass through to the medulla in *dri* mutant eye mosaics.

### *6.3.1 Dri appears to define a new transcriptional regulatory component of photoreceptor axonogenesis*

A transcriptional hierarchy has been identified for R1-R6 axon targeting. In the wild type situation, Run is expressed exclusively in R7 and R8 cells, which terminate in the medulla. Misexpression of *run* in R2 and R5 cells results in all the R cell axons terminating in the medulla, showing that *run* is a key regulator of axonogenesis in R7 and R8 cells. It has recently been shown that Brakeless (Bks) represses *runt* (*run*) expression in R2 and R5 cells (Kaminker et al., 2002). Interestingly, the *bks* mutant eye mosaic phenotype does not recapitulate the severe phenotype of misexpressing Run in R2 and R5 cells, indicating that another factor may also be repressing *run* expression in R2 and R5 cells. Given the similarity in phenotype between *bks* and *dri* mutant eye mosaics, it was possible that Dri acts in this regulatory hierarchy to repress *run* expression. Thus, *dri* mutants would lead to ectopic *run* expression. However, this study has shown that *run* expression is unaffected in *dri* mutant eye mosaics and therefore that Dri is not co-operating with Bks to repress *run* expression in R2 and R5 cells. Furthermore *dri* expression was not affected by the misexpression of Runt in R2 and R5 cells, suggesting that *dri* is not downstream of *run* and therefore lies in a different transcriptional pathway. The loss of *run* specifically in the *Drosophila* eye has no phenotype, indicating redundancy with two suggested *runt*-domain containing proteins (Kaminker et al., 2002). It is possible that *dri* is acting in a similar fashion to *bks* and repressing one or both of the other *runt*-domain containing proteins, so that the loss of *dri* would result in the inappropriate expression of the *runt*-domain containing proteins in R1-R6 cells, resulting in a pass-through phenotype.

To test one possible explanation for why a subset of R1-R6 axons pass through to the medulla in *dri* mutant eye mosaics, lamina glial cell migration was investigated. Previously it has been established that R cells are required for the correct migration of lamina glial cells to the lamina plexus (Suh et al., 2002) and the incorrect migration of lamina glial cells result in the R1-R6 axons passing through the lamina to the medulla (Perez and Steller, 1996; Huang et al., 1998; Poeck et al., 2001; Suh et al., 2002). Furthermore, in the embryo, *dri* is expressed in the longitudinal glial cells in the CNS and in a *dri* mutant embryo these cells fail to migrate (Shandala et al., 2003). Work presented in this thesis established that the glial cells migrate correctly to the lamina plexus in *dri* mutant eye mosaics, indicating that *dri* is not regulating a factor in R cells that is required for migration of the lamina glial cells.

If *dri* is not regulating a factor required for the migration of glial cells then it must be regulating one or more factors within the R cells that are important for the attachment or guidance of the R cell axons. There are many genes that have been identified as being important for R1-R6 axon targeting but most of these are also involved in R7 axon targeting, a cell type in which *dri* is not expressed. At present, of the published proteins involved in R1-R6 targeting, the two best candidates for *dri* regulation in R1-R6 cells are the Ste-20 kinase, Misshapen (Msn) and a protein that re-organises F-actin, Bifocal (Bif) (Ruan et al., 1999; Ruan et al., 2002). Not only do the R1-R6 axons pass-through to the medulla in both *msn* and *bif* mutants, but in *bif* mutant eye mosaics the R7 axons target correctly, suggesting that *bif* is either redundant or not expressed in R7 cells, a pattern similar to that of Dri expression. Furthermore, tangential sections of *msn* clones display the same ectopic inner R cell as *dri* mutant clones, as well as ommatidial mis-orientation defects (Treisman et al., 1997a; Paricio et al., 1999/this study). The ommatidia of *bif* mutant clones do not display the ectopic inner R cells observed in *dri* mutant eye mosaics, but *bif* mutant eye mosaics do have misshaped and enlarged rhabdomeres (Bahri et al., 1997), which are also observed in *dri* mutant eye mosaic clones. Taken together, these observations suggest that *dri* is regulating either or both of these genes. To investigate if this is so, *in situ* hybridisation and real time PCR analysis could be undertaken to determine if the transcription level of both *msn* and *bif* in *dri* mutant eye mosaic eye discs is different to *FRT* controls.

Although a target gene for *dri* regulation has not been identified in this study, many candidate genes can be suggested on the basis of the phenotypes described in this thesis. In addition to the *runt*-domain containing proteins, *misshapen* and *bifocal*, Dri may be regulating any of the known or yet to be identified factors important in R1-R6 targeting. Given the large number of candidate genes, an appropriate and comprehensive approach to finding the targets of *dri* regulation would be a microarray-based approach.

### *6.3.2 Dri is required for correct growth cone shape in R8 cells*

If *dri* is not present in R8 cells during the third larval instar stage then the growth cones of the R8 axons do not form the correct "inverted Y" shaped. However, the R8 axons are targeted to the correct layer, the medulla, in both the third larval instar and adult optic lobes. It would be of interest to determine if the R8 axon phenotype observed during the third larval instar was transient or if the aberrant "inverted Y" shape had a lasting effect on the function of these axons. Exposing the flies to green light could test the function of the R8 cells. If the R8 axons are functional in a *dri* mutant eye mosaic, then the flies would move towards the light.

The loss of the R8 axon "inverted Y" morphology in *dri* mutant eye mosaics may indicate cytoskeletal defects in the growth cone or a reduced adhesion to the target region. Such defects could also account for the morphological structure of the adult mutant eye, in which both R7 and R8 rhabdomeres are present in the same ommatidium. The misplaced inner R cell may be due to problems in the morphogenesis of the R8 cells. Alternatively, the incorrectly positioned inner R cell may be the result of loss of adhesion between the R1-R6 cells and the R7 and R8 inner R cells. Restoring *dri* expression specifically in R8 cells, and examining if the correct array of rhabdomeres within the ommatidium is re-established, would show if the inner R cell phenotype was a result of an R8 cell-autonomous role of *dri*, consistent with the first explanation. Unfortunately, a GAL-4 driver that could be used to rescue the expression of *dri* in R8 cells alone, during both the third larval instar and up to 21 hours after puparium formation, was not available.

During pupal development, at approximately 21 hours APF, *dri* expression is downregulated in R8 cells. This transient expression in R8 cells, the disruption of the "inverted-Y" shape and the mis-orientation of the R cells observed in *dri* mutant eye mosaics is similar to the *flamingo* expression pattern and mutant phenotype (Senti et al., 2003, this study). Flamingo is a cadherin-like membrane protein that is expressed in R1-R6 cells but differs from the role of *dri* in those cells. *dri* is required for R1-R6 axons to terminate in the lamina while *flamingo* is not. However, *flamingo* is required for neural superposition, a process where axons from neighbouring ommatidia synapse with each other in an organised fashion. While this thesis has not addressed if *dri* is required for the R1-R6 axons from neighbouring ommatidia to synapse correctly, I have established that *dri* is expressed in R1-R6 cells at the correct time to have a role in neural superposition.

## 6.4 The role of *dri* in the adult eye

### *6.4.1 Rhodopsin 1 fails to accumulate in* dri *mutant eye mosaics*

None of the phenotypes observed during the third larval instar stage of eye development appear sufficient to explain the loss of vision that is observed in *dri* mutant eye mosaic flies. Under normal conditions, *dri* is expressed in R1-R6 cells in the adult eye and this expression pattern is reminiscent of *ninaE* expression. *ninaE* encodes Rhodopsin 1 (Rh1), the R1-R6 specific light sensing protein (Scavarda et al., 1983; Zuker et al., 1985a; Feiler et al., 1988; OTousa et al., 1989) and a loss of Rh1 protein was observed in *dri* mutant eye mosaics. Together these data suggested that one of the roles for *dri* might be to directly regulate *ninaE* expression. However, no differences in *ninaE* transcript levels were observed between *dri* mutant eye mosaics and *FRT42D* control heads, indicating that *dri* is not

regulating *ninaE* transcription. This does not exclude *dri* from acting as a repressor of one or more of the other rhodopsin proteins whose normal expression pattern is found in R7 or R8 cells. An example of a rhodopsin gene repressor is the transcription factor *orthodentical*, which has been shown to repress Rh6 transcription in R1-R6 cells but is also required to activate expression of Rh3 in R7 cells and Rh5 in R8 cells (Tahayato et al., 2003). Immunohistochemical staining with antibodies raised against Rh2, Rh3, Rh4, Rh5 and Rh6 would show whether these genes are ectopically expressed in *dri* mutant R1-R6 cells.

Interestingly, less Rh1 protein was present in both light- and dark-reared conditions when Dri is absent. The lower level of Rh1 protein not only explains the blindness observed in *dri* mutant eye mosaic flies but also suggests that *dri* is required for the processing and/or stability of Rh1. Consistent with this finding, *dri* dependent retinal degeneration occurred slowly in a light-independent manner after eclosion, but it is yet to be determined whether the ommatidial defects observed at eclosion are due to light-independent degeneration, or are morphogenetic defects that arise during pupal development. These possibilities could be experimentally tested as discussed in Chapter 5.

### *6.4.2 Light-dependent degeneration in* dri *mutant eyes*

This study has shown that retinal degeneration in *dri* mutant adult eyes is greatly enhanced in the presence of light. Although this could be due to the effect of light on the already limiting levels of Rh1, it could also result from a role for *dri* in the maintenance of the visual reception and transduction pathway. There is no simple explanation for this role, as *dri* expression is restricted to R1-R6 cells while known members of the light pathway, other than the rhodopsins, are expressed in all R cells, not specifically in R1-R6 cells. Transcription factors such as *glass*, *spalt major*, *prospero* and *orthodentical* are required for the regulation of the expression of the different Rhodopsins in different cell types (Mismer et al., 1988; Mismer and Rubin, 1989; Moses et al., 1989; Moses and Rubin, 1991; Mollereau et al., 2001; Tahayato et al., 2003; Cook et al., 2003). To date, however, Pph13, a homeodomain containing transcription factor, is the only transcription factor that has been identified as regulating members of the light pathway, and Pph13 is expressed in all R cells (Zelhof et al., 2003). Dri may be a second transcription factor that regulates members of the light pathway.

Further characterisation of the nature of the retinal degeneration that is occurring in *dri* mutant eye mosaics may help identify potential targets of Dri regulation. It has been shown that necrosis of R cells occurs when there is an uncontrolled influx of calcium into the cell, for example, as a result of the loss of Trp channels or hypomophic mutations in *rdgA*

and *arr2* genes (Davidson and Steller, 1998; Alloway et al., 2000; Raghu et al., 2000; Yoon et al., 2000). Apoptosis, on the other hand, occurs when a stable rhodopsin-arrestin complex is formed (Alloway and Dolph, 1999; Alloway et al., 2000; Kiselev et al., 2000). It has been shown that apoptosis of photoreceptor cells can be suppressed by the caspase inhibitor, *p35*, or by inhibiting the endocytic pathway via the introduction of a dominant form of the dynamin encoded by *shibire*, while necrosis of the photoreceptor cells will continue even if these proteins are present (Davidson and Steller, 1998; Alloway and Dolph, 1999; Alloway et al., 2000; Kiselev et al., 2000). Therefore, expressing *p35* or *shibire* in a *dri* mutant eye mosaic background and observing if the photoreceptor cells continue to degenerate in a light-dependent manner would discriminate between these types of degeneration. The retinal degeneration observed in *dri* mutant eye mosaics may be due to apoptosis, as a reduction in Rh1 levels is observed in *dri* mutant eyes and in *rdgB* and *rdgC* mutants, where retinal degeneration has been shown to occur by apoptosis (Alloway et al., 2000; Kiselev et al., 2000). A detailed discussion of the types of possible *dri* targets in the light pathway has been presented in Chapter 5.

### *6.4.3 Does* dri *play an evolutionarily conserved role in eye development?*

Many of the roles of proteins involved in the *Drosophila* light pathway are conserved in the vertebrate visual transduction pathway (Hardie and Raghu, 2001). It would be interesting to determine if *dri* regulation of light pathway members has been conserved during animal evolution. If this were true, the loss of the mammalian homologues of *dri*, DRIL1 and Bright Dead ringer Protein (BDP), could also result in light-dependent retinal degeneration. DRIL1 (also known as E2F Binding Protein 1) is expressed in a number of different tissues but it has not been established if it is expressed in the eye. A conditional knockout of the DRIL1 and BDP genes in the eye could be undertaken to determine if light-dependent retinal degeneration occurs in vertebrates.

## 6.5 Conclusion

The transcription factor gene, *dri*, is expressed in a dynamic pattern in both the *Drosophila* embryo and eye. This thesis has identified pleiotropic roles for *dri* in eye development and in adult eye function. In the developing eye, *dri* is required by the R cells for formation of the correct R1-R6 axon connections in the lamina of the optic lobe. Moreover *dri* was found not to be involved in the *brakeless-runt* transcriptional hierarchy, the only axonal transcriptional pathway in the eye identified so far. The task is now to identify other components of the *dri* pathway and the target genes of this pathway that are required

for an R cell axon to reach the optic lobe, the target area of the brain, and to terminate in the correct location.

In the adult eye, *dri* is required for Rh1 protein accumulation, the integrity of the rhabdomeres and vision. However, the molecular mechanism by which *dri* is acting is yet to be elucidated. Future work should focus on the identification of Dri target genes in the eye. Identification of these genes will provide a molecular basis for the roles of Dri in axon behaviour, Rh1 accumulation and ommatidial stability.

# Appendices

**Ct values used to determine the relative expression of *ninaE* and *rp49* in *FRT42D* and *dri*$^2$.**

| | *FRT42D rp49* | *FRT42D ninaE* | *dri*$^2$ #1 *rp49* | *dri*$^2$ #1 *ninaE* |
|---|---|---|---|---|
| **#1** | 20.9829 | 18.3148 | 20.4759 | 18.435 |
| | 21.2207 | 18.2448 | 20.5348 | 18.3371 |
| | 21.1268 | 18.4449 | 20.6552 | 18.3604 |
| **Average** | 21.11013 | 18.33483 | 20.5553 | 18.3775 |
| **Standard deviation** | 0.119773 | 0.101543 | 0.091391 | 0.051141 |
| | | | | |
| **#2** | 20.9067 | 18.0878 | 20.6941 | 18.121 |
| | 21.1925 | 18.2128 | 20.8087 | 18.2156 |
| | 21.1867 | 18.1536 | 20.7219 | 18.1293 |
| **Average** | 21.0953 | 18.1514 | 20.74157 | 18.1553 |
| **Standard deviation** | 0.163358 | 0.062529 | 0.059778 | 0.052386 |
| | | | | |
| **#3** | | 17.8157 | 21.0109 | 18.0714 |
| | 21.1805 | 18.0607 | 20.8367 | 18.0341 |
| | 21.1948 | 17.9868 | 20.9501 | 17.8177 |
| **Average** | 21.18765 | 17.9544 | 20.93257 | 17.9744 |
| **Standard deviation** | 0.010112 | 0.125672 | 0.088414 | 0.136982 |

Equations used to determine the relative expression (Muller et al., 2002).

$$MNE = \frac{(E_{target})^{\frac{CTtarget,well1 CTtarget,well2, CTtarget,well3}{3}}}{(E_{ref})^{\frac{CTref,well1 CTref,well2, CTref,well3}{3}}} = \frac{(E_{target})^{CTtarget\ mean}}{(E_{ref})^{CTref\ mean}}$$

***FRT42D* CT values for the standard curve**

| *ninaE* | | *rp49* | |
|---|---|---|---|
| 100ng | 24.6424 | 100ng | 20.1513 |
| 100ng | 24.6745 | 100ng | 20.4124 |
| 100ng | 24.7999 | 100ng | |
| Average | 24.7056 | Average | 20.28185 |
| Standard deviation | 0.067956 | Standard deviation | 0.184626 |
| | | | |
| 50ng | 25.1075 | 50ng | 20.3725 |
| 50ng | 24.9305 | 50ng | 20.5294 |
| 50ng | 24.8924 | 50ng | 20.5351 |
| Average | 24.9768 | Average | 20.479 |
| Standard deviation | 0.093719 | Standard deviation | 0.092276 |
| | | | |
| 10ng | | 10ng | 24.0664 |
| 10ng | 28.1486 | 10ng | |
| 10ng | 28.4879 | 10ng | 24.0521 |
| Average | 28.31825 | Average | 24.05925 |
| Standard deviation | 0.16965 | Standard deviation | 0.010112 |
| | | | |
| 5ng | 28.2387 | 5ng | |
| 5ng | 27.9911 | 5ng | 23.5748 |
| Average | 28.175 | 5ng | 23.4351 |
| Standard deviation | 28.13493 | Average | 23.50495 |
| | 0.104978 | Standard deviation | 0.06985 |
| | | | |
| 1ng | 30.422 | 1ng | 26.8925 |
| 1ng | 30.2881 | 1ng | |
| Average | | 1ng | 27.0694 |
| Standard deviation | 30.35505 | Average | 26.98095 |
| | 0.06695 | Standard deviation | 0.08845 |

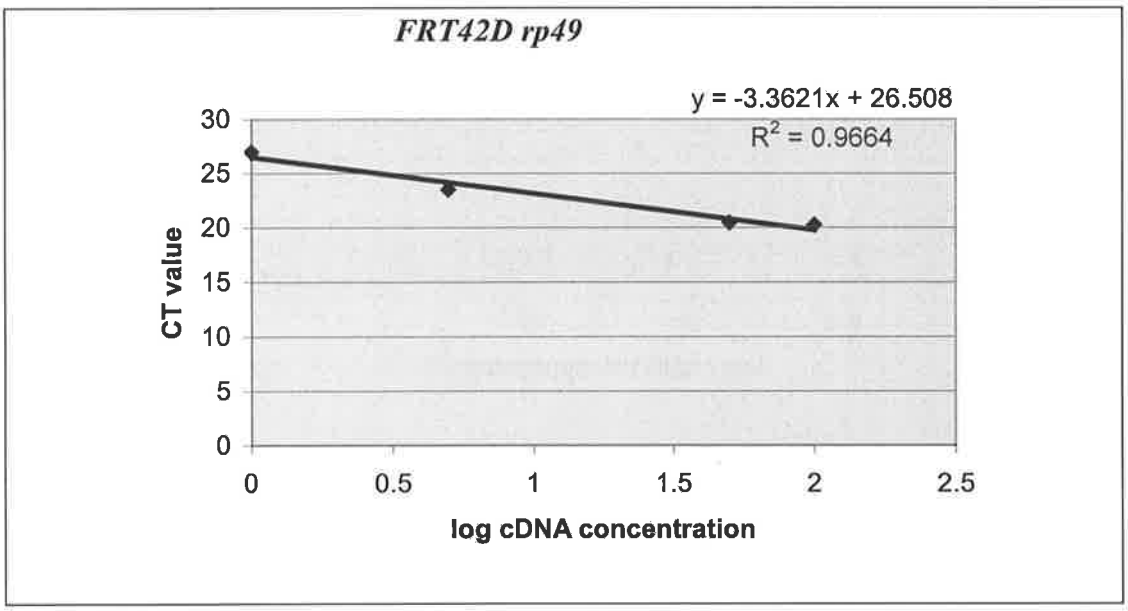


*FRT42D rp49* standard curve

| cDNA concentration | Average Ct value | |
|---|---|---|
| Log(100ng) | 20.28185 | |
| Log(50ng) | 20.479 | |
| Log(5ng) | 23.50495 | |
| Log(1ng) | 26.98095 | Slope = -3.621 |

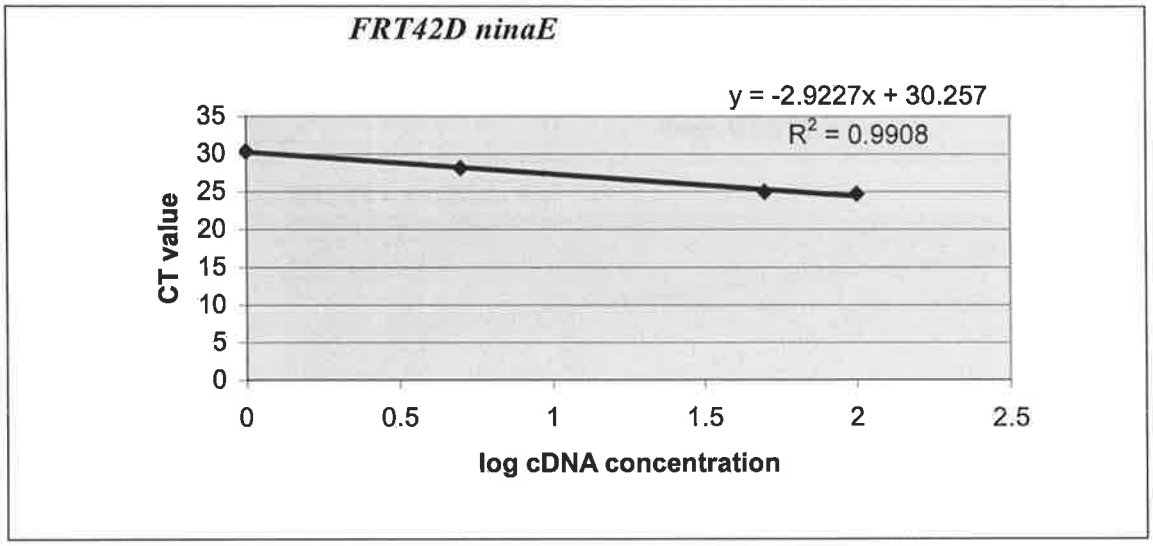


*FRT ninaE* standard curve

| cDNA concentration | Average Ct value | |
|---|---|---|
| Log(100ng) | 24.7056 | |
| Log(50ng) | 24.9768 | |
| Log(5ng) | 28.13493 | |
| Log(1ng) | 30.35505 | Slope = -2.9227 |

# References

**Acharya, U., Mowen, M. B., Nagashima, K. and Acharya, J. K.** (2004). Ceramidase expression facilitates membrane turnover and endocytosis of rhodopsin in photoreceptors. *Proc Natl Acad Sci U S A* **101**, 1922-6.

**Acharya, U., Patel, S., Koundakjian, E., Nagashima, K., Han, X. and Acharya, J. K.** (2003). Modulating sphingolipid biosynthetic pathway rescues photoreceptor degeneration. *Science* **299**, 1740-1743.

**Agulnik, A. I., Mitchell, M. J., Lerner, J. L., Woods, D. R. and Bishop, C. E.** (1994b). A mouse Y chromosome gene encoded by a region essential for spermatogenesis and expression of male-specific minor histocompatibility antigens. *Hum Mol Genet* **3**, 873-8.

**Agulnik, A. I., Mitchell, M. J., Mattei, M. G., Borsani, G., Avner, P. A., Lerner, J. L. and Bishop, C. E.** (1994a). A novel X gene with a widely transcribed Y-linked homologue escapes X-inactivation in mouse and human. *Hum Mol Genet* **3**, 879-84.

**Alloway, P. G. and Dolph, P. J.** (1999). A role for the light-dependent phosphorylation of visual arrestin. *Proc Nat Acad Sci USA* **96**, 6072-6077.

**Alloway, P. G., Howard, L. and Dolph, P. J.** (2000). The formation of stable rhodopsin-arrestin complexes induces apoptosis and photoreceptor cell degeneration. *Neuron* **28**, 129-138.

**Applebury, M. L., Antoch, M. P., Baxter, L. C., Chun, L. L., Falk, J. D., Farhangfar, F., Kage, K., Krzystolik, M. G., Lyass, L. A., Robbins, J. T. et al.** (2000). The murine cone photoreceptor: a single cone type expresses both S and M opsins with retinal spatial patterning. *Neuron* **27**, 513-23.

**Ausuble, S. F., Brent, R., Kingston, R. E., Moore, D., Seideman, J. G., Smith, J. A. and Struhl, K.** (1994). Current Protocols in Molecular Biology. New York: Weily.

**Bahri, S. M., Yang, X. and Chia, W.** (1997). The *Drosophila* bifocal gene encodes a novel protein which colocalizes with actin and is necessary for photoreceptor morphogenesis. *Molecular and Cellular Biology* **17**, 5521-9.

**Baker, N. E. and Yu, S. Y.** (1997). Proneural function of neurogenic genes in the developing *Drosophila* eye. *Curr Biol* **7**, 122-32.

**Barrett, A., Madsen, B., Copier, J., Lu, P. J., Cooper, L., Scibetta, A. G., Burchell, J. and Taylor-Papadimitriou, J.** (2002). PLU-1 nuclear protein, which is upregulated in breast cancer, shows restricted expression in normal human adult tissues: a new cancer/testis antigen? *Int J Cancer* **101**, 581-8.

**Balciunas, D. and Ronne, H.** (2000). Evidence of domain swapping within the jumonji family of transcription factors. *Trends in Biochemical Sciences* **25**, 274-276.

**Bentrop, J.** (1998). Rhodopsin mutations as the cause of retinal degeneration - Classification of degeneration phenotypes in the model system *Drosophila melanogaster*. *Acta Anatomica* **162**, 85-94.

**Berge-Lefranc, J. L., Jay, P., Massacrier, A., Cau, P., Mattei, M. G., Bauer, S., Marsollier, C., Berta, P., Fontes, M., Barrett, A. et al.** (1996). Characterization of the human *jumonji* gene. *Hum Mol Genet* **5**, 1637-41.

**Brady-Kalnay, S. M., Mourton, T., Nixon, J. P., Pietz, G. E., Kinch, M., Chen, H. Y., Brackenbury, R., Rimm, D. L., Del Vecchio, R. L. and Tonks, N. K.** (1998). Dynamic interaction of PTP mu with multiple cadherins *in vivo*. *Journal of Cell Biology* **141**, 287-296.

**Brand, A. H. and Perrimon, N.** (1993). Targeted Gene-Expression as a Means of Altering Cell Fates and Generating Dominant Phenotypes. *Development* **118**, 401-415.

**Brennan, C. A. and Moses, K.** (2000). Determination of *Drosophila* photoreceptors: timing is everything. *Cellular and Molecular Life Sciences* **57**, 195-214.

**Briscoe, A. D., Townson, S. M., Chang, B. S., Salcedo, E., Chadwell, L. V., Pierce, N. E., Britt, S. G., Vandendries, E. R., Johnson, D. and Reinke, R.** (2000). Six opsins from the butterfly Papilio glaucus: molecular phylogenetic evidence for paralogous origins of red-sensitive visual pigments in insects. *J Mol Evol* **51**, 110-21.

**Brumby, A. M., Zraly, C. B., Horsfield, J. A., Secombe, J., Saint, R., Dingwall, A. K. and Richardson, H.** (2002). *Drosophila* cyclin E interacts with components of the Brahma complex. *Embo J* **21**, 3377-89.

**Buchner, E., Buchner, S., Heisenberg, M. and Hofbauer, A.** (1987). Cell-Specific Staining by Immunocytochemistry in the Visual-System of *Drosophila* - Towards Cellular Characterization of Mutant Brain Defects. *Journal of Neurogenetics* **4**, 117-118.

**Canon, J. and Banerjee, U.** (2000). Runt and Lozenge function in *Drosophila* development. *Semin Cell Dev Biol* **11**, 327-36.

**Chan, S. W. and Hong, W.** (2001). Retinoblastoma-binding protein 2 (Rbp2) potentiates nuclear hormone receptor-mediated transcription. *J Biol Chem* **276**, 28402-12.

**Chang, H. Y. and Ready, D. F.** (2000). Rescue of photoreceptor degeneration in *rhodopsin*-null *Drosophila* mutants by activated Rac1. *Science* **290**, 1978-80.

**Chasan, R. and Anderson, K. V.** (1993). Maternal control of dorsal-ventral polarity and pattern in the embryo. In The Development of *Drosophila melanogaster*, M. Bate and A. Martinex Arias (Cold Spring Harbor Laboratory Press), 387-424.

**Chevesich, J., Kreuz, A. J. and Montell, C.** (1997). Requirement for the PDZ domain protein, INAD, for localization of the TRP store-operated channel to a signaling complex. *Neuron* **18**, 95-105.

**Choi, K. W. and Benzer, S.** (1994). Migration of glia along photoreceptor axons in the developing *Drosophila* eye. *Neuron* **12**, 423-31.

**Chou, W. H., Hall, K. J., Wilson, D. B., Wideman, C. L., Townson, S. M., Chadwell, L. V. and Britt, S. G.** (1996). Identification of a novel *Drosophila* opsin reveals specific patterning of the R7 and R8 photoreceptor cells. *Neuron* **17**, 1101-1115.

**Chou, W. H., Huber, A., Bentrop, J., Schulz, S., Schwab, K., Chadwell, L. V., Paulsen, R. and Britt, S. G.** (1999). Patterning of the R7 and R8 photoreceptor cells of *Drosophila*: evidence for induced and default cell-fate specification. *Development* **126**, 607-616.

**Chyb, S., Raghu, P. and Hardie, R. C.** (1999). Polyunsaturated fatty acids activate the *Drosophila* light-sensitive channels TRP and TRPL. *Nature* **397**, 255-259.

**Clandinin, T. and Zipursky, S.** (2000). Afferent Growth Cone Interactions Control Synaptic Specificity in the *Drosophila* Visual System. *Neuron* **28**, 427-436.

**Clandinin, T. R., Lee, C. H., Herman, T., Lee, R. C., Yang, A. Y., Ovasapyan, S. and Zipursky, S. L.** (2001). *Drosophila* LAR regulates R1-R6 and R7 target specificity in the visual system. *Neuron* **32**, 237-48.

**Colley, N. J., Cassill, J. A., Baker, E. K. and Zuker, C. S.** (1995). Defective Intracellular-Transport Is the Molecular-Basis of Rhodopsin-Dependent Dominant Retinal Degeneration. *Proc Nat Acad Sci USA* **92**, 3070-3074.

**Collins, R. T., Furukawa, T., Tanese, N. and Treisman, J. E.** (1999). Osa associates with the Brahma chromatin remodeling complex and promotes the activation of some target genes. *Embo J* **18**, 7029-40.

**Collins, R. T. and Treisman, J. E.** (2000). Osa-containing Brahma chromatin remodeling complexes are required for the repression of wingless target genes. *Genes Dev* **14**, 3140-52.

**Cook, T., Pichaud, F., Sonneville, R., Papatsenko, D. and Desplan, C.** (2003). Distinction between color photoreceptor cell fates is controlled by Prospero in *Drosophila*. *Dev Cell* **4**, 853-64.

**Cowman, A. F., Zuker, C. S. and Rubin, G. M.** (1986). An Opsin Gene Expressed in Only One Photoreceptor Cell Type of the *Drosophila* Eye. *Cell* **44**, 705-710.

**Dallas, P. B., Pacchione, S., Wilsker, D., Bowrin, V., Kobayashi, R. and Moran, E.** (2000). The human SWI-SNF complex protein p270 is an ARID family member with non-sequence-specific DNA binding activity. *Molecular and Cellular Biology* **20**, 3137-46.

**Davidson, F. F. and Steller, H.** (1998). Blocking apoptosis prevents blindness *Drosophila* retinal degeneration mutants. *Nature* **391**, 587-591.

**Dickson, B. J. and Hafen, E.** (1993). Genetic dissection of eye development in *Drosophila* In The Development of *Drosophila melanogaster*, M. Bate and A. Martinex Arias (Cold Spring Harbor Laboratory Press), 1327-1362.

**Dokucu, M. E., Zipursky, S. L. and Cagan, R. L.** (1996). Atonal, rough and the resolution of proneural clusters in the developing *Drosophila* retina. *Development (Cambridge, England)* **122**, 4139-47.

**Dolph, P. J., Ranganathan, R., Colley, N. J., Hardy, R. W., Socolich, M. and Zuker, C. S.** (1993). Arrestin Function in Inactivation of G-Protein Coupled Receptor Rhodopsin Invivo. *Science* **260**, 1910-1916.

**Fattaey, A. R., Helin, K., Dembski, M. S., Dyson, N., Harlow, E., Vuocolo, G. A., Hanobik, M. G., Haskell, K. M., Oliff, A., Defeo-Jones, D. et al.** (1993). Characterization of the retinoblastoma binding proteins RBP1 and RBP2. *Oncogene* **8**, 3149-56.

**Feiler, R., Bjornson, R., Kirschfeld, K., Mismer, D., Rubin, G. M., Smith, D. P., Socolich, M. and Zuker, C. S.** (1992). Ectopic Expression of Ultraviolet-Rhodopsins in the Blue Photoreceptor Cells of *Drosophila* - Visual Physiology and Photochemistry of Transgenic Animals. *Journal of Neuroscience* **12**, 3862-3868.

**Feiler, R., Harris, W. A., Kirschfeld, K., Wehrhahn, C. and Zuker, C. S.** (1988). Targeted Misexpression of a *Drosophila* Opsin Gene Leads to Altered Visual Function. *Nature* **333**, 737-741.

**Ferbeyre, G., de Stanchina, E., Querido, E., Baptiste, N., Prives, C. and Lowe, S. W.** (2000). PML is induced by oncogenic ras and promotes premature senescence. *Genes Dev* **14**, 2015-27.

**Fischbach, K. F. and Dittrich, A. P. M.** (1989). The Optic Lobe of *Drosophila-Melanogaster* .1. A Golgi Analysis of Wild-Type Structure. *Cell and Tissue Research* **258**, 441-475.

**Fortini, M. E. and Rubin, G. M.** (1990). Analysis of Cis-Acting Requirements of the Rh3 and Rh4 Genes Reveals a Bipartite Organization to Rhodopsin Promoters in *Drosophila-Melanogaster. Genes & Development* **4**, 444-463.

**Frankfort, B. J., Nolo, R., Zhang, Z. H., Bellen, H. and Mardon, G.** (2001). *senseless* repression of *rough* is required for R8 photoreceptor differentiation in the developing *Drosophila* eye. *Neuron* **32**, 403-414.

**Freeman, M.** (1996). Reiterative use of the EGF receptor triggers differentiation of all cell types in the *Drosophila* eye. *Cell* **87**, 651-660.

**Freeman, M.** (1997). Cell determination strategies in the *Drosophila* eye. *Development* **124**, 261-270.

**Frost, J. A., Xu, S., Hutchison, M. R., Marcus, S., Cobb, M. H., Zhao, Z. S., Manser, E., Chen, X. Q., Chong, C., Leung, T. et al.** (1996). Actions of Rho family small G proteins and p21-activated protein kinases on mitogen-activated protein kinase family members. *Molecular and Cellular Biology* **16**, 3707-13.

**Fryxell, K. J. and Meyerowitz, E. M.** (1987). An Opsin Gene That Is Expressed Only in the R7 Photoreceptor Cell of *Drosophila*. *Embo Journal* **6**, 443-451.

**Fukuyo, Y., Mogi, K., Tsunematsu, Y., Nakajima, T., Ferbeyre, G., de Stanchina, E., Querido, E., Baptiste, N., Prives, C. and Lowe, S. W.** (2004). E2FBP1/hDril1 modulates cell growth through downregulation of promyelocytic leukemia bodies. *Cell Death Differ* **12**, 12-25.

**Garrity, P. A., Lee, C. H., Salecker, I., Robertson, H. C., Desai, C. J., Zinn, K. and Zipursky, S. L.** (1999). Retinal axon target selection in *Drosophila* is regulated by a receptor protein tyrosine phosphatase. *Neuron* **22**, 707-17.

**Garrity, P. A., Rao, Y., Salecker, I., McGlade, J., Pawson, T. and Zipursky, S. L.** (1996). *Drosophila* photoreceptor axon guidance and targeting requires the dreadlocks SH2/SH3 adapter protein. *Cell* **85**, 639-50.

**Gerresheim, F.** (1988). Isolation of *Drosophila Melanogaster* Mutants with a Wavelength-Specific Alteration in Their Phototactic Response. *Behavior Genetics* **18**, 227-246.

**Gildea, J. J., Lopez, R. and Shearn, A.** (2000). A screen for new trithorax group genes identified *little imaginal discs*, the *Drosophila melanogaster* homologue of human *retinoblastoma binding protein 2*. *Genetics* **156**, 645-63.

**Gong, L., Kamitani, T., Fujise, K., Caskey, L. S., Yeh, E. T., Negorev, D., Ishov, A. M., Maul, G. G., Bell, P., Seeler, J. S. et al.** (1997). Preferential interaction of sentrin with a ubiquitin-conjugating enzyme, Ubc9. *J Biol Chem* **272**, 28198-201.

**Gregory, S. L., Kortschak, R. D., Kalionis, B. and Saint, R.** (1996). Characterization of the *dead ringer* gene identifies a novel, highly conserved family of sequence-specific DNA-binding proteins. *Molecular and Cellular Biology* **16**, 792-9.

**Haberman, A. S., Isaac, D. D. and Andrew, D. J.** (2003). Specification of cell fates within the salivary gland primordium. *Dev Biol* **258**, 443-53.

**Hader, T., Wainwright, D., Shandala, T., Saint, R., Taubert, H., Bronner, G. and Jackle, H.** (2000). Receptor tyrosine kinase signaling regulates different modes of Groucho-dependent control of Dorsal. *Curr Biol* **10**, 51-4.

**Hardie, R. C.** (1991). Whole-Cell Recordings of the Light-Induced Current in Dissociated *Drosophila* Photoreceptors - Evidence for Feedback by Calcium Permeating the Light-Sensitive Channels. *Proceedings of the Royal Society of London Series B-Biological Sciences* **245**, 203-210.

**Hardie, R. C.** (2003). Regulation of TRP channels via lipid second messengers. *Annual Review of Physiology* **65**, 735-759.

**Hardie, R. C. and Raghu, P.** (2001). Visual transduction in *Drosophila*. *Nature* **413**, 186-193.

**Harris, W. A. and Stark, W. S.** (1977). Hereditary retinal degeneration in Drosophila melanogaster. A mutant defect associated with the phototransduction process. *J Gen Physiol* **69**, 261-91.

**Hart, A. C., Kramer, H., Van Vactor, D. L., Jr., Paidhungat, M. and Zipursky, S. L.** (1990). Induction of cell fate in the *Drosophila* retina: the bride of sevenless protein is predicted to contain a large extracellular domain and seven transmembrane segments. *Genes Dev* **4**, 1835-47.

**Hauck, B., Gehring, W. J. and Walldorf, U.** (1999). Functional analysis of an eye specific enhancer of the *eyeless* gene in *Drosophila*. *Proc Nat Acad Sci USA* **96**, 564-569.

**Heberlein, U., Wolff, T. and Rubin, G. M.** (1993). The TGF beta homolog *dpp* and the segment polarity gene *hedgehog* are required for propagation of a morphogenetic wave in the *Drosophila* retina. *Cell* **75**, 913-26.

**Heitzler, P., Vanolst, L., Biryukova, I. and Ramain, P.** (2003). Enhancer-promoter communication mediated by Chip during Pannier-driven proneural patterning is regulated by Osa. *Genes Dev* **17**, 591-6.

**Herrscher, R. F., Kaplan, M. H., Lelsz, D. L., Das, C., Scheuermann, R. and Tucker, P. W.** (1995). The immunoglobulin heavy-chain matrix-associating regions are bound by Bright: a B cell-specific trans-activator that describes a new DNA-binding protein family. *Genes Dev* **9**, 3067-82.

**Hicks, J. L., Liu, X. R. and Williams, D. S.** (1996). Role of the NinaC proteins in photoreceptor cell structure: Ultrastructure of NinaC deletion mutants and binding to actin filaments. *Cell Motility and the Cytoskeleton* **35**, 367-379.

**Hing, H., Xiao, J., Harden, N., Lim, L. and Zipursky, S. L.** (1999). Pak functions downstream of Dock to regulate photoreceptor axon guidance in *Drosophila*. *Cell* **97**, 853-63.

**Hsu, C. D., Whaley, M. A., Frazer, K., Miller, D. A., Mitchell, K. A., Adams, S. M. and O'Tousa, J. E.** (2004). Limited role of developmental programmed cell death pathways in *Drosophila norpA* retinal degeneration. *The Journal of Neuroscience* **24**, 500-7.

**Huang, T. H., Oka, T., Asai, T., Okada, T., Merrills, B. W., Gertson, P. N., Whitson, R. H. and Itakura, K.** (1996). Repression by a differentiation-specific factor of the human cytomegalovirus enhancer. *Nucleic Acids Res* **24**, 1695-701.

**Huang, Z., Shilo, B. Z. and Kunes, S.** (1998). A retinal axon fascicle uses spitz, an EGF receptor ligand, to construct a synaptic cartridge in the brain of *Drosophila*. *Cell* **95**, 693-703.

**Huber, A., Sander, P., Gobert, A., Bahner, M., Hermann, R. and Paulsen, R.** (1996a). The transient receptor potential protein (Trp), a putative store-operated Ca2+ channel essential for phosphoinositide-mediated photoreception, forms a signaling complex with NorpA, InaC and InaD. *Embo J* **15**, 7036-45.

**Huber, A., Sander, P. and Paulsen, R.** (1996b). Phosphorylation of the *InaD* gene product, a photoreceptor membrane protein required for recovery of visual excitation. *Journal of Biological Chemistry* **271**, 11710-11717.

**Huber, A., Schulz, S., Bentrop, J., Groell, C., Wolfrum, U. and Paulsen, R.** (1997). Molecular cloning of *Drosophila* Rh6 rhodopsin: The visual pigment of a subset of R8 photoreceptor cells. *Febs Letters* **406**, 6-10.

**Hummel, T., Attix, S., Gunning, D. and Zipursky, S. L.** (2002). Temporal control of glial cell migration in the *Drosophila* eye requires *gilgamesh*, *hedgehog*, and eye specification genes. *Neuron* **33**, 193-203.

**Hurlstone, A. F., Olave, I. A., Barker, N., van Noort, M. and Clevers, H.** (2002). Cloning and characterization of hELD/OSA1, a novel BRG1 interacting protein. *Biochem J* **364**, 255-64.

**Inoue, H., Furukawa, T., Giannakopoulos, S., Zhou, S., King, D. S. and Tanese, N.** (2002). Largest subunits of the human SWI/SNF chromatin-remodeling complex promote transcriptional activation by steroid hormone receptors. *J Biol Chem* **277**, 41674-85.

**Iwahara, J. and Clubb, R. T.** (1999). Solution structure of the DNA binding domain from Dead ringer, a sequence-specific AT-rich interaction domain (ARID). *Embo J* **18**, 6084-94.

**Iwahara, J., Iwahara, M., Daughdrill, G. W., Ford, J. and Clubb, R. T.** (2002). The structure of the Dead ringer-DNA complex reveals how AT-rich interaction domains (ARIDs) recognize DNA. *Embo J* **21**, 1197-209.

**Iwaki, D. D., Johansen, K. A., Singer, J. B. and Lengyel, J. A.** (2001). *drumstick*, *bowl*, and *lines* are required for patterning and cell rearrangement in the *Drosophila* embryonic hindgut. *Dev Biol* **240**, 611-26.

**Jarman, A. P., Grell, E. H., Ackerman, L., Jan, L. Y. and Jan, Y. N.** (1994). Atonal is the proneural gene for *Drosophila* photoreceptors. *Nature* **369**, 398-400.

**Jarman, A. P., Sun, Y., Jan, L. Y. and Jan, Y. N.** (1995). Role of the proneural gene, *atonal*, in formation of *Drosophila* chordotonal organs and photoreceptors. *Development* **121**, 2019-30.

**Jasper, H., Benes, V., Atzberger, A., Sauer, S., Ansorge, W. and Bohmann, D.** (2002). A genomic switch at the transition from cell proliferation to terminal differentiation in the *Drosophila* eye. *Dev Cell* **3**, 511-21.

**Johnson, K., Grawe, F., Grzeschik, N. and Knust, E.** (2002). *Drosophila* crumbs is required to inhibit light-induced photoreceptor degeneration. *Curr Biol* **12**, 1675-80.

**Kahn, E. S. and Matsumoto, H.** (1997). Calcium/calmodulin-dependent kinase II phosphorylates *Drosophila* visual arrestin. *Journal of Neurochemistry* **68**, 169-175.

**Kaminker, J. S., Canon, J., Salecker, I. and Banerjee, U.** (2002). Control of photoreceptor axon target choice by transcriptional repression of Runt. *Nature Neuroscience* **5**, 746-50.

**Kania, M. A., Bonner, A. S., Duffy, J. B. and Gergen, J. P.** (1990). The *Drosophila* segmentation gene *runt* encodes a novel nuclear regulatory protein that is also expressed in the developing nervous system. *Genes Dev* **4**, 1701-13.

**Kaplan, M. H., Zong, R. T., Herrscher, R. F., Scheuermann, R. H. and Tucker, P. W.** (2001). Transcriptional activation by a matrix associating region-binding protein - Contextual requirements for the function of Bright. *Journal of Biological Chemistry* **276**, 21325-21330.

**Kas, E., Poljak, L., Adachi, Y. and Laemmli, U. K.** (1993). A Model for Chromatin Opening - Stimulation of Topoisomerase-Ii and Restriction Enzyme Cleavage of Chromatin by Distamycin. *Embo Journal* **12**, 2231-2231.

**Kim, T. G., Kraus, J. C., Chen, J. Q. and Lee, Y.** (2003). JUMONJI, a critical factor for cardiac development, functions as a transcriptional repressor. *Journal of Biological Chemistry* **278**, 42247-42255.

**Kimmel, B. E., Heberlein, U. and Rubin, G. M.** (1990). The homeo domain protein rough is expressed in a subset of cells in the developing *Drosophila* eye where it can specify photoreceptor cell subtype. *Genes Dev* **4**, 712-27.

**Kiselev, A., Socolich, M., Vinos, J., Hardy, R. W., Zuker, C. S. and Ranganathan, R.** (2000). A molecular pathway for light-dependent photoreceptor apoptosis in *Drosophila*. *Neuron* **28**, 139-152.

**Kitajima, K., Kojima, M., Kondo, S. and Takeuchi, T.** (2001). A role of *jumonji* gene in proliferation but not differentiation of megakaryocyte lineage cells. *Exp Hematol* **29**, 507-14.

**Kitamoto, J., Ozaki, K., Arikawa, K., Briscoe, A. D., Townson, S. M., Chang, B. S., Salcedo, E., Chadwell, L. V., Pierce, N. E., Britt, S. G. et al.** (2000). Ultraviolet and violet receptors express identical mRNA encoding an ultraviolet-absorbing opsin: identification and histological localization of two mRNAs encoding short-wavelength-absorbing opsins in the retina of the butterfly *Papilio xuthus*. *J Exp Biol* **203**, 2887-94.

**Kortschak, R. D.** (1999). Molecular biology of the *dead ringer* gene. In *Genetics Department*, ed. Adelaide: University of Adelaide.

**Kortschak, R. D., Reimann, H., Zimmer, M., Eyre, H. J., Saint, R. and Jenne, D. E.** (1998). The human *dead ringer/bright* homolog, *DRIL1*: cDNA cloning, gene structure, and mapping to D19S886, a marker on 19p13.3 that is strictly linked to the Peutz-Jeghers syndrome. *Genomics* **51**, 288-92.

**Kortschak, R. D., Tucker, P. W. and Saint, R.** (2000). ARID proteins come in from the desert. *Trends Biochem Sci* **25**, 294-9.

**Kozmik, Z., Machon, O., Kralova, J., Kreslova, J., Paces, J. and Vlcek, C.** (2001). Characterization of mammalian orthologues of the *Drosophila osa* gene: cDNA cloning, expression, chromosomal localization, and direct physical interaction with Brahma chromatin-remodeling complex. *Genomics* **73**, 140-8.

**Kramer, H., Cagan, R. L. and Zipursky, S. L.** (1991). Interaction of bride of sevenless membrane-bound ligand and the sevenless tyrosine-kinase receptor. *Nature* **352**, 207-12.

**Kumar, J. P. and Ready, D. F.** (1995a). Photoreceptor Degeneration in *Drosophila* Rhodopsin Mutants. *Investigative Ophthalmology & Visual Science* **36**, S918-S918.

**Kumar, J. P. and Ready, D. F.** (1995b). Rhodopsin plays an essential structural role in *Drosophila* photoreceptor development. *Development* **121**, 4359-4370.

**Kurada, P. and O'Tousa, J. E.** (1995). Retinal Degeneration Caused by Dominant Rhodopsin Mutations in *Drosophila*. *Neuron* **14**, 571-579.

**Kurada, P. and White, K.** (1998). Ras promotes cell survival in *Drosophila* by downregulating *hid* expression. *Cell* **95**, 319-329.

**Kypta, R. M., Su, H. and Reichardt, L. F.** (1996). Association between a transmembrane protein tyrosine phosphatase and the cadherin-catenin complex. *Journal of Cell Biology* **134**, 1519-1529.

**Lahoud, M. H., Ristevski, S., Venter, D. J., Jermiin, L. S., Bertoncello, I., Zavarsek, S., Hasthorpe, S., Drago, J., de Kretser, D., Hertzog, P. J. et al.** (2001). Gene targeting of Desrt, a novel ARID class DNA-binding protein, causes growth retardation and abnormal development of reproductive organs. *Genome Res* **11**, 1327-34.

**Lee, C. H., Herman, T., Clandinin, T. R., Lee, R. and Zipursky, S. L.** (2001). N-cadherin regulates target specificity in the *Drosophila* visual system. *Neuron* **30**, 437-50.

**Lee, R. C., Clandinin, T. R., Lee, C. H., Chen, P. L., Meinertzhagen, I. A. and Zipursky, S. L.** (2003a). The protocadherin Flamingo is required for axon target selection in the *Drosophila* visual system. *Nature Neuroscience* **6**, 557-63.

**Lee, S. J. and Montell, C.** (2001). Regulation of the rhodopsin protein phosphatase, RDGC, through interaction with calmodulin. *Neuron* **32**, 1097-1106.

**Lee, S. J., Xu, H., Kang, L. W., Amzel, L. M. and Montell, C.** (2003b). Light adaptation through phosphoinositide-regulated translocation of *Drosophila* visual arrestin. *Neuron* **39**, 121-132.

**Leonard, D. S., Bowman, V. D., Ready, D. F. and Pak, W. L.** (1992). Degeneration of photoreceptors in rhodopsin mutants of *Drosophila*. *Journal of Neurobiology* **23**, 605-26.

**Liu, M., Parker, L. L., Wadzinski, B. E. and Shieh, B. H.** (2000). Reversible phosphorylation of the signal transduction complex in *Drosophila* photoreceptors. *J Biol Chem* **275**, 12194-9.

**Lu, P. J., Sundquist, K., Baeckstrom, D., Poulsom, R., Hanby, A., Meier-Ewert, S., Jones, T., Mitchell, M., Pitha-Rowe, P., Freemont, P. et al.** (1999). A novel gene (PLU-1) containing highly conserved putative DNA/chromatin binding motifs is specifically up-regulated in breast cancer. *J Biol Chem* **274**, 15633-45.

**Lyapina, S., Cope, G., Shevchenko, A., Serino, G., Tsuge, T., Zhou, C. S., Wolf, D. A., Wei, N. and Deshaies, R. J.** (2001). Promotion of NEDD8-CUL1 conjugate cleavage by COP9 signalosome. *Science* **292**, 1382-1385.

**Ma, C. and Moses, K.** (1995). Wingless and patched are negative regulators of the morphogenetic furrow and can affect tissue polarity in the developing *Drosophila* compound eye. *Development* **121**, 2279-89.

**Ma, K., Araki, K., Ichwan, S. J., Suganuma, T., Tamamori-Adachi, M. and Ikeda, M. A.** (2003). E2FBP1/DRIL1, an AT-Rich Interaction Domain-Family Transcription Factor, Is Regulated by p53. *Mol Cancer Res* **1**, 438-44.

**Matsumoto, E., Hirosawa, K., Takagawa, K., Hotta, Y., Harris, W. A. and Stark, W. S.** (1988). Structure of retinular cells in a Drosophila melanogaster visual mutant, rdgA, at early stages of degeneration. *Cell Tissue Res* **252**, 293-300.

**Maul, G. G., Negorev, D., Bell, P., Ishov, A. M., Seeler, J. S. and Dejean, A.** (2000). Review: properties and assembly mechanisms of ND10, PML bodies, or PODs. *J Struct Biol* **129**, 278-87.

**Maurel_Zaffran, C., Suzuki, T., Gahmon, G., Treisman, J. E. and Dickson, B. J.** (2001). Cell-autonomous and -nonautonomous functions of LAR in R7 photoreceptor axon targeting. *Neuron* **32**, 225-35.

**Meinertzhagen, I. A. and Hanson, T. E.** (1993). The development of the optic lobe In The Development of *Drosophila melanogaster*, M. Bate and A. Martinex Arias (Cold Spring Harbor Laboratory Press), 1363-1491.

**Mismer, D., Michael, W. M., Laverty, T. R. and Rubin, G. M.** (1988). Analysis of the Promoter of the Rh2 Opsin Gene in *Drosophila*-Melanogaster. *Genetics* **120**, 173-180.

**Mismer, D. and Rubin, G. M.** (1989). Definition of Cis-Acting Elements Regulating Expression of the *Drosophila*-Melanogaster-Ninae Opsin Gene by Oligonucleotide-Directed Mutagenesis. *Genetics* **121**, 77-87.

**Mohrmann, L., Langenberg, K., Krijgsveld, J., Kal, A. J., Heck, A. J. and Verrijzer, C. P.** (2004). Differential targeting of two distinct SWI/SNF-related *Drosophila* chromatin-remodeling complexes. *Molecular and Cellular Biology* **24**, 3077-88.

**Mollereau, B., Dominguez, M., Webel, R., Colley, N. J., Keung, B., de Celis, J. F. and Desplan, C.** (2001). Two-step process for photoreceptor formation in *Drosophila*. *Nature* **412**, 911-3.

**Montell, C., Jones, K., Zuker, C. and Rubin, G.** (1987). A 2nd Opsin Gene Expressed in the Ultraviolet-Sensitive R7 Photoreceptor Cells of *Drosophila*-Melanogaster. *Journal of Neuroscience* **7**, 1558-1566.

**Moses, K., Ellis, M. C. and Rubin, G. M.** (1989). The Glass Gene Encodes a Zinc-Finger Protein Required by *Drosophila* Photoreceptor Cells. *Nature* **340**, 531-536.

**Moses, K. and Rubin, G. M.** (1991). Glass Encodes a Site-Specific DNA-Binding Protein That Is Regulated in Response to Positional Signals in the Developing *Drosophila* Eye. *Genes & Development* **5**, 583-593.

**Muller, P. Y., Janovjak, H., Miserez, A. R. and Dobbie, Z.** (2002). Processing of gene expression data generated by quantitative real-time RT-PCR. *Biotechniques* **32**, 1372-4, 1376, 1378-9.

**Negorev, D., Ishov, A. M., Maul, G. G., Bell, P., Seeler, J. S. and Dejean, A.** (2001). Evidence for separate ND10-binding and homo-oligomerization domains of Sp100. *J Cell Sci* **114**, 59-68.

**Nevins, J. R.** (1998). Toward an understanding of the functional complexity of the E2F and retinoblastoma families. *Cell Growth Differ* **9**, 585-93.

**Newsome, T. P., Asling, B. and Dickson, B. J.** (2000a). Analysis of *Drosophila* photoreceptor axon guidance in eye-specific mosaics. *Development* **127**, 851-60.

**Newsome, T. P., Schmidt, S., Dietzl, G., Keleman, K., Asling, B., Debant, A. and Dickson, B. J.** (2000b). Trio combines with dock to regulate Pak activity during photoreceptor axon pathfinding in *Drosophila*. *Cell* **101**, 283-94.

**Nie, Z., Xue, Y., Yang, D., Zhou, S., Deroo, B. J., Archer, T. K. and Wang, W.** (2000). A specificity and targeting subunit of a human SWI/SNF family-related chromatin-remodeling complex. *Molecular and Cellular Biology* **20**, 8879-88.

**Numata, S., Claudio, P. P., Dean, C., Giordano, A. and Croce, C. M.** (1999). Bdp, a new member of a family of DNA-binding proteins, associates with the *retinoblastoma* gene product. *Cancer Res* **59**, 3741-7.

**O'Tousa, J. E., Kurada, P., Tonini, T. and Adams, S.** (1995). Dominant Rhodopsin Mutations of *Drosophila*. *Investigative Ophthalmology & Visual Science* **36**, S637-S637.

**O'Tousa, J. E., Leonard, D. S. and Pak, W. L.** (1989). Morphological Defects in Orajk84 Photoreceptors Caused by Mutation in R1-6 Opsin Gene of *Drosophila*. *Journal of Neurogenetics* **6**, 41-52.

**Papatsenko, D., Nazina, A. and Desplan, C.** (2001). A conserved regulatory element present in all *Drosophila* rhodopsin genes mediates Pax6 functions and participates in the fine-tuning of cell-specific expression. *Mech Dev* **101**, 143-53.

**Papatsenko, D., Sheng, G. and Desplan, C.** (1997). A new rhodopsin in R8 photoreceptors of *Drosophila*: evidence for coordinate expression with Rh3 in R7 cells. *Development* **124**, 1665-73.

**Paricio, N., Feiguin, F., Boutros, M., Eaton, S., Mlodzik, M., Treisman, J. E., Ito, N. and Rubin, G. M.** (1999). The *Drosophila* STE20-like kinase *misshapen* is required downstream of the Frizzled receptor in planar polarity signaling *Embo J* **18**, 4669-78.

**Peeper, D. S., Shvarts, A., Brummelkamp, T., Douma, S., Koh, E. Y., Daley, G. Q. and Bernards, R.** (2002). A functional screen identifies hDRIL1 as an oncogene that rescues RAS-induced senescence. *Nat Cell Biol* **4**, 148-53.

**Pemov, A., Bavykin, S. and Hamlin, J. L.** (1998). Attachment to the nuclear matrix mediates specific alterations in chromatin structure. *Proc Natl Acad Sci U S A* **95**, 14757-14762.

**Perez, S. E. and Steller, H.** (1996). Migration of glial cells into retinal axon target field in *Drosophila melanogaster*. *Journal of Neurobiology* **30**, 359-73.

**Peterson, C. L. and Herskowitz, I.** (1992). Characterization of the Yeast Swi1, Swi2, and Swi3 Genes, Which Encode a Global Activator of Transcription. *Cell* **68**, 573-583.

**Poeck, B., Fischer, S., Gunning, D., Zipursky, S. and Salecker I.** (2001). Glial Cells Mediate Target Layer Selection of Retinal Axons in the Developing Visual System of *Drosophila*. *Neuron* **29**, 99-113.

**Pollock, J. A. and Benzer, S.** (1988). Transcript localization of four opsin genes in the three visual organs of *Drosophila*; RH2 is ocellus specific. *Nature* **333**, 779-82.

**Porter, J. A., Minke, B., Montell, C., Yu, M., Doberstein, S. K., Pollard, T. D., Scott, K., Sun, Y., Beckingham, K. and Zuker, C. S.** (1995). Calmodulin binding to *Drosophila* NinaC required for termination of phototransduction. *Embo J* **14**, 4450-9.

**Porter, J. A., Yu, M., Doberstein, S. K., Pollard, T. D., Montell, C.** (1993) Dependence of calmodulin localization in the retina on the NINAC unconventional myosin. *Science* **262**, 1038-42

**Punzo, C., Kurata, S. and Gehring, W. J.** (2001). The *eyeless* homeodomain is dispensable for eye development in *Drosophila*. *Genes & Development* **15**, 1716-1723.

**Quadbeck-Seeger, C., Wanner, G., Huber, S., Kahmann, R. and Kamper, J.** (2000). A protein with similarity to the human retinoblastoma binding protein 2 acts specifically as a repressor for genes regulated by the b mating type locus in *Ustilago maydis*. *Mol Microbiol* **38**, 154-66.

**Raghu, P., Usher, K., Jonas, S., Chyb, S., Polyanovsky, A. and Hardie, R. C.** (2000). Constitutive activity of the light-sensitive channels TRP and TRPL in the *Drosophila* diacylglycerol kinase mutant, *rdgA*. *Neuron* **26**, 169-179.

**Ranganathan, R., Harris, G. L., Stevens, C. F. and Zuker, C. S.** (1991). A *Drosophila* Mutant Defective in Extracellular Calcium-Dependent Photoreceptor Deactivation and Rapid Desensitization. *Nature* **354**, 230-232.

**Rangarajan, R., Gong, Q. and Gaul, U.** (1999). Migration and function of glia in the developing *Drosophila* eye. *Development* **126**, 3285-92.

**Rao, Y., Pang, P., Ruan, W., Gunning, D. and Zipursky, S. L.** (2000). brakeless is required for photoreceptor growth-cone targeting in *Drosophila*. *Proc Natl Acad Sci U S A* **97**, 5966-71.

**Rao, Y. and Zipursky, S. L.** (1998). Domain requirements for the Dock adapter protein in growth- cone signaling. *Proc Natl Acad Sci U S A* **95**, 2077-82.

**Ready, D. F., Hanson, T. E. and Benzer, S.** (1976). Development of the *Drosophila* retina, a neurocrystalline lattice. *Dev Biol* **53**, 217-40.

**Ristevski, S., Tam, P. P., Kola, I. and Hertzog, P.** (2001). Desrt, an AT-rich interaction domain family transcription factor gene, is an early marker for nephrogenic mesoderm and is expressed dynamically during mouse limb development. *Mech Dev* **104**, 139-42.

**Ruan, W., Long, H., Vuong, D. and Rao, Y.** (2002). Bifocal Is a Downstream Target of the Ste20-like Serine/Threonine Kinase Misshapen in Regulating Photoreceptor Growth Cone Targeting in *Drosophila*. *Neuron* **36**, 831-842.

**Ruan, W., Pang, P. and Rao, Y.** (1999). The SH2/SH3 adaptor protein dock interacts with the Ste20-like kinase misshapen in controlling growth cone motility. *Neuron* **24**, 595-605.

**Salcedo, E., Huber, A., Henrich, S., Chadwell, L. V., Chou, W. H., Paulsen, R. and Britt, S. G.** (1999). Blue- and green-absorbing visual pigments of *Drosophila*: Ectopic expression and physiological characterization of the R8 photoreceptor cell-specific Rh5 and Rh6 rhodopsins. *Journal of Neuroscience* **19**, 10716-10726.

**Salecker, I., Clandinin, T. R. and Zipursky, S. L.** (1998). Hedgehog and spitz: Making a match between photoreceptor axons and their targets. *Cell* **95**, 587-590.

**Sanbrook, J., Fritsch, E. F. and Maniatis, T.** (1989). Molecular cloning: a laboratory manual. Cold Spring Harbor, New York: Cold Spring Harbor Laboratory Press.

**Scavarda, N. J., Otousa, J. and Pak, W. L.** (1983). *Drosophila* Locus with Gene-Dosage Effects on Rhodopsin. *Proc Natl Acad Sci U S A* **80**, 4441-4445.

**Schwechheimer, C. and Deng, X. W.** (2001). COP9 signalosome revisited: a novel mediator of protein degradation. *Trends in Cell Biology* **11**, 420-426.

**Scott, K., Sun, Y., Beckingham, K. and Zuker, C. S.** (1997). Calmodulin regulation of *Drosophila* light-activated channels and receptor function mediates termination of the light response *in vivo*. *Cell* **91**, 375-83.

**Seeler, J. S. and Dejean, A.** (1999). The PML nuclear bodies: actors or extras? *Curr Opin Genet Dev* **9**, 362-7.

**Senti, K., Keleman, K., Eisenhaber, F. and Dickson, B. J.** (2000). *brakeless* is required for lamina targeting of R1-R6 axons in the *Drosophila* visual system. *Development* **127**, 2291-301.

**Senti, K., Usui, T., Boucke, K., Greber, U., Uemura, T. and Dickson, B.** (2003). Flamingo Regulates R8 Axon-Axon and Axon-Target Interactions in the *Drosophila* Visual System. *Current Biology* **13**, 828-832.

**Shaham, S. and Bargmann, C. I.** (2002). Control of neuronal subtype identity by the *C. elegans* ARID protein CFI-1. *Genes Dev* **16**, 972-83.

**Shandala, T., Kortschak, R. D., Gregory, S. and Saint, R.** (1999). The *Drosophila dead ringer* gene is required for early embryonic patterning through regulation of *argos* and *buttonhead* expression. *Development* **126**, 4341-9.

**Shandala, T., Kortschak, R. D. and Saint, R.** (2002). The *Drosophila retained/dead ringer* gene and ARID gene family function during development. *Int J Dev Biol* **46**, 423-30.

**Shandala, T., Takizawa, K. and Saint, R.** (2003). The *dead ringer/retained* transcriptional regulatory gene is required for positioning of the longitudinal glia in the *Drosophila* embryonic CNS. *Development* **130**, 1505-13.

**Sheng, G., Thouvenot, E., Schmucker, D., Wilson, D. S. and Desplan, C.** (1997). Direct regulation of *rhodopsin 1* by Pax-6/eyeless in *Drosophila*: evidence for a conserved function in photoreceptors. *Genes Dev* **11**, 1122-31.

**Shetty, K. M., Kurada, P. and O'Tousa, J. E.** (1998). Rab6 regulation of rhodopsin transport in *Drosophila*. *Journal of Biological Chemistry* **273**, 20425-20430.

**Shieh, B. H. and Niemeyer, B.** (1995). A Novel Protein Encoded by the *Inad* Gene Regulates Recovery of Visual Transduction in *Drosophila*. *Neuron* **14**, 201-210.

**Shieh, B. H., Zhu, M. Y., Lee, J. K., Kelly, I. M., Bahiraei, F., Huber, A., Sander, P., Gobert, A., Bahner, M., Hermann, R. et al.** (1997). Association of INAD with NORPA is essential for controlled activation and deactivation of *Drosophila* phototransduction *in vivo*. *Proc Natl Acad Sci U S A* **94**, 12682-7.

**Song, J., Wu, L., Chen, Z., Kohanski, R. A. and Pick, L.** (2003). Axons guided by insulin receptor in *Drosophila* visual system. *Science* **300**, 502-5.

**Staehling-Hampton, K., Ciampa, P. J., Brook, A. and Dyson, N.** (1999). A genetic screen for modifiers of E2F in *Drosophila melanogaster*. *Genetics* **153**, 275-87.

**Stein, G. S., van Wijnen, A. J., Stein, J. L., Lian, J. B., Pockwinse, S. M. and McNeil, S.** (1998). Linkages of nuclear architecture to biological and pathological control of gene expression. *Journal of Cellular Biochemistry*, 220-31.

**Stowers, R. S. and Schwarz, T. L.** (1999). A genetic method for generating *Drosophila* eyes composed exclusively of mitotic clones of a single genotype. *Genetics* **152**, 1631-9.

**Su, Y. C., Maurel_Zaffran, C., Treisman, J. E. and Skolnik, E. Y.** (2000). The Ste20 kinase *misshapen* regulates both photoreceptor axon targeting and dorsal closure, acting downstream of distinct signals. *Molecular and Cellular Biology* **20**, 4736-44.

**Su, Y. C., Treisman, J. E. and Skolnik, E. Y.** (1998). The *Drosophila* Ste20-related kinase *misshapen* is required for embryonic dorsal closure and acts through a JNK MAPK module on an evolutionarily conserved signaling pathway. *Genes & Development* **12**, 2371-2380.

**Suh, G., Poeck, B., Chouard, T., Oron, E., Segal, D., Chamovitz, D. and Zipursky, S.** (2002). *Drosophila* JAB1/CSN5 Acts in Photoreceptor Cells to Induce Glial Cells. *Neuron* **33**, 35-46.

**Tahayato, A., Sonneville, R., Pichaud, F., Wernet, M. F., Papatsenko, D., Beaufils, P., Cook, T. and Desplan, C.** (2003). Otd/Crx, a dual regulator for the specification of ommatidia subtypes in the *Drosophila* retina. *Dev Cell* **5**, 391-402.

**Takeuchi, T., Yamazaki, Y., Katoh-Fukui, Y., Tsuchiya, R., Kondo, S., Motoyama, J. and Higashinakagawa, T.** (1995). Gene trap capture of a novel mouse gene, *jumonji*, required for neural tube formation. *Genes Dev* **9**, 1211-22.

**Tomlinson, A.** (1985). The cellular dynamics of pattern formation in the eye of *Drosophila*. *J Embryol Exp Morphol* **89**, 313-31.

**Tomlinson, A., Bowtell, D. D., Hafen, E. and Rubin, G. M.** (1987). Localization of the sevenless protein, a putative receptor for positional information, in the eye imaginal disc of *Drosophila*. *Cell* **51**, 143-50.

**Townson, S. M., Chang, B. S., Salcedo, E., Chadwell, L. V., Pierce, N. E., Britt, S. G., Vandendries, E. R., Johnson, D. and Reinke, R.** (1998). Honeybee blue- and ultraviolet-sensitive opsins: cloning, heterologous expression in *Drosophila*, and physiological characterization. *The Journal of Neuroscience* **18**, 2412-22.

**Toyoda, M., Kojima, M. and Takeuchi, T.** (2000). Jumonji is a nuclear protein that participates in the negative regulation of cell growth. *Biochem Biophys Res Commun.* 274, 332-6.

**Treisman, J. E. and Heberlein, U.** (1998). Eye development in *Drosophila*: formation of the eye field and control of differentiation. *Curr Top Dev Biol* **39**, 119-58.

**Treisman, J. E., Ito, N. and Rubin, G. M.** (1997a). *misshapen* encodes a protein kinase involved in cell shape control in *Drosophila*. *Gene* **186**, 119-25.

**Treisman, J. E., Luk, A., Rubin, G. M. and Heberlein, U.** (1997b). eyelid antagonizes wingless signaling during *Drosophila* development and has homology to the Bright family of DNA-binding proteins. *Genes Dev* **11**, 1949-62.

**Tsunoda, S., Sierralta, J., Sun, Y. M., Bodner, R., Suzuki, E., Becker, A., Socolich, M. and Zuker, C. S.** (1997). A multivalent PDZ-domain protein assembles signalling complexes in a g-protein-coupled cascade. *Nature* **388**, 243-249.

**Valentine, S. A., Chen, G., Shandala, T., Fernandez, J., Mische, S., Saint, R. and Courey, A. J.** (1998). Dorsal-mediated repression requires the formation of a multiprotein repression complex at the ventral silencer. *Molecular and Cellular Biology* **18**, 6584-94.

**Vandendries, E. R., Johnson, D. and Reinke, R.** (1996). *orthodenticle* is required for photoreceptor cell development in the *Drosophila* eye. *Dev Biol* **173**, 243-55.

**Vazquez, M., Moore, L. and Kennison, J. A.** (1999). The trithorax group gene *osa* encodes an ARID-domain protein that genetically interacts with the brahma chromatin-remodeling factor to regulate transcription. *Development* **126**, 733-42.

**Watanabe, M., Layne, M. D., Hsieh, C. M., Maemura, K., Gray, S., Lee, M. E. and Jain, M. K.** (2002). Regulation of smooth muscle cell differentiation by AT-rich interaction domain transcription factors Mrf2alpha and Mrf2beta. *Circ Res* **91**, 382-9.

**Webb, C. F.** (2001). The transcription factor, Bright, and immunoglobulin heavy chain expression. *Immunologic Research* **24**, 149-161.

**Webb, C. F., Smith, E. A., Medina, K. L., Buchanan, K. L., Smithson, G. and Dou, S.** (1998). Expression of *bright* at two distinct stages of B lymphocyte development. *J Immunol* **160**, 4747-54.

**Wes, P. D., Xu, X. Z., Li, H. S., Chien, F., Doberstein, S. K. and Montell, C.** (1999). Termination of phototransduction requires binding of the NINAC myosin III and the PDZ protein INAD. *Nature Neuroscience* **2**, 447-53.

**Wills, Z., Bateman, J., Korey, C. A., Comer, A. and Van Vactor, D.** (1999). The tyrosine kinase Abl and its substrate Enabled collaborate with the receptor phosphatase Dlar to control motor axon guidance. *Neuron* **22**, 301-312.

**Wilsker, D., Patsialou, A., Dallas, P. B. and Moran, E.** (2002). ARID proteins: a diverse family of DNA binding proteins implicated in the control of cell growth, differentiation, and development. *Cell Growth Differ* **13**, 95-106.

**Wolff, T. and Ready, D. F.** (1991). The Beginning of Pattern-Formation in the *Drosophila* Compound Eye - the Morphogenetic Furrow and the 2nd Mitotic Wave. *Development* **113**, 841-50.

**Wolff, T. and Ready, D. F.** (1993). Pattern formation in the *Drosophila* retina., In The Development of *Drosophila melanogaster*, M. Bate and A. Martinex Arias (Cold Spring Harbor Laboratory Press), 1277-1326.

**Wu, J., Ellison, J., Salido, E., Yen, P., Mohandas, T. and Shapiro, L. J.** (1994). Isolation and characterization of XE169, a novel human gene that escapes X-inactivation. *Hum Mol Genet* **3**, 153-60.

**Xu, H., Lee, S. J., Suzuki, E., Dugan, K. D., Stoddard, A., Li, H. S., Chodosh, L. A., Montell, C., Johnson, K., Grawe, F. et al.** (2004). A lysosomal tetraspanin associated with retinal degeneration identified via a genome-wide screen *Drosophila crumbs* is required to inhibit light-induced photoreceptor degeneration. *Embo J* **23**, 811-22. Epub 2004 Feb 12.

**Xu, T. and Rubin, G. M.** (1993). Analysis of Genetic Mosaics in Developing and Adult *Drosophila* Tissues. *Development* **117**, 1223-1237.

**Xu, X. Z. S., Choudhury, A., Li, X. L. and Montell, C.** (1998a). Coordination of an array of signaling proteins through homo- and heteromeric interactions between PDZ domains and target proteins. *Journal of Cell Biology* **142**, 545-555.

**Xu, X. Z. S., Wes, P. D., Chen, H., Li, H. S., Yu, M. J., Morgen, S., Liu, Y. and Montell, C.** (1998b). Retinal targets for calmodulin include proteins implicated in synaptic transmission. *Journal of Biological Chemistry* **273**, 31297-31307.

**Yoon, J., Ben-Ami, H. C., Hong, Y. S., Park, S., Strong, L. L. R., Bowman, J., Geng, C. X., Baek, K., Minke, B. and Pak, W. L.** (2000). Novel mechanism of massive photoreceptor degeneration caused by mutations in the *trp* gene of *Drosophila*. *Journal of Neuroscience* **20**, 649-659.

**Zanolari, B., Friant, S., Funato, K., Sutterlin, C., Stevenson, B. J. and Riezman, H.** (2000). Sphingoid base synthesis requirement for endocytosis in *Saccharomyces cerevisiae*. *Embo Journal* **19**, 2824-2833.

**Zelhof, A. C., Koundakjian, E., Scully, A. L., Hardy, R. W. and Pounds, L.** (2003). Mutation of the photoreceptor specific homeodomain gene Pph13 results in defects in phototransduction and rhabdomere morphogenesis. *Development* **130**, 4383-92.

**Zhao, Z. S., Manser, E., Chen, X. Q., Chong, C., Leung, T. and Lim, L.** (1998). A conserved negative regulatory region in alphaPAK: inhibition of PAK kinases reveals their morphological roles downstream of Cdc42 and Rac1. *Molecular and Cellular Biology* **18**, 2153-63.

**Zhou, C. S., Wee, S., Rhee, E., Naumann, M., Dubiel, W. and Wolf, D. A.** (2003). Fission yeast COP9/signalosome suppresses cullin acivity through recruitment of the deubiquitylating enzyme Ubp12p. *Molecular Cell* **11**, 927-938.

**Zhu, L., Hu, J., Lin, D., Whitson, R., Itakura, K. and Chen, Y.** (2001). Dynamics of the Mrf-2 DNA-binding domain free and in complex with DNA. *Biochemistry* **40**, 9142-50.

**Zong, R. T., Das, C. and Tucker, P. W.** (2000). Regulation of matrix attachment region-dependent, lymphocyte-restricted transcription through differential localization within promyelocytic leukemia nuclear bodies. *Embo Journal* **19**, 4123-4133.

**Zuker, C., Cowman, A., Montell, C. and Rubin, G.** (1987). Molecular-Genetics of Rhodopsin and Phototrans Duction in the Visual-System of *Drosophila*. *Federation Proceedings* **46**, 2052-2052.

**Zuker, C. S., Cowman, A. F. and Rubin, G. M.** (1985a). Isolation and Structure of a Rhodopsin Gene from *Drosophila*-Melanogaster. *Cell* **40**, 851-858.

**Zuker, C. S., Cowman, A. F., Rubin, G. M., Pollock, J. A. and Benzer, S.** (1985b). Isolation and structure of a rhodopsin gene from D. melanogaster Transcript localization of four opsin genes in the three visual organs of *Drosophila*; RH2 is ocellus specific. *Cell* **40**, 851-8.